Ph.D Dissertation

UNIVERSITY OF TRENTO

Doctoral School in Mathematics

Human behaviour in epidemic modelling

Piero Poletti

Advisor:
Prof. Andrea Pugliese

Co-Advisor:
Dr. Stefano Merler

December 2010

Contents

Chapter 1

Introduction

1.1 Human behavior in response to epidemics

Mathematical models represent a powerful tool for investigating human infection diseases, providing useful predictions about the potential transmissibility of a disease and the effectiveness of possible control measures.

As well known, the characteristics of the pathogen responsible for the infections [6, 19] play a central role in the spread of an infectious disease. Nonetheless, one of the most central aspects of the human infection dynamics is the heterogeneity in behavioral patters adopted by the host population. Actually, the role played by human mobility patterns [84, 38, 151, 11, 112], the sociodemographic structure of the population [112] and intervention measures [6, 92] has been deeply investigated.

However, changes in human behaviors caused by the reaction to the disease can play a crucial role as well [56, 52]. Beyond behavioral changes imposed by public authorities, human behavioral changes can be triggered by uncoordinated responses driven by risk perception and fear of diseases (eventually of unknown fatality). Indeed, some studies on recent outbreaks of infectious disease have shown that people are prone to reduce risky behaviors [144, 98, 90, 125].

While behavioral responses to the spread of a diseases have been frequently reported anecdotally, there has been relatively little systematic investigation into their nature and on how they can affect the spread of infectious diseases. Behavioral changes are sometimes cited in the interpretation of outbreak data to explain drops in the transmission rate [132, 121], yet rarely spontaneous behavioral changes are explicitly modeled and investigated.

Efforts to study human behavior in the context of epidemics usually concentrated on evaluating the effectiveness of various institutionally enforced measures such as school closures [21, 80, 28, 27]. Recently, however, the impact of self-protective actions on the dynamics of an infectious disease has received increased attention [147, 42, 53, 93, 67, 66, 17, 15, 16, 29, 48, 47, 49, 45, 108, 61, 131, 69, 129, 72, 127, 130]. In fact, human spontaneous responses to an epidemic can affect remarkably the infection spread, and their interactions with disease dynamics require a proper investigation in order to better understand what happens when a disease spreads through human populations [56, 52].

With *spontaneous behavioral responses* here we define the changes in human behavioral patterns that involve personal decisions based on the available information about the disease or on individuals' beliefs and attitudes. This phenomenon is completely different from scenarios where the public is expected to comply with recommendations or control measures imposed by institutions.

Common childhood diseases, such as chickenpox and measles, provide a suitable example of when personal decisions are relevant. In fact, the decision whether or not to vaccinate a child is ultimately a personal decision and thus it has a strong behavioral component. Similarly, it is reasonable that during a severe epidemic outbreak individuals try to reduce the number of potentially infectious contacts. The avoidance of crowded environments, usage of face masks, practice of better hygiene protocols and self-restriction in traveling represent examples of self-imposed measures that can remarkably affect the disease spread.

During the 1918 influenza pandemic people eventually stayed away from congregated places [40]. In 1995, a supposed outbreak of bubonic plague in Sura, India, caused widespread panic on hundreds of thousands of people remarkably changing their traveling patterns [24]. When the Severe Acute Respiratory Syndrome (SARS) emerged in 2003, the usage of face masks became widespread in affected areas [98], and many individuals changed their traveling behavior [98, 58]. More recently, a high risk perception, possibly as a consequence of the exposure to a massive information campaign (media) on the risks of an emerging influenza pandemic, was detected during the 2009 H1N1 pandemic influenza [90] and, despite the low fatality associated to the event [128], behavioral response apparently played a relevant role during the early stages of the pandemic as well [144]. On the other hand, it was observed an increase in protective behavior as the prevalence of the disease was increasing, for both measles [125] and HIV [2]. Finally, concerns about proclaimed risks of vaccines have probably driven a widespread refusal of vaccination, leading to drops in vaccine uptake. This was the case of pertussis in the 1970s [70] and more recently of measles-mumps-rubella (MMR) vaccine [89].

As a matter of fact, attitudes, belief systems, available information about the risk associated to a disease can change over time. The dynamics of these attributes is a relevant element to understand the impact of behavioral responses to a disease [68]. Thus, infection dynamics should be considered as a coupled dynamics where the transmission of the pathogen is driven by human behavior dynamics, and vice versa. The investigation of this complex interplay would be helpful for giving insight to public health policy makers, for planning public health control strategies (e.g., vaccination) and better estimating the burden for health care centers over time.

Two specific phenomena are discussed in this thesis. The first one is represented by vaccination choices during a not compulsory vaccination program for childhood diseases. The second one is represented by spontaneous social distancing during an emerging epidemic outbreak.

By a modeling point of view, effects of spontaneous behavioral responses on the infec-

tion dynamics are very different in these two specific situations. Vaccination may result in moving individuals directly from the susceptible compartment to the removed compartment, i.e. those individuals that have developed immunity for the disease. On the other hand a reduced exposure to diseases, as a reaction to the presence of either the disease or certain beliefs about the disease, could be modeled either as a reduction in the number of contacts (e.g., reduced travel behavior), or as a reduction of intensity of contacts (e.g., usage of face mask). Thus models dealing with spontaneous social distancing, usually, assume a change in parameters (mainly the transmission rate or the recovery rate) or changes in population structure. Moreover, unless one considers vaccines that require boosting at regular intervals because of waning immunity or because of pathogen evolution (e.g. seasonal influenza), the decision to vaccinate is usually not reversible. On the opposite, social distancing triggered by risk perception, may depend on the dynamics of the risk of infection.

1.2 State of Art

There are various ways to model behavioral changes over time. Different assumption can be made not only on the effect of behavioral changes on the epidemic dynamics, but also on source and type of available information and the way the information spreads in the population. In addition, more sophisticated models can explicitly include spatial or contact network structure. In this case behavioral response to epidemics can change in the network structure as well.

1.2.1 Spontaneous social distancing during an epidemic outbreak

A number of studies have considered extensions of the simple SIR model in which the incidence rate is not bilinear in susceptible and infective individuals, but is modeled through a more general function, to include effects of saturation. Basically, the assumption is that, in the presence of a very large number of infective individuals, the population may tend to reduce the number of contacts per time [25]. These models have been shown to yield rich complex dynamics [101, 100], but human behavior and its dynamics are not explicitly modeled in order to account for a specific reaction to the disease [68].

Arguably, also behavioral response which affects the disease transmission can spread among individuals. Recently a class of models accounting for such phenomenon has been proposed. Such models share the idea that the spread of responsiveness is driven by the diffusion of fear, which can be modeled as a parallel infection [147, 42, 53, 93, 67, 66].

In [147], two different types of behaviors, labeled as "careful" and "risky", are considered and their frequencies in the population change over time according to social interactions. Interestingly, this work shows that *responsive behavior* (i.e. behavior which would guarantee a better protection from the disease and labeled as "careful") has an inherent evolutionary advantage if riskier behavior leads to faster progression to infection

and death. In general, the impact on disease dynamics can be quite remarkable if protective behavior is triggered by fear or awareness of a disease spread. In [53] it is assumed that people remove themselves from the circulation of a disease completely when they are affected by fear from the epidemic; in this case the modeled infection dynamics can lead to multiple epidemic waves as a consequence of the subsequent return into circulation of the individuals, as fear decreases [53]. In [93], it is assumed that individuals avoid infection or seek treatment earlier as they become aware of a disease; as a consequence, the diffusion of health information can reduce the prevalence of infection. In [42], behavioral responses can produce a reduction in both the basic reproductive number of the disease and the final epidemic size as a consequence of people entering a class of low activity at a given rate depending on the prevalence of a disease.

As for models involving more complex structures, if susceptibility of individuals is reduced as a direct consequence of having infectious contacts in a social network, it has been shown that a disease can be brought to extinction when self-protection is strong enough [9]. Moreover, it was shown that behavioral response results particularly effective when the network of information spread overlaps with the contact network of disease transmission [67, 66].

The behavior of infected individuals has also been considered in several works [77, 141, 167]. The underlying idea is that individuals that develop symptoms alter their contact patters as a consequence of their sickness. More specifically, models based on contact network assume that individuals who stay at home or avoid infected peers can be seen as cutting links of possible contagion. For instance, in [77, 141, 167], it was assumed that healthy individuals completely remove contacts with infected peers (eventually reconnecting them with the rest of the population). However, changing network structure removing only existing link is often unrealistic (e.g., it could be "realistic" only in the specific context of sexually transmitted diseases). The effect of cutting links of possible contagion is very similar to a reduction in the transmission rate [68].

1.2.2 Vaccination choices in not compulsory vaccination program

Vaccination policies of a large number of countries are based on voluntary compliance [68]. Some recent outbreaks of vaccine preventable diseases occurred in groups opposing vaccination on ideological grounds [79] or in communities beyond the reach of health care authorities [35]. Although forms of exemption to vaccination have always existed [139], the *natural history* of vaccination programs has always been pervaded by a high degree of optimism [29]. However, this optimistic view has increasingly been challenged in recent years. Indeed, concerns about proclaimed risks of vaccines can produce widespread refusal of vaccination and consequent drops in vaccine uptake.

For example, opposition to the whole-cell pertussis vaccine in the 1970s [70], the thimerosal case [106], and more recently the MMR scare [89, 135, 64, 142, 163] can be considered evidence that, in industrialized countries, the success story of vaccination is feeding back on itself. This is the consequence of two different processes. On the one

hand, the high degree of herd immunity achieved by decades of successful immunization programs has reduced the incidence of many infections to negligible levels. On the other hand, the large, and increasing, number of vaccines routinely administered every year yields steady flows of vaccine-associated side effects [160, 159]. In the US approximately 30,000 reports of Vaccine Adverse Events are notified annually, with 10–15% classified as serious [62]. In such circumstances the perception of the public will likely rank the perceived risk of suffering a *vaccine side effect* (VSE) as much higher than the corresponding risk of infection.

A common example is poliomyelitis in industrialized countries. In Italy during 1980-2000 the number of vaccine-induced polio cases was three times higher than wild polio cases [43]. In addition, it is well known that there can be a significant imbalance between perceived and real risk. An example of misperception of risk is the belief that the MMR vaccine can cause autism [120, 146]. In fact, such belief has spread widely despite the overwhelming evidences that reject such a causality [146].

Drops in vaccination coverage have led to increased interest in so-called *rational* vaccination decisions and their effects on the epidemiology of vaccine preventable infectious diseases. Many epidemiological modelers have turned to game theory and focused on the dilemma introduced by voluntary vaccination.

The "free riding" problem and the rational exemption in vaccination

Under voluntary vaccination high degrees of *herd immunity* might incentives vaccination *free riding* [145, 23, 131].

The name "free rider" comes from a historical example for public transportation: people using a bus without paying the fare are free riders. The free rider problem raises when too many individuals becomes free riders and thereby the system has not enough money to operate. Herd immunity consists in the indirect protection for unvaccinated individuals provided by vaccinated individuals, as the latter will not contract and transmit the disease. The notion of free riding in vaccination means that, if vaccination is perceived to come with risk or side-effects, the better strategy can appear not vaccinating, thus avoiding any risk of vaccine side effects, while relying on the rest of the population to keep the coverage high enough to provide herd immunity.

The *rational exemption*, as defined in [48, 108], represents the parents' decision not to immunize children after a seemingly "rational" comparison between the perceived utility of vaccination, i.e. protection from the risk of infection – perceived as very low as a consequence of the high herd immunity due to decades of successful vaccination policies – with its disutility, i.e. the risk of vaccine associated side effects. Actually, a behavior, resulting from the optimization performed by rational agents, might well turn out to be *myopically* rational, since it considers only the current perceived risk of disease, and not the risk of its future resurgence due to declining coverage. Several evidence of rational exemption behavior are documented by surveys of vaccination lifestyles [8, 107, 163, 64].

A series of recent intriguing works have attempted to explain rational exemption in its most appropriate framework, i.e. game theory [16, 15, 36, 131]. These papers have

provided the first game-theoretic proof of the *elimination impossible* result, and various implications of rational exemption. These implications suggest potential difficulties for global eradication plans, both at the national and international level [13, 55].

The game theoretical approach

When vaccination decisions are investigated using the game theory framework, it can be shown that the vaccination level attained from individuals acting only in their best self-interest is always below the optimal for the community. This result implies that it is impossible to eradicate a disease under voluntary vaccination [17, 15, 16, 29, 48, 23, 61, 48, 47, 49, 45, 131, 69, 129, 69, 72].

Moreover, models based on game theory have shown that the coupled dynamics of vaccination coverage and disease prevalence can lead to oscillations with outbreaks following upsurges in vaccination coverage and subsequent epidemic troughs. Such results comes from the assumption that vaccination decisions are made by imitating other individuals at a rate depending on the individual benefit [15, 131]. Actually, similar results have also been found by assuming that decisions are based on past prevalence of a disease (e.g. by considering time delays and memory mechanisms [131, 150, 48, 49, 22, 45]).

Works focusing on influenza [69] and on human papillomavirus (HPV) [14], in which the model is parametrized using the results of population surveys, confirmed the problem that, with individuals acting rationally according to their perceived risk, the population does not achieve vaccination levels that minimize disease prevalence in the population. Moreover, a similar approach (leading to similar results) has been applied to the study of vaccination against smallpox to prepare for bioterrorism [17], to childhood diseases [16, 48, 49], to seasonal influenza [150] and to yellow fever [34].

However, it was recently suggested that elimination might become possible when more realistic contact network structures are considered [124]. Specifically, in [124] it has been shown that voluntary ring-vaccination of individuals can reduce local outbreaks if contacts are sufficiently local and the response is fast enough.

Beyond investigations based on game theory framework, models have recently been proposed to base vaccination behavior on the spread of opinions in a social neighborhood rather than assuming individual rational behavior. In that case, it was shown that clusters of unvaccinated individuals can make outbreaks more likely to occur [138, 50].

1.3 Innovative aspects

Spontaneous human behavioral response is rarely considered explicitly in epidemic modeling. This Ph.D. thesis attempts to shed some light on the potential impact of behavioral changes on infection dynamics. Spontaneous social distancing is investigated in order to assess how and when behavioral changes can affect the spread of an epidemic. As a second topic, the problem of rational exemption is faced in order to investigate whether vaccine preventable diseases can be eliminated through not compulsory vaccination programs.

1.3.1 Spontaneous social distancing

While the game theoretical approach has been shared by many modelers for investigating the problem of vaccination choices, to the best of my knowledge, no efforts, but for a very recent ones [130], were developed for investigating spontaneous social distancing during an outbreak by using this framework. Moreover, still few works, e.g. [15], deal with the evolutionary game theory framework, instead of considering classic and static games. The approach of considering dynamical games allows to explicitly model the coupled dynamics of disease transmission and behavioral changes based on the risk perception.

Actually, most models accounting for spontaneous social distancing, assume a priori human response to the infection or consider only the behavioral response induced by the diffusion of fear, which is modeled as a parallel infection [42, 147, 53, 93, 67, 66]. However, an alternative mechanisms can contribute to the diffusion of responsiveness in a population. In fact, information diffusion may also spread through person to person contacts and can be modeled as an imitation process in which the convenience of different behaviors depends on the perceived risk of infection [9, 52].

Other novelties introduced in this thesis consist in considering: **(i)** asymptomatic infective individuals' behavior in response to the risk of infection; **(ii)** the effect of risk misperception; **(iii)** time delays and memory mechanisms in the risk perception of infection;

An innovative, in my opinion, aspect of this thesis is the investigation of an actual epidemic through a theoretical model explicitly considering human behavior. Indeed, the application to the 2009 H1N1 pandemic influenza may represent a further step to empirically assess quantitative and qualitative effects of spontaneous human response to perceived risk of infection.

Actually, most modeling efforts undertaken so far to study the impact of human behavior on the spread of infectious diseases are based on anecdotal evidence and common sense. Such models are almost never validated against quantifiable observations. Undeniably, a lot of data would be needed for model validation and parametrization. Recently, in order to answer questions like "where people obtain their information from", "which of information available to them they trust", "if and how they act upon the information" and "how-effective this reaction is", several surveys have been performed [98, 90, 82, 39]. However, even if many works share the insight on the effect of behavioral response on the epidemic spread, it is still difficult quantify human behavior with robust estimates [68]. Nonetheless, coupling the analysis of epidemiological data with drug purchase data, as discussed in chapter 4, could represent a promising solution.

At the current stage, proposed models could hardly be used for real time predictions since our knowledge on model parameters related to human behavior is only preliminary. However, further investigations, perhaps including results coming from surveys, can lead to gain a major consciousness on how spontaneous human behavior could affect epidemic dynamics.

1.3.2 Vaccination choices

Vaccination choices are investigated in chapters 5, 6 through different frameworks and assumptions, e.g. by considering families as representative agents and investigating different static and dynamic games.

Recent literature has highlighted that human perception of risk plays a central role in the dynamics of vaccination choices [17, 15, 16, 29, 48, 23, 61, 48, 47, 49, 45, 131, 69, 129, 69, 72], and thus strongly affects the chance of diseases' elimination. As discussed in sec. 1.2, elimination of vaccine preventable diseases becomes a challenge when vaccine are perceived as risky. Actually, the mismatch between subjective and objective assessment of risk has been demonstrated experimentally [166] and some of the key factors contributing to this mismatch have been deeply investigated [65, 91].

One innovative aspect of proposed models is represented by considering misperception of risks induced by partial or incorrect information, both concerning the infection and vaccine side effects. Actually, the imbalance between perceived and real risk play a central role in determining the possibility of eliminating a vaccine preventable disease. For example, the investigation carried out in chapter 5 highlight that elimination turns out to be possible when individuals are not fully informed about herd immunity or about the existence of a critical vaccination coverage.

Other novelties introduced in this thesis consist in considering: **(i)** the case of heterogeneous predisposition to vaccinate, assuming the population divided in groups that have different perceptions about risk of VSEs; **(ii)** nonlinear perceived costs of infection; **(iii)** the possibility that the perceived costs of infection and vaccination are evaluated by the public using past values of state variables, for example due to information delay or of the perception of long-term vaccine side effects.

The model introduced in chapter 6 makes, in my opinion, useful contributions to the investigation of the problem of rational exemption. The main innovation is to model the perceived risk of vaccination as a function of the incidence of vaccine side effects. If available information on vaccine side effects is becoming the main driving force of vaccine demand, as strongly supported by empirical evidence [135], this work may represent an appropriate description of the future evolution of immunization programs in voluntary vaccination regimes.

1.4 Structure of the Thesis

This thesis is structured as follows. In the next chapter, a simple model coupling an SIR transmission process with an imitation process is introduced in order to investigate effects of spontaneous social distancing during an epidemic outbreak. Specifically, the model assume that individuals are able to reduce their susceptibility. The potential impact of behavioral response on the final epidemic size and the temporal dynamics of the epidemic is assessed, and the chance of multiple epidemic waves is discussed. An accurate theoretical investigation is also carried out, capturing essential patterns of the infection dynamics when behavioral changes are much faster than the epidemic transmission.

In chapter 3, an extension of the model presented in chapter 2 is described. Both behavioral response performed by infected individuals and the effect of a memory mechanism in perception of risk are considered. The aim of this chapter is to investigate when and how the behavioral response affects the epidemic spread, clarifying the role of the key features describing human response. Moreover, scenarios accounting for the chance of delayed warning and behavioral responses triggered by the misperception of risk are analyzed.

In chapter 4, this approach is applied for investigating the specific case of the 2009 H1N1 pandemic influenza in Italy. The chapter is mainly focused on the analysis of real datasets. The hypothesis of an initial overestimation of risk by the host population is advanced, as a plausible explanation for the unusual and notable pattern observable in the ILI incidence reported to the national surveillance system. Such hypothesis is supported by empirical evidences, such as the temporal pattern of drug purchase and some (sporadic) reactive school closure ("self-imposed" by the scholastic board or suggested by local authorities).

Chapter 5, is devoted to the discussion of the problem of rational exemption in developed countries, through a set of simple static models for vaccination behavior. Firstly the problem is investigated trough the hypothesis of representative agent and, secondly, considering game strategic interactions, including the Stackelberg competition and the analysis of Nash Equilibria. The case of partial information about the risk of an epidemic is considered and the effect of heterogeneity in the perception of risks associated to vaccination is investigated as well.

In chapter 6, a transmission model with dynamic vaccine demand based on an imitation mechanism and with the perceived risk of vaccination modeled as a function of the incidence of VSEs is introduced. The analysis of the equilibria is performed and noteworthy inferences as regards both the past and future lifetime of vaccination programs are drown.

Finally, in chapter 7 includes a summary of work made during the thesis project and a discussion on several open issues about human spontaneous behavior in epidemic modeling.

Chapter 2

Spontaneous behavioral response to an epidemic outbreak

2.1 Introduction

The epidemic dynamics depends on the complex interplay between the characteristics of the pathogens' transmissibility and the structure and behaviour of the host population. Spontaneous change of behaviour in response to epidemics [56], possibly related to risk perception [9, 133, 141], has been recently proposed as a relevant factor in the comprehension of infection dynamics. While the merits and influence of such phenomena are still debated [48, 117], experience from the 1918-19 pandemic indicates that a better understanding of behavioural patterns is crucial to improve model realism and enhance the effectiveness of containment/mitigation policies [21].

Human behaviour is driven by evaluation of prospective outcomes deriving from alternative decisions and cost-benefit considerations. Past experience, response to the action of others and changes in exogenous conditions all contribute to the balance, to which game theory provides a rich and natural modelling framework [154, 81]. It is not surprising, therefore, that looking at behaviours through the lens of game theory has recently attracted the attention of the epidemiology community, for example when modelling the evolution over time of voluntary vaccination uptakes [16, 15].

In this paper we model a fairly general situation in which a population of individuals is subject to an epidemic outbreak developing according to an SIR model, but in which contact rates depend on the behavioural patterns adopted across the population. More specifically, all susceptible individuals can conform to either one or the other of two different behaviours, b_a and b_n, respectively corresponding to an "altered" and a "normal" behavioural pattern. The first gives the individuals an advantage in terms of reduced risk of infection, yet at some extra cost. For example, avoidance of crowded environments reduces the risk of infection, but also entails disadvantages deriving from greater isolation. Individuals adopting the second (b_n) are exposed to a normal risk of infection, but are spared the extra cost associated with b_a. Individuals may choose to switch between b_a and b_n at any time, depending on cost-benefit assessments based on the perception of risk.

The resulting model consists in the coupling of two dynamical systems, one describing the epidemic transmission and the other describing the behavioural changes. In principle, there is no reason for the two phenomena to evolve at the same speed. It is therefore crucial to study the model allowing for different time–scales, embodied in different time-units.

We give a full description of the model when the dynamics of the behavioural changes are "fast" with respect to the epidemic transmission. In particular, we provide sufficient conditions on the parameters for generating sequences of epidemic waves. Moreover, we show that the model is able to account for "asymmetric waves", i.e., infection waves whose rising and decaying phases differ in slope. However, similar patterns can also be observed when the time–scales of the two dynamics are comparable. When the dynamic of behavioural changes is "slow", the model basically reduces to a classical SIR.

The model's dynamics gives rise to patterns that are morphologically compatible with multiple outbreaks and the same-wave asymmetric slopes recently reported for the Spanish influenza of the 1918–19 [32, 31, 58, 115]. For these phenomena (trivially incompatible with the classical SIR model) a variety of alternative explanations have in fact been advanced: military demobilization at the end of the First World War [58], genetic variation of the influenza virus [26, 7, 20], exogenous time changes in transmission rates, such as seasonal forcing [38, 37]. Other explanations have been proposed invoking coinfection scenarios [111, 1, 51, 114]

Finally, and regardless of the relative speeds of dynamics, we show that the fraction of susceptible individuals at the end of the epidemic is always larger than that of a classical SIR model in which all individuals adopt the normal behaviour (b_n) with the same parameters.

2.2 The Model

Our model consists of the coupling of two mutually influencing phenomena: a) the epidemic transitions; b) the behavioural changes in the population of susceptible individuals.

As for the epidemic transitions, whose time unit is t, our model is based on an $S \to I \to R$ scheme[1]. We consider that susceptible individuals may adopt two mutually exclusive behaviours, b_n ("normal") and b_a ("altered"). Specifically, we assume that individuals adopting behaviour b_a are able to reduce the number of contacts in the time unit with respect to individuals adopting behaviour b_n. Thus, two transmission rates are considered for the two groups, accounting for the different contact rates associated with behaviours b_a and b_n. In particular, susceptible individuals adopting behaviour b_n, $S_n(t)$, become infected at a rate $\beta_n I(t)$ (and thus $\dot{S}_n(t) = -\beta_n S_n(t) I(t)$), where $I(t)$ represents the pool of infectious individuals, while susceptible individuals adopting behaviour b_a, $S_a(t)$, become infected at a rate $\beta_a I(t)$ (and thus $\dot{S}_a(t) = -\beta_a S_a(t) I(t)$), with $\beta_a < \beta_n$. Introducing the variables $S(t) = S_a(t) + S_n(t)$ and $x(t) = S_n(t)/(S_n(t) + S_a(t))$, corresponding to the

[1]Since we model single epidemic outbreaks, the vital dynamics of the population is not taken into account.

whole susceptible population and to the fraction of susceptibles adopting behaviour b_n respectively, the epidemic model can be written as:

$$
\left\{
\begin{array}{rcl}
\dfrac{dS}{dt}(t) &=& -\left[\beta_n S(t)x(t) + \beta_a S(t)(1-x(t))\right] I(t) \\
\dfrac{dI}{dt}(t) &=& \left[\beta_n S(t)x(t) + \beta_a S(t)(1-x(t))\right] I(t) - \gamma I(t) \\
\dfrac{dR}{dt}(t) &=& \gamma I(t) \\
\dfrac{dx}{dt}(t) &=& x(t)(1-x(t))(\beta_a - \beta_n) I(t) \ .
\end{array}
\right. \tag{2.1}
$$

Notice that the last equation describes the change of behaviours distribution in susceptible individuals deriving from the different rates of infection, β_n and β_a.

We now allow susceptible individuals to change their behaviour spontaneously, following cost/benefit considerations. This phenomenon can be cast in the language of evolutionary game theory, in which behaviours correspond to strategies in a suitable game, with certain expected payoffs. Adopting b_a reduces the risk of infection, but it is more costly. On the other hand, individuals adopting b_n are exposed to a higher risk of infection. It is clear that whether it is more convenient to adopt the first behaviour or the second depends on the state of the epidemic.

Of course, the two phenomena may not have the same time scales. In fact, while epidemic transmission can occur only through person-to-person contacts, it is fairly reasonable to consider that individuals can access the information required to decide whether to adopt either b_n or b_a, much more frequently by telephone, email, the Internet and, in general, the media.

Let us therefore introduce τ as the time unit of behavioural changes, and let us assume that $t = \alpha\tau$ with $\alpha > 0$.

Payoffs can now be modelled as it follows. All individuals pay a cost for the risk of infection, which we assume depends linearly on the fraction of infected individuals, $I(\tau)$, and it is higher for b_n than for b_a. Moreover, individuals playing b_a pay an extra, fixed cost k. It may be convenient to think of k as deriving from reducing the contacts with people, and therefore less traveling, working, attending school, visiting friends and relatives, etc.. Yet, it is more general than that, as it can account, in fact, for the cost of any self-imposable prophylactic measure. The payoffs associated with b_n and b_a are:

$$
\begin{array}{rcl}
p_n(\tau) &=& -m_n I(\tau) \\
p_a(\tau) &=& -k - m_a I(\tau) \quad ,
\end{array} \tag{2.2}
$$

with $m_n > m_a$. We may think of m_n and m_a as parameters related to the risk of developing symptoms (especially for the lethal infections) induced by the two different behaviours b_n and b_a.

The dynamics of behaviours is modelled as a selection dynamics based on imitation (*Imitation Dynamics* [81, 122]). A fraction of the individuals playing strategy b_n can switch to strategy b_a after having compared the payoffs of the two strategies, at a rate proportional to the difference between payoffs, $\Delta P(\tau) = p_n(\tau) - p_a(\tau)$, with proportionality constant ρ. Conversely for the fraction of the individuals playing b_a.

The last equation of system (2.1), in the time scale of infection transmission, thus becomes:

$$\begin{aligned} \frac{dx}{dt}(t) &= x(t)(1-x(t))(\beta_a - \beta_n)I(t) + \\ &+ \frac{\rho}{\alpha}x(t)(1-x(t))(k-(m_n-m_a)I(t)) \ . \end{aligned} \tag{2.3}$$

Notice that the first component of the time derivative of $x(t)$ is negative, meaning that the fraction of susceptible individuals adopting the normal beahviour b_n can only decrease over time as an effect of the *selection of behaviours* induced by the epidemic. On the other hand, whenever b_n is more convenient than b_a ($p_n(t) > p_a(t)$), the fraction in the population of susceptibles playing b_n can grow.

Let us briefly comment on the second component of the time derivative of $x(t)$. In principle, since the number of susceptible individuals decreases over time, one can argue that spontaneous changes of behaviour must depend explicitly on $S(t)$, because of the diminished number of contacts among susceptible individuals. However, here we assume that susceptible individuals take their decision on the basis of the composition of the pool of susceptible individuals that they are able to meet somehow (by looking only at the fractions of susceptible individuals adopting the two behaviours b_n and b_a, without considering the size of the sample).

It is worth noticing that $x = 0$ and $x = 1$ are equilibria for Eq. (8.7). This in particular implies that there is no way to switch to a different strategy (independently of whether it would be convenient) unless there is a non zero fraction of individuals already playing it. To circumvent this (which one may regard as an undesirable effect of strict imitation), *irrational behaviour* can be introduced which allows for rare (in τ time units) random switches of behaviour independent of encounters. Assuming a constant rate, $\chi > 0$, equal for both behaviours, the resulting equation for x is:

$$\begin{aligned} \frac{dx}{dt}(t) &= x(t)(1-x(t))(\beta_a - \beta_n)I(t) + \\ &+ \frac{\rho}{\alpha}x(t)(1-x(t))(k-(m_n-m_a)I(t)) + \\ &+ \frac{\chi}{\alpha}(1-x(t)) - \frac{\chi}{\alpha}x(t) \ . \end{aligned} \tag{2.4}$$

Therefore, the complete dynamics of infection (coupling behaviour with epidemic tran-

Table 2.1: *Model variables and parameters*

Notation	Description
S	Fraction of susceptible individuals
I	Fraction of infectious individuals
R	Fraction of recovered individuals
x	Fraction of susceptibles individuals adopting the "normal" behaviour
β_n	Transmission rate of individuals adopting the "normal" behaviour
β_a	Transmission rate of individuals adopting the "altered" behaviour
γ	Recovery rate
$1/m$	Threshold value determining the switch between "normal" and "altered" behaviour
μ	Irrational behaviour rate
ϵ	Relative speed of SIR dynamics and behavioural response

sitions) is given by:

$$
\left\{
\begin{array}{rcl}
\dfrac{dS}{dt}(t) &=& -\left[\beta_n S(t)x(t) + \beta_a S(t)(1-x(t))\right] I(t) \\
\dfrac{dI}{dt}(t) &=& \left[\beta_n S(t)x(t) + \beta_a S(t)(1-x(t))\right] I(t) - \gamma I(t) \\
\dfrac{dR}{dt}(t) &=& \gamma I(t) \\
\epsilon\dfrac{dx}{dt}(t) &=& x(t)(1-x(t))(1-mI(t)) + \mu(1-2x(t)) \ .
\end{array}
\right. \tag{2.5}
$$

where $\epsilon = \dfrac{\alpha}{k\rho}$, $m = (m_n - m_a)/k + \epsilon(\beta_n - \beta_a)$ and $\mu = \dfrac{\chi}{k\rho}$. As for the constraints on the models parameters, we have: $0 < \beta_a < \beta_n$, $0 < \gamma < \beta_n$[2], $\epsilon > 0$, $m > \epsilon(\beta_n - \beta_a)$ and $\mu > 0$. For facilitating the reader's understanding, the definitions of the variables recurring throughout the paper are reported in Tab. 2.1.

2.3 Study of Dynamics

System (2.5) admits the disease free equilibrium $(S, I, R, x) = (1, 0, 0, x^\star)$[3], with

$$
x^\star = \frac{1 - 2\mu + \sqrt{1 + 4\mu^2}}{2} \ , \tag{2.6}
$$

[2]This constraint is required only to ensure that the epidemic occurs (see Eq. 3.3).

[3]System (2.5) admits a continuum of equilibria, namely $(S^\star, 0, 1 - S^\star, x^\star)$ with $S^\star \in [0, 1]$. However, here we consider in detail only the "pandemic" case $S^\star = 1$.

which is unstable when $\beta_n x^\star + \beta_a(1-x^\star) > \gamma$. Thus, we assume that the initial values for system (2.5) are the following: $(S(0), I(0), R(0), x(0)) = (1 - I_0, I_0, 0, x^\star)$ with I_0 close to 0. Note that $1/2 < x^\star < 1$ and $x^\star \to 1$ when $\mu \to 0$. Moreover, this equilibrium is stable as long as $R_0 < 1$ where the basic reproductive number of system (2.5) is:

$$R_0 = \frac{\beta_n x^\star + \beta_a(1-x^\star)}{\gamma} \ . \tag{2.7}$$

Let us introduce the basic quantities $R_0^n = \beta_n/\gamma$ and $R_0^a = \beta_a/\gamma$. We can rewrite Eq. (3.3) as $R_0 = R_0^n x^\star + R_0^a(1-x^\star)$. The quantities R_0^n and R_0^a are reproduction numbers themselves: R_0^n characterizes the situation where the susceptible pool is fully composed by individuals adopting the normal behaviour b_n, whereas R_0^a characterizes the situation where the susceptible pool is fully composed by individuals spontaneously reducing their contacts (behaviour b_a). Thus, Eq. (3.3) has a straightforward interpretation: a typical infective individual behaving according to b_n (a case occurring with probability $x^\star$) would cause R_0^n new infections during his/her whole period of infectivity. Similarly for R_0^a in case he/she adopts the altered behaviour b_a (which occurs with probability $1-x^\star$). Note that $R_0 \simeq R_0^n$ for $x^\star \simeq 1$.

We start by analyzing the dynamics of system (2.5) in two extreme cases, namely $\epsilon \to 0$ and $\epsilon \to +\infty$, which correspond respectively to the situation when the dynamics of the behavioural changes is "fast" or "slow" with respect to the epidemic transmission.

Let us consider first the case $\epsilon \to +\infty$. In this case, the solutions of system (2.5) approximate those of system (2.1), which is a classical SIR model with two classes of susceptibility. Since $\dot{x}(t) < 0$, the fraction of individuals adopting the normal behaviour b_n will decrease over time as a consequence of the selection of the behaviour b_a induced by the epidemic, even in the absence of spontaneous behavioural changes.

For the case $\epsilon \to 0$ (which is more interesting from both the mathematical and the biological point of view) we are going to apply the singular perturbation methods [123].

The solutions of the singularly perturbed initial value problem (2.5) is approximated by that of the degenerate system:

$$\left\{ \begin{array}{rcl} \dfrac{dS}{dt}(t) & = & -\left[\beta_n S(t)x(t) + \beta_a S(t)(1-x(t))\right] I(t) \\ \dfrac{dI}{dt}(t) & = & \left[\beta_n S(t)x(t) + \beta_a S(t)(1-x(t))\right] I(t) - \gamma I(t) \\ \dfrac{dR}{dt}(t) & = & \gamma I(t) \\ 0 & = & x(t)(1-x(t))(1-mI(t)) + \mu(1-2x(t)) \ , \end{array} \right. \tag{2.8}$$

obtained from (2.5) by formally setting $\epsilon = 0$, provided that in the last of (2.8) we use an asymptotically stable equilibrium of the boundary–layer system

$$\frac{dx}{ds}(s) = x(s)(1-x(s))(1-mI) + \mu(1-2x(s)) \ , \tag{2.9}$$

obtained by making the transformation of independent variable $s = t/\epsilon$, and then setting $\epsilon = 0$ (which in particular implies that $S(s)$, $I(s)$ and $R(s)$ are constant) [148, 83].

Notice that, after having set $\epsilon = 0$, parameter m reduces to $(m_n - m_a)/k$. Consequently, as it may be expected, the effect of the selection of behaviours induced by the epidemic is negligible when the dynamics of behaviours is much faster than that of the infection transmission.

We start by analyzing the solutions of Eq. (2.9), where the fraction of infected individuals I is assumed to be constant. Eq. (2.9) admits the following equilibrium:

$$x^\star(I) = \begin{cases} \dfrac{1-2P+\sqrt{1+4P^2}}{2} & \text{if} \quad I < 1/m \iff P > 0 \\ \dfrac{1-2P-\sqrt{1+4P^2}}{2} & \text{if} \quad I > 1/m \iff P < 0 \\ \dfrac{1}{2} & \text{if} \quad I = 1/m \ , \end{cases} \tag{2.10}$$

where $P = \frac{\mu}{1-mI}$, which is asymptotically stable (comparing Eq. (2.6), note that $x^\star = x^\star(0)$). In conclusion, the following Proposition holds:

Proposition 2.3.1. *The boundary–layer system* (2.9) *admits the asymptotically stable equilibrium* (2.10) *and, independently on* I, $x^\star(I) \to 1$ *if* $I < 1/m$ *and* $x^\star(I) \to 0$ *if* $I > 1/m$ *when* $\mu \to 0$.

As regards the stability of the equilibrium (2.10), it is sufficient to observe that the equation of $\dot{x}$ is a parabola (which reduces to a straight line when $I = 1/m$) and that the sign of $\dot{x}$ is positive for $x < x^\star(I)$ and negative for $x > x^\star(I)$.

The following Proposition characterizes the solutions of system (2.5) when the dynamics of the behavioural changes is fast with respect to that of the epidemic transmission and irrational behaviour rate is small.

Proposition 2.3.2. *Under the assumptions* $R_0^n > 1$ *and* $1/m < I_p$ *where* $I_p = 1 - \frac{1}{R_0^n} + \frac{1}{R_0^n}\log\frac{1}{R_0^n}$, *if* $\epsilon \to 0$ *and* $\mu = o(\epsilon^k)$ *with* $k \geq 1$, *the solutions of system* (2.5) *are characterized as follows:*

S1 *there exists a finite time* $t_1 > 0$ *such that the solutions of system* (2.5) *approximate those of a classical SIR model with* $R_0 = R_0^n$ *on the interval* $(0, t_1)$ *and* $I(t_1) = 1/m$;

S2.1 *If* $R_0^a S(t_1) \leq 1$, *there exists a finite time* $t_2' > t_1$ *such that the solution of system* (2.5) *can be approximated in the time interval* (t_1, t_2'), *where* $t_2' = t_1 + \frac{m}{\gamma}(S(t_1) - \frac{1}{R_0^n})$, *by* $S(t) = S(t_1) - \frac{\gamma}{m}(t - t_1)$ *and* $I(t) = 1/m$. *Afterwards, the solutions of system* (2.5) *approximate those of a classical SIR model (in its decaying phase) with* $R_0 = R_0^n$ *on the interval* $(t_2', +\infty)$;

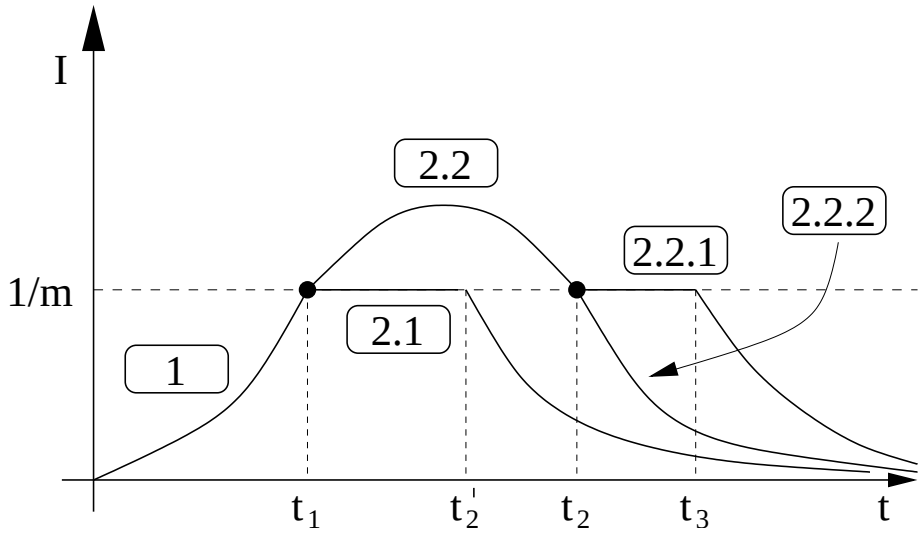

Figure 2.1: Possible temporal evolution of the fraction of infected individuals I. Regions above and below $1/m$ correspond to $x^\star(I) \to 0$ and $x^\star(I) \to 1$, respectively. In the two regions the solutions of system (2.5) approximate those of classical SIR models with basic reproductive numbers $R_0 = R_0^a$ and $R_0 = R_0^n$ respectively.

S2.2 *If $R_0^a S(t_1) > 1$ there exists a finite time $t_2 > t_1$ such that the solutions of system (2.5) approximate those of a classical SIR model with $R_0 = R_0^a$ on the interval (t_1, t_2) and $I(t_2) = 1/m$;*

S2.2.1 *If $R_0^n S(t_2) > 1$ there exists a finite time $t_3 > t_2$ such that the solutions of system (2.5) can be approximated in the time interval (t_2, t_3), where $t_3 = t_2 + \frac{m}{\gamma}(S(t_2) - \frac{1}{R_0^n})$, by $S(t) = S(t_2) - \frac{\gamma}{m}(t - t_2)$ and $I(t) = 1/m$. Afterwards, the solutions of system (2.5) approximate those of a classical SIR model (in its decaying phase) with $R_0 = R_0^n$ on the interval $(t_3, +\infty)$;*

S2.2.2 *If $R_0^n S(t_2) \leq 1$ the solutions of system (2.5) approximate those of a classical SIR model (in its decaying phase) with $R_0 = R_0^n$ on the interval $(t_2, +\infty)$.*

Therefore, under the hypotheses of Prop. 2.3.2, solutions of system (2.5) can be classified in the three following types:

C1 Solution *S1* in $[0, t_1)$ and *S2.1* in $[t_1, +\infty)$;

C2 Solution *S1* in $[0, t_1)$, *S2.2* in $[t_1, t_2)$ and *S2.2.1* in $[t_2, +\infty)$;

C3 Solution *S1* in $[0, t_1)$, *S2.2* in $[t_1, t_2)$ and *S2.2.2* in $[t_2, +\infty)$.

The possible behaviours of the solutions of system (2.5), which depends on the values of R_0^a and R_0^n, are shown in Fig. 2.1.

Let us briefly comment on the hypotheses of Prop. 2.3.2. The condition $R_0^n > 1$ is the obvious threshold condition for an epidemic to occur. $I_p = 1 - \frac{1}{R_0^n} + \frac{1}{R_0^n} \log \frac{1}{R_0^n}$ is the fraction of infected individuals at the peak for the classical SIR model with basic reproductive number $R_0 = R_0^n$ (this can be easily established by considering that the fraction of infected individuals at the peak is $\frac{1}{R_0}$ and by employing the SIR invariant $S(t) + I(t) - \frac{1}{R_0} \log S(t) = \text{const}$). Thus the condition $1/m < I_p$ imposes that behaviour b_a starts being convenient at some point before the epidemic reaches its peak. Basically, if the condition is not satisfied, system (2.5) is of scarce interest since all individuals adopt the normal behaviour b_n during the course of the epidemic; thus, system (2.5) would be equivalent to a classical SIR model with basic reproductive number $R_0 = R_0^n$. No explicit condition is needed on R_0^a. In particular, R_0^a can be less than 1 (which means that no epidemic will occur if the susceptible pool is fully composed by individuals adopting the altered behaviour b_a). Clearly, in this case the solutions of system (2.5) can only be of type *C1*.

Full proof of Prop. 2.3.2 is given in App 8.1.1. Here we only observe that when $I(t) < 1/m$ we have $x^\star(I) \to 1$ (see Prop. 2.3.1). Thus, the solutions of the degenerate system (2.8), obtained by solving the system of differential equations after having substituted $x(t) = 1$, are those of a classical SIR model with basic reproductive number $R_0 = R_0^n$. The same happens when $I(t) > 1/m$, but now $x^\star(I) \to 0$, which results in $R_0 = R_0^a$. Let us now assume that ϵ is close to 0. The time intervals in which $I(t) \approx 1/m$ (for solutions of type *C1* or *C2*) can be interpreted as time intervals in which the fraction of infected individuals $I(t)$ is characterized by a sequence of "micro–waves". In fact, as soon as $I(t) > 1/m$, $x(t)$ gets close to 1, so that the effective reproductive number ($R_0^a S(t_1)$ for solutions of type *C1* and $R_0^a S(t_2)$ for solutions of type *C2*) is not sufficiently large to sustain the epidemic and thus $I(t)$ decreases below $1/m$. However, as soon as $I(t) < 1/m$, $x(t)$ gets close to 1, so that the effective reproductive number ($R_0^n S(t_1)$ for solutions of type *C1* and $R_0^n S(t_2)$ for solutions of type *C2*) is sufficient to sustain the epidemic and thus $I(t)$ increases over $1/m$. The process is repeated as long as the fraction of susceptible individuals in the population is sufficiently large ($R_0^n S(t) > 1$). In the limit $\epsilon \to 0$, these switches are instantaneous, and the solution $I(t)$ is approximately always equal to $1/m$. Finally, as soon as $R_0^n S(t) \leq 1$, the fraction of infected individuals $I(t)$ will start decreasing to 0 over time. In Prop. 2.3.3 we give sufficient conditions for solutions of type *C1* or *C2* to occur, which in particular implies the presence of sequences of "micro–waves" for small value of ϵ.

Proposition 2.3.3. *Under the assumptions* $R_0^n > 1$ *and* $1/m < I_p$, *where* $I_p = 1 - \frac{1}{R_0^n} + \frac{1}{R_0^n} \log \frac{1}{R_0^n}$, *if* $\epsilon \to 0$, $\mu = o(\epsilon^k)$ *with* $k > 1$ *and* R_0^a *satisfies the inequalities* $1 < R_0^a < R_0^n \exp\{-R_0^a(1 - 1/R_0^n)\}$ *then the solution of system* (2.5) *are of type* C1 *or* C2.

First of all, we comment on the hypotheses of Prop. 2.3.3. Clearly, if $R_0^a S(t_1) \leq 1$ the solutions of system (2.5) can only be of type *C1*. Condition $R_0^a S(t_1) > 1$ (which in particular implies $R_0^a > 1$) is thus required for solutions of type *C2* to occur, in particular to have that $I(t)$ is increasing in t_1. Condition $R_0^a < R_0^n \exp\{-R_0^a(1 - 1/R_0^n)\}$ is necessary

to have that the fraction of susceptible individuals does not decrease too much in the time interval (t_1, t_2), where system (2.5) is equivalent to an SIR model with basic reproductive number $R_0 = R_0^a$. In fact, if $S(t)$ decreases so much that $R_0^n S(t_2) < 1$, $I(t)$ will decrease again for $t > t_2$, resulting in a solution of type *C3*. Full proof of Prop. 2.3.3 is given in App. 8.1.1.

Prop. 2.3.3 guarantees that, under certain conditions, one (or more) epidemic waves will occur after the first when $\epsilon > 0$ is sufficiently small; here, a solution showing two (or more) epidemic waves is one for which $\dot{I}(t) > 0$ in two time intervals separated by one interval in which $\dot{I}(t) < 0$. A concrete example is shown in Fig. 2.2a. In this case, a sequence of small epidemic waves is observed for $t > t_2$. In fact, as soon as the fraction of infected individuals becomes larger than the threshold $1/m$, the dynamics is the same as that of an SIR model with $R_0 = R_0^a$ for which there are not enough susceptible individuals to sustain the epidemic. Thus, the fraction of infected individuals decreases below the threshold value (see the inset in Fig. 2.2a). A series of waves therefore follows, as long as $R_0^n S(t) > 1$. Fig. 2.2b shows that, as stated in Prop. 2.3.2, $S(t)$ decreases linearly while $I(t)$ undergoes this sequence of waves.

Convergence of the solutions of the singularly perturbed system (2.5) to those of the degenerate system (Eq. 2.8, $\epsilon = 0$) for $\epsilon \to 0$ is shown in Fig. 2.2c-d.

If we consider greater values of the parameter ϵ (about which proposition 2.3.3 does not say anything), the fraction of infected individuals reaches a higher peak, and thus the fraction of susceptible individuals decreases in the time interval (t_1, t_2) more than that of a SIR model with $R_0 = R_0^a$. However, if R_0^a is not too large, the fraction of susceptible individuals at time $t = t_2$ can be sufficient to generate at least a second epidemic wave (see Fig. 2.3a), that is now quite relevant in size.

As observed previously, if R_0^a is not sufficiently small (as required by Prop. 2.3.3) the fraction of susceptible individuals in the time interval (t_1, t_2) may decrease so much that $R_0^n S(t_2) < 1$. In this case, no additional waves will be generated and only a change in the slope during the decaying phase may be observed (see Fig. 2.3b).

One may ask how large ϵ can be to give rise to a second epidemic wave of the type shown in Fig. 2.3a. Fig. 2.4a shows a numerical approximation to the minimum value, ϵ_{min}^{-1}, of $1/\epsilon$ giving rise to sequences of at least two epidemic waves, as a function of the threshold parameter m. In this respect, it should be observed that computing, given m, the value of ϵ at which multiple waves start to occur is essentially equivalent to the problem of locating the zero (if it exists) of a one-variable monotonic function, within a suitable interval. It can be observed that ϵ_{min}^{-1} decreases with m and $\epsilon_{min}^{-1} \searrow 0$ as $m \to +\infty$. Moreover, m has to be larger than the theoretical minimum $m = 1/I_p$ (shown as the dotted vertical line in Fig. 2.4a) in the assumptions of Prop. 2.3.2; indeed ϵ_{min}^{-1} goes to ∞ (i.e. ϵ_{max} goes to 0) as $m \to 1/I_p$.

The following Proposition shows that, independently of ϵ, the fraction of susceptible individuals at the end of an epidemic described by an SIR model with $R_0 = R_0^n$ is always smaller than that obtained with model (2.5):

Proposition 2.3.4. *$S_\infty > S_\infty^{SIR}$, where S_∞^{SIR} is the fraction of susceptible individuals at the end of an epidemic described by a classical SIR model with transmission rate β_n and*

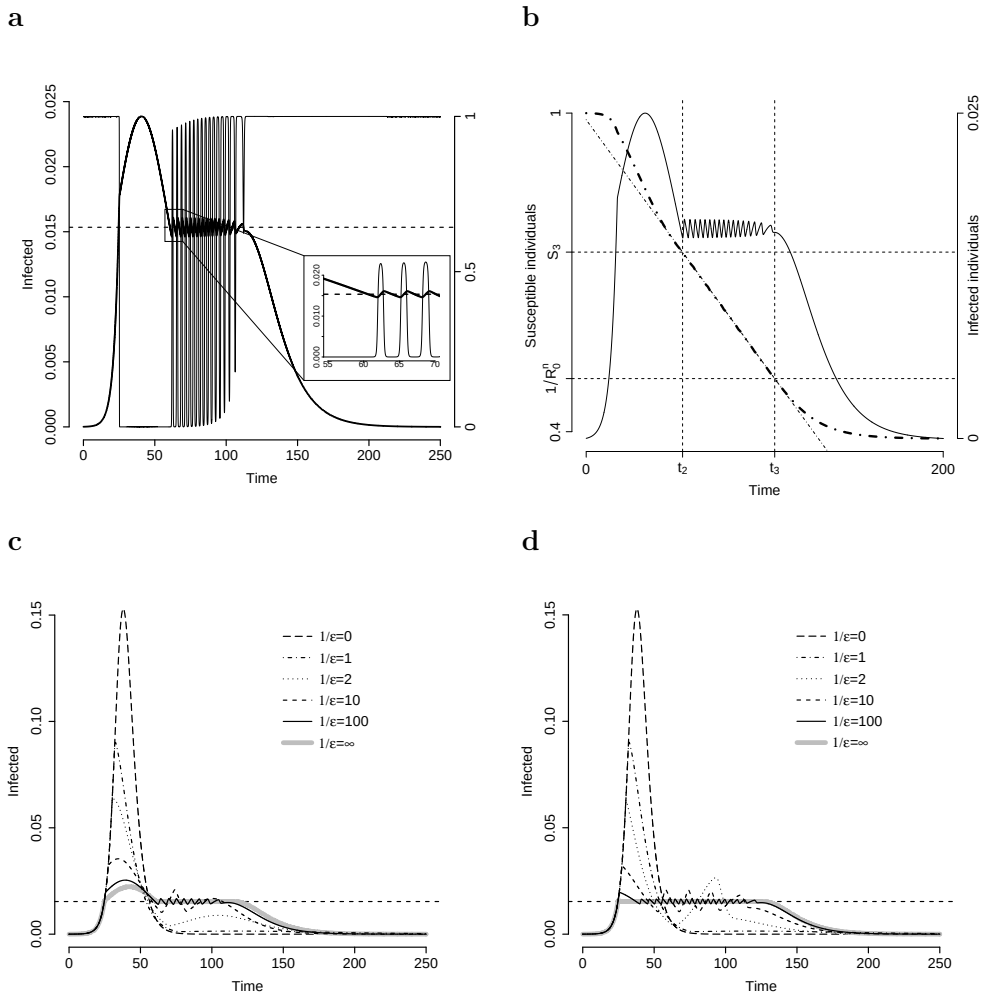

Figure 2.2: **a** Fraction of infected individuals (solid bold line, scale on the left) and fraction of individuals playing strategy b_n (solid tiny line, scale on the right) over time for system (2.5). Parameters employed: $\beta_n = 0.6$, $\gamma = 0.3$, $\beta_a = 0.35$, $\epsilon = 3.33 \cdot 10^{-3}$, $m = 65$, $\mu = 10^{-7}$. The dashed line represents the threshold value $1/m$. **b** Fraction of infected individuals (solid line, scale on the right) and susceptible individuals (bold dot-dashed line, scale on the left) in the same example as in panel **a**. We also plot the straight line $S(t) = S(t_1) - \frac{\gamma}{m}(t - t_1)$ (tiny dot-dashed line, scale on the left)to show the linearity of $S(t)$ in $[t_2, t_3]$ as predicted by Prop. 2.3.2. **c** Fraction of infected individuals vs. time for different choices of the parameter ϵ (thin black lines) and the piecewise solution of system (2.5) (heavy gray line) as in Fig. 2.1; other parameters as in panel **a**. **d** Like panel **c** but with $\beta_a = 0.3$; this implies $R_0^a S(t_1) < 1$ so that the solution is of type C1.

S_∞ is the fraction of susceptible individuals at the end of an epidemic described by system (2.5).

Finally, for $\epsilon \approx 0$, the dependence of S_∞ from m is clarified by the following:

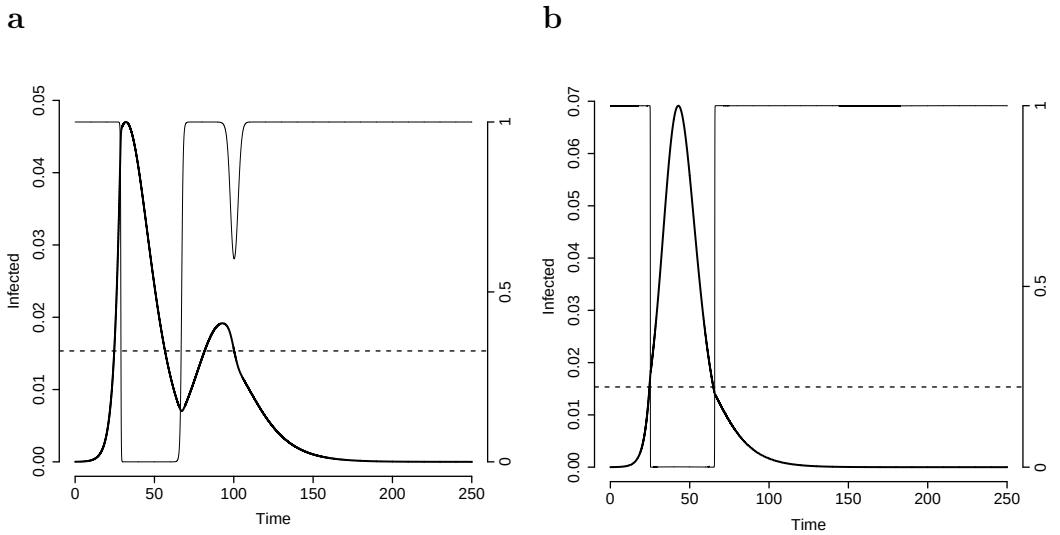

Figure 2.3: Other possible behaviour of solutions of system (2.5). **a** As in Fig. 2.2a but with $\epsilon = 0.25$. **b** As in Fig. 2.2a, but with $\beta_a = 0.45$.

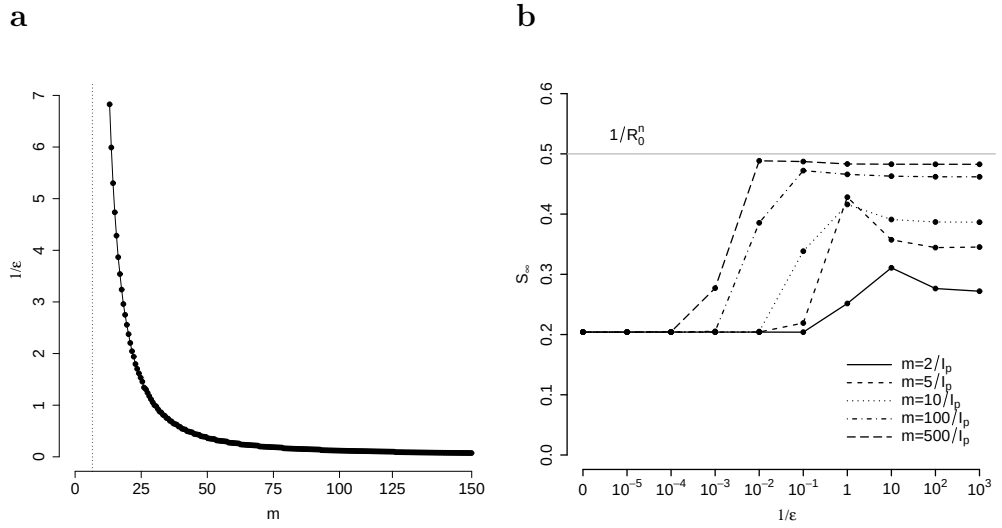

Figure 2.4: **a** The minimum values of $1/\epsilon$ giving rise to a sequence of at least two epidemic waves are plotted against m, for system (2.5). Parameters employed: $\beta_n = 0.6$, $\gamma = 0.3$, $\beta_a = 0.33$, $\mu = 10^{-7}$. The vertical dotted line represents the value of m such that $m = 1/I_p$. Notice that for such choice of parameters, the conditions of Prop. 2.3.3 are satisfied, which implies that epidemic waves will occur for $\epsilon \to 0$. Notice how multiple waves can occur even for "slow" changes in behaviour (large ϵ values). **b** S_∞ as a function of $1/\epsilon$ for different choices of m for system (2.5). Parameters employed: $\beta_n = 0.6$, $\gamma = 0.3$, $\beta_a = 0.35$, $\mu = 10^{-7}$.

Proposition 2.3.5. *Under the assumptions $R_0^n > 1$ and $1/m < I_p$, where $I_p = 1 - \frac{1}{R_0^n} + \frac{1}{R_0^n} \log \frac{1}{R_0^n}$, in the limit $\epsilon \to 0$, $\mu = o(\epsilon^k)$ with $k \geq 1$, if R_0^a satisfies the inequalities*

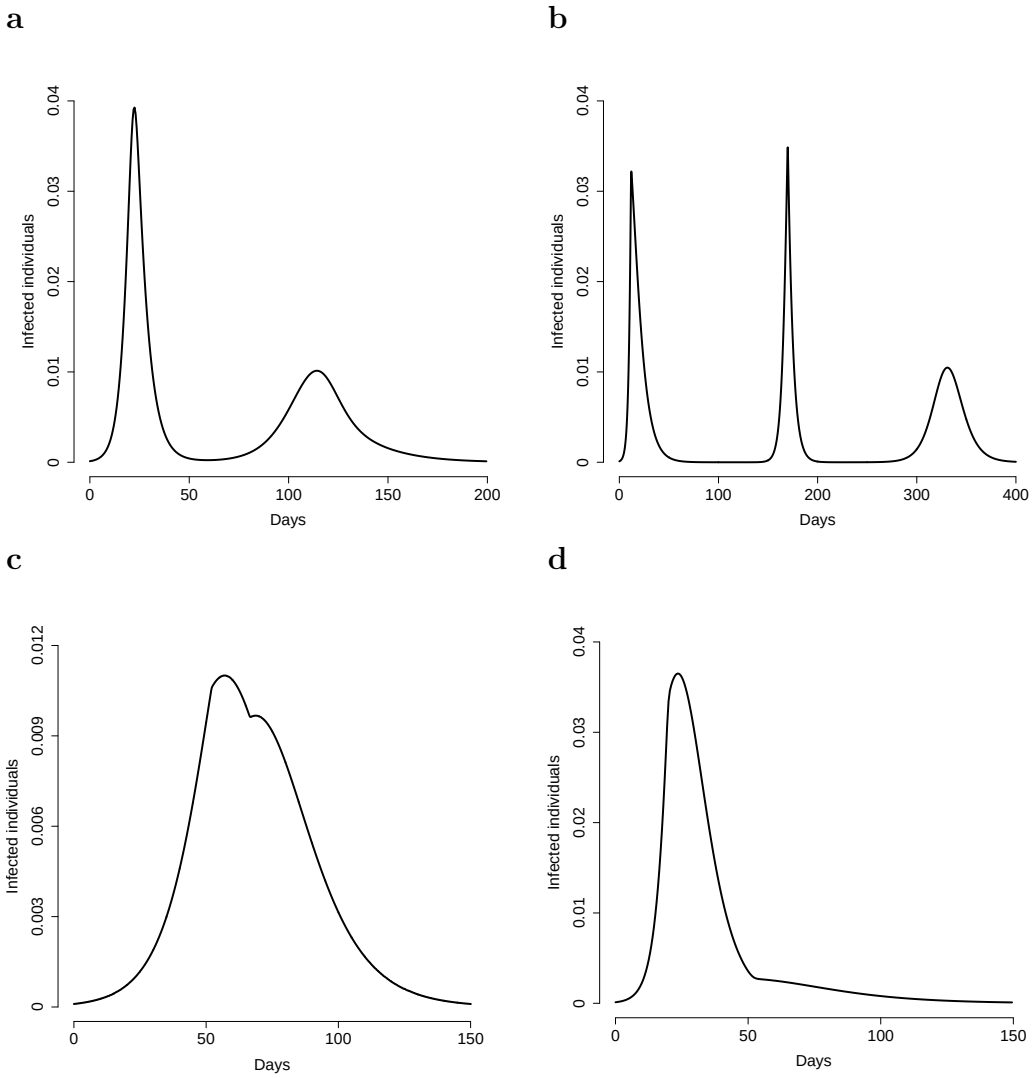

Figure 2.5: The model (2.5) accounts for interesting epidemic patterns: **a** Parameters employed: $m = 150$, $\beta_n = 0.8$, $\beta_a = 0.4$, $\gamma = 0.5$, $\mu = 0.01$, $\epsilon = 10$. **b** Parameters employed: $m = 300$, $\beta_n = 1$, $\beta_a = 0.48$, $\gamma = 0.5$, $\mu = 10^{-10}$, $\epsilon = 2$. **c** Parameters employed: $m = 100$, $\beta_n = 0.6$, $\beta_a = 0.54$, $\gamma = 0.5$, $\mu = 10^{-5}$, $\epsilon = 0.01$. **d** Parameters employed: $m = 100$, $\beta_n = 0.8$, $\beta_a = 0.6$, $\gamma = 0.5$, $\mu = 10^{-5}$, $\epsilon = 1$.

$1 < R_0^a < R_0^n \exp\{-R_0^a(1-1/R_0^n)\}$ *then the fraction of susceptible individuals at the end of the epidemic* ($S_\infty(m)$) *is an increasing function of* m *and* $S_\infty(m) \to 1/R_0^n$ *when* $1/m \to 0$.

Proofs of Prop. 2.3.4 and 2.3.5 are in appendix 8.1.1. In Fig. 2.4b the values of S_∞ are reported for increasing values of $1/\epsilon$ and for different choices of m. We can see that S_∞ is non monotonic in neither $1/\epsilon$ nor in m. However, when $1/\epsilon$ is sufficiently large, S_∞ increases by decreasing $1/m$ and $S_\infty \to 1/R_0^n$ when $1/m \to 0$. For small values of $1/\epsilon$, S_∞ is equivalent to that obtained by employing a classical SIR model with $R_0 = R_0^n$.

We conclude the analysis of the proposed model by showing that, with suitable choices

of parameters, its solutions can exhibit some interesting patterns (unaccessible to any classical SIR model), that are morphologically compatible with the evolution of past pandemics. For example, two epidemic waves can be obtained (see Fig. 2.5a) in the same epidemic episode. However, more than two epidemic waves can be obtained (as it was in fact observed in the 1918-19 Spanish pandemic). Moreover, the peak daily attack rate of the sequence of waves is not necessarily decreasing over time (see Fig. 2.5b). Difference in slope in the decaying phase (reminiscent of those observed in the Fall wave of the 1918-19 Spanish pandemic in the UK) can also be captured by our model (see Fig. 2.5c and [33] for a brief discussion). Finally, very long decaying phases, making the epidemic curve strongly asymmetric, can also be obtained (see Fig. 2.5d).

2.4 Discussion

When studying the spread of epidemics, behaviour and contact patterns are typically considered "background" for the infection – i.e., they are not themselves variables of the dynamics. It is interesting, however, to address cases for which the population behaviour cannot be merely considered as an independent (though time-varying) parameter, but it is better modelled as a variable whose evolution influences, and is influenced by, the dynamics of the infection.

With the introduction of an explicit model for behavioural changes, infection and behaviour both contribute to define the context for the other. Symmetry between these two key-factors is therefore restored, and no *by-principle* prevalence is given (even formally) to one over the other. Not only the dynamics of infection depends now on both the transmission and behaviour, but also the behaviour dynamics depends on behaviour (and infection as well). This is what makes evolutionary game theory especially suited to the case as compared to classical game theory. In fact, application of the latter would result in (rational) instantaneous best responses to the infection dynamics, regardless of the current distribution of behavioural strategies.

The model we propose is (deliberately) simple, and exhibits a transmission dynamics driven by an $S \to I \to R$ scheme coupled with behavioural (contact) patterns driven by imitation dynamics. Still, we were able to prove that the model accounts for multiple waves occurring within the same outbreak, and is able to explain "asymmetric waves", i.e., infection waves whose rising and decaying phases differ in slope. As an interesting feature, the attack rate for the model is always smaller than that of the equivalent SIR model (obtained by fixing $x(t) = 1$).

It should be observed that the model is based on two implicit, yet crucial assumptions: a) that the benefits of behavioral changes be immediately clear to the individuals; b) that individuals be able to recognize whether their contacts are susceptible, infective or removed (since susceptible individuals can change their behaviour only through encounters with other susceptible individuals). Consequently, our model applies better to severe epidemics, in which it is more likely that these requirements are actually met.

Coming to discuss possible variants and extensions, a first remark concerns the dy-

namics of behavioural changes that we have adopted. In particular, the payoffs of the underlying game are modelled as the *perceived* risk of infection. Our choice was for a simple linear dependence from the fraction of currently infected individuals. Of course, a number of different options are available; for example one may tie the perception of risk to the number of new infections, or consider the actual probability of infection in place of perceived risk. Cumulation of risk over time could also be addressed by introducing appropriate memory mechanisms.

Independently of how the risk is specifically reckoned, the access to information pertaining the relative efficacy of behaviours may also be collected across more structured networks (e.g., the media). In this respect, considering different time units adds some flexibility to the model, in that it allows for different speeds in the diffusion of infection and behaviour. For example, tuning of key parameter ϵ may be obtained on the basis of empirical evidence.

At first sight, introduction of irrational behaviour may appear unnecessary, and contrasting with the model simplicity we tried to keep throughout. Yet, by avoiding extinction of allowed behaviours, irrational behaviour overtakes an unrealistic (and undesirable) effect of strict imitation: the pool of strategies from which an individual can choose is limited to those effectively represented in the population. By allowing exploration of *all possible* behaviours, irrational behaviours may account for erroneous decisions or idiosyncratic attitudes always present in human societies.

The focus of this work is to investigate the effects that behavioural change as a protective response to the state of infection has on the spread of a (severe) epidemic. That's why the behavioural change modelled here affects only susceptible individuals (infected individuals may of course change behaviour as an effect of their status, regardless of the state of epidemic). As a side remark, notice that quarantine or isolation of infected individuals can already be described by our model since they can be modelled as a reduction of the transmission parameters.

A wider class of models can also be considered. The model of behavioural changes can in fact be extended to infected individuals subdivided in symptomatic and asymptomatic, for example treating the infected asymptomatics as susceptibles for anything concerning the behavioural dynamics. A specific class for latent individuals could also be introduced, thereby delaying the epidemic spread and affecting behavioural changes. In general, considering more than two behavioural classes would provide greater flexibility and realism, while of course opening to technical problems of increased complexity.

The class of models introduced in this paper may contribute to elucidate phenomena for which a behavioural basis is apparent, as in reaction to alerts [157], or hypothesized, as for superspreading events [102]. In fact, empirical estimation of epidemic parameters (as, for example, the basic reproduction number) or the comparison between intervention strategies have to be carefully reconsidered whenever an underlying behavioural dynamics is suspected. Finally, a better understanding of the distinction between spontaneous and induced changes of behaviour is key for the implementation of more realistic and effective social distancing measures.

Chapter 3

Effectiveness of spontaneous social distancing and risk perception

3.1 Introduction

Among the many factors known to influence the spread of epidemics across human populations, a central role is played by the heterogeneity in human behaviors and contact patterns [156, 103, 57, 151, 3, 76, 11, 112]. Human spontaneous behavioral response to the risk of infection is largely suspected to play a crucial role as well [71, 132, 56, 21, 52]. In fact, it is expected that, during an epidemic outbreak, individuals change their behavior in order to reduce the risk of infection, especially if serious consequences are involved. As mathematical modeling has increasingly become a powerful tool for decision making, knowing in advance how to account for spontaneous behavioral changes would greatly improve the predictive power of epidemic transmission models and the evaluation of the effectiveness of control strategies. Actually, the impact of risk perception on the spontaneous behavioral response, and in turn on the epidemic spread, is largely acknowledged and several models have been proposed in order to investigate such phenomenon [42, 147, 53, 93, 67, 66, 9, 137, 138, 127, 90, 130, 68]. Nonetheless, most models in literature either assume a priori human response to the infection or consider only the behavioral response as driven by the diffusion of fear, which is modeled as a parallel infection [42, 147, 53, 93, 67, 66]. Evolutionary game theory represents a rich and natural framework for modeling human behavior[153, 158, 81]. Both traditional and evolutionary game theory have recently been employed to investigate individuals' choices in voluntary vaccination programs resulting in interesting and non trivial insights [17, 15, 109, 124], promoting this approach as very promising.

The aim of this study is to propose the evolutionary game theory framework to model explicitly the infection dynamics as a complex interplay between the disease transmission process and spontaneous human defensive response. The dynamics of an epidemic outbreak is modeled by an SIR transmission scheme, where the force of infection depends on the behavioral patterns of individuals involved. Behavior of individuals is assumed to change over time in response to the perceived risk of infection [9, 127], based on the

perceived prevalence [52]. Specifically, at any time, each individual can choose to adopt or not a self-protection strategy, altering contact patterns and usual habits, in order to reduce the risk of infection. A recent work [127] has investigated the simple case in which only choices of susceptible individuals are modeled. Here, an extension of this work, which includes the investigation of behavioral response performed by infected individuals, is presented.

Two possible responses are considered. The first one accounts for changes in contact patterns involving individuals that suffers symptoms, as a consequence of their sickness (workplaces and school attendance can drastically reduced during a serious infection outbreak [119, 152]). Such defensive response depends on the severity of symptoms and appears regardless of the current state of the epidemic in the population, the behavior of other individuals and the current risk of infection. Hence, we assume that symptomatic infected individuals perform the same defensive response. This assumption results in considering a different transmission rate for symptomatic individuals, which can take into account also a possible increased infectivity of symptomatic infections. The second behavioral response considered, accounts for a spontaneous defensive self-protection in response to the perceived risk of infection. In particular, individuals are supposed to be able to reduce their susceptibility. Such defensive response takes into account both reduction in physical contacts – e.g. through the avoidance of crowded environments or by limiting travels [98, 59] – and, more in general, all self-prophylaxis measures which can reduce the transmission probability during these contacts – e.g. achievable by increasing wariness in usual activities, as recommended by WHO during 2009 pandemic influenza [161], or by using face masks, as during the 2003 SARS outbreak [98]. Actually, only susceptible individuals are exposed to the risk of infection. On the other hand, in principle, asymptomatic infective individuals, and recovered individuals that have not experienced symptoms, have no reason to behave differently from susceptibles. Self-protective behavior eventually adopted by asymptomatic infective individuals results in a reduction of the force of infection. On the contrary, neither symptomatic infective individuals, nor recovered individuals that have already experienced the symptoms of the infection can achieve any benefit through a reduction of the risk of infection. Therefore, they are not considered in such mechanism of self–protection.

This manuscript investigates the impact of the behavioral response on the spread of an epidemic and clarifies the role of key parameters regulating such mechanism, in order to capture essential patterns of the interplay between the risk perception and the transmission process.

3.2 The model

The disease transmission process is based on a simple SIR model where individuals may adopt two mutually exclusive behaviors, *normal* and *altered*, on the basis of the perceived risk of infection. Individuals adopting the altered behavior are supposed to be able to reduce the force of infection.

Cast in the language of evolutionary game theory, the dynamics of self-protection can be modeled as a suitable dynamic game, where behaviors adopted by individuals correspond to strategies with certain expected payoffs. The altered behavior gives the individuals an advantage of reducing the risk of infection, but it is more costly (in absence of infection the normal behavior is more convenient). The diffusion of the strategies in the population is modeled as an imitation process [158, 81, 15, 127]: individuals change strategy as they become aware, through encounters with other individuals, that their payoff can increase by adopting another behavior. Which behavior is more convenient to adopt clearly depends on the state of the epidemic. The balance of the payoff between the two possible strategies is determined by the perceived risk of infection, which depends on the cost associated to the risk of infection and on the perceived prevalence in the population, which is considered as a measure of such risk. The perceived prevalence is modeled by assuming an exponential fading memory mechanism (such in [48]), taking into account the number of infections occurred over a certain (past) period of time.

Let denote with S, I_S, I_A, R_S, R_A the fraction of susceptible, symptomatic and asymptomatic infective individuals and recovered individuals that has experienced symptoms or not respectively. By introducing the variables x, describing the fraction of individuals adopting the normal behavior, and M, describing the perceived prevalence of infection in the population, the system of ordinary differential equations regulating the above described process can be written as follows:

$$
\left\{
\begin{array}{lcl}
\dot{S} & = & -\lambda[x + q(1-x)]S \\
\dot{I}_S & = & p\lambda[x + q(1-x)]S - \gamma I_S \\
\dot{I}_A & = & (1-p)\lambda[x + q(1-x)]S - \gamma I_A \\
\dot{R}_S & = & \gamma I_S \\
\dot{R}_A & = & \gamma I_A \\
\dot{M} & = & -p\dot{S} - \nu M \\
\dot{x} & = & x(1-x)\frac{pS}{(1-R_S-I_S)}\lambda(q-1) \\
 & + & \rho[x(1-x)(1-I_S-R_S)(1-mM) + \mu(1-2x)]
\end{array}
\right. \tag{3.1}
$$

where p denotes the probability of developing symptoms, $1/\gamma$ is the average length of the infectivity period (corresponding here to the generation time), ν weighs the decay of the perceived prevalence M (which is based on symptomatic cases), $0 \leq q \leq 1$ represents the reduction of contagious contact rate induced by the altered behavior; finally, λ is the force of infection, which is modeled as follows:

$$
\lambda = \beta_S I_S + \beta_A I_A x + q\beta_A I_A(1-x) \tag{3.2}
$$

where β_S and β_A are the transmission rate for symptomatic and asymptomatic infectives respectively. The force of infection λ is the result of three contribution: first, the transmission associated to symptomatic infected individuals ($\beta_S I_S$); second, the transmission associated to asymptomatic infected adopting the normal behavior ($\beta_S I_S x$); third, the transmission associated to asymptomatic infected adopting the altered behavior ($q\beta_S I_S(1-x)$).

Moreover, the susceptibility of individuals is reduced by q for those susceptibles that adopt the altered behavior, i.e. a fraction $1-x$ of susceptible individuals (see first eq. of system (3.1)).

The first term of the equation for x (i.e., $x(1-x)\frac{pS}{(1-R_S-I_S)}\lambda(q-1)$) represents a natural selection, embedded into the transmission process, that favors individuals reducing the risk of infection. The second one (i.e., $\rho[x(1-x)(1-I_S-R_S)(1-mM)+\mu(1-2x)]$) accounts for spontaneous changes in individual behaviors. Specifically, $x(1-x)(1-I_S-R_S)$ is the fraction of useful encounter for having a switch of strategy by imitation; $1-mM$ represent the balance between the payoff associated with the two possible behavior; m defines a threshold determining which behavior would represent the most convenient choice; the term $\mu(1-2x)$ represents the possibility that individuals, rarely (at a rate $\mu << 1$), change strategy independently by the payoff values, by performing an irrational exploration of strategies [81, 127, 149]; ρ is the imitation rate and essentially represents the speed of the behavioral dynamics with respect to the disease transmission dynamics. In fact, in general, as imitation is based on the diffusion of information rather than on physical contacts between individuals, the speed of behavioral changes may be different from that of the disease transmission.

For large values of ρ (and small values of μ) the sign of $\dot{x}$ essentially depends on the balance of payoff between the two possible behavior $(1-mM)$. When the perceived prevalence M is over $1/m$ (hereafter referred to as *prevalence threshold* or *risk threshold*), the altered behavior is perceived as the most convenient, and thus x decreases. It is worth of noticing that in the special case of $\nu = \gamma$, the perceived prevalence is exactly the prevalence of symptomatic infection in the population ($M = I_S$).

3.3 Reproductive number and model parametrization

The basic reproductive number R_0, which is essentially the average number of secondary infections that results from a single infectious individual in a fully susceptible population [6], can be computed by using next generation technique [44]. In this case, the resulting basic reproductive number is

$$R_0 = (1-p)\frac{\beta_A}{\gamma}[x+q(1-x)]^2 + p\frac{\beta_S}{\gamma}[x+q(1-x)] \tag{3.3}$$

which can be interpreted as a combination of two basic reproductive numbers:

$$R_0^n = (1-p)\frac{\beta_A}{\gamma} + p\frac{\beta_S}{\gamma},$$

the reproductive number for a population where all individuals are adopting the normal behavior ($x = 1$) and

$$R_0^a = q^2(1-p)\frac{\beta_A}{\gamma} + qp\frac{\beta_S}{\gamma},$$

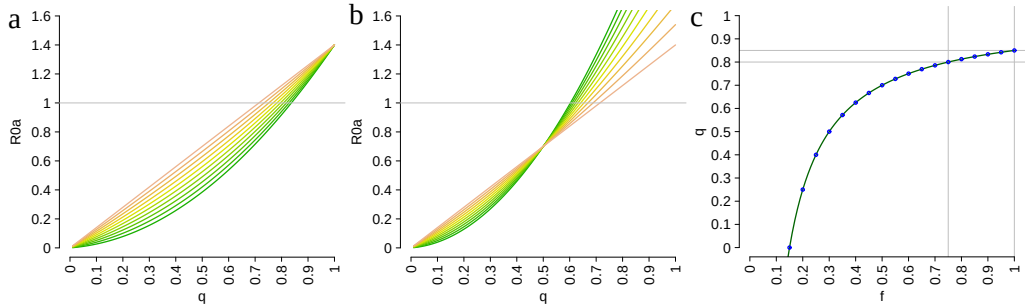

Figure 3.1: **a** R_0^a as a function of q where $\beta_S = \beta_A = 0.5$. Colors from green to orange correspond to different values of p ranging from 0 to 1. **b** As in **a** but for $\beta_S = 2\beta_A$, where $\beta_A = 0.5$. **c** $\tilde{q} = (q + f - 1)/f$ where f is the fraction of individuals able to reduce their contacts, obtained by keeping R_0^a constant. For instance, the figure shows that a reduction of $q = 0.85$ in contacts performed by all individuals has the same effect on R_0^a that a reduction of $q = 0.8$ performed only by 75% of individuals.

the reproductive number for a population where all individuals are adopting the altered behavior (i.e. $x = 0$). As $0 \leq q \leq 1$ and $0 \leq p \leq 1$, $R_0^a \leq R_0^n$. The reduction in the number of contagious contacts cumulates when both susceptibles and asymptomatic infective individual are adopting the altered behavior; this leads the term q^2 in R_0^a.

Equation (3.3) highlights that R_0 depends on the fraction of individuals in the population who are adopting either normal or altered behavior. It is easy to check that if $x(0) = 1$ and $\rho = 0$ the system (3.1) reduces to a classical SIR model (with the distinction on symptomatic and asymptomatic individuals) driven by R_0^n; on the contrary, if $x(0) = 0$ and $\rho = 0$ it reduces to a classical SIR model driven by R_0^a. The smaller is q, the smaller R_0^a and the larger the effect of self-protection when individuals are performing the altered behavior. Moreover, if $\beta_S = \beta_A$, i.e. the transmissibility of the disease is assumed equal for both symptomatic and asymptomatic individuals, a larger fraction of asymptomatic infections (small values of p) corresponds to a larger impact of self-protection because of the quadratic form of R_0^a in q (see Fig.3.1a). On the other hand, if $\beta_S > \beta_A$ a larger fraction of asymptomatic infections corresponds to a larger impact of self-protection only for small value of q (see Fig.3.1b).

Two important assumptions characterize this model: **(i)** all individuals are able to perform a self-protection strategy; **(ii)** only two possible behavior are available and is assumed that all individuals adopting the altered behavior perform the same reduction q. Nevertheless, as the payoff are linear and a population of players is considered, such assumptions are analogous to consider a population of individuals that can choose among the infinite set of mixed strategies defined by the linear convex combination of this two pure strategies. Moreover, assumption **(i)** is not constrictive. In fact, assuming that all individuals are reducing contagious contacts by q, is similar to assume that only a fraction $\tilde{x}$ act a reduction of $\tilde{q}$ with $\tilde{q} = (q - \tilde{x})/(1 - \tilde{x})$ or that only a fraction of f of individuals is able to reduce their contacts by acting a reduction of $\tilde{q}$ with $\tilde{q} = (q + f - 1)/f$ (see

Fig.3.1c)[1].

In general, the transmission rate for symptomatic and asymptomatic individuals can be different, as a consequence of a larger infectivity of symptomatic infections or as a consequence of changes in usual habits (e.g. a lower workplaces and school attendance associated with sickness). However, such difference does not vary over the course of the epidemic. In fact, behavioral changes adopted by symptomatic individuals are performed in order to face sickness rather than to reduce the risk of infection and thus they are performed regardless of the perceived risk and the behavior adopted by other individuals. Therefore, in order to investigate the interplay between risk perception and the epidemic diffusion, the specific choice of the value of the transmission rates is not crucial (here we made the simplest assumption $\beta_S = \beta = A$).

In this study the spread of a "generic" influenza-like infection is simulated. Therefor, parameters that merely characterize the disease transmission process are taken from literature. Specifically, the basic reproductive number is assumed 1.4 [63, 118, 74, 165, 4] and the generation time is assumed 2.8 days [74, 165].

On the other hand, estimates of most of parameters introduced for characterizing the human behavioral response are uncertain and a deep investigation would be required to produce reliable estimates. In order to give insights on qualitative dynamics triggered by human self-protection and to assess when and how human response affects the epidemic spread, plausible (expected) ranges for those parameters are explored. The impact of different behavioral response on the epidemic is investigated, varying one-by-one the parameters starting from a *baseline* configuration of parameters and initial conditions (see table Tab.3.1).

3.4 Results

Baseline scenario

In the baseline scenario (parameters as in Tab.3.1) all infections are symptomatic ($p = 1$), the perceived prevalence is exactly the fraction of symptomatic infections I_S ($\gamma = \nu$) and the epidemic is initially perceived as not risky ($M(0) = 0 < 1/m$). The resulting dynamics of the system (3.1) Fig.3.2a and Fig.3.2b. After an initial growth of the epidemic, the perceived prevalence reaches the prevalence threshold $1/m$ and the altered behavior becomes more convenient than the normal one; then, after few days, the altered behavior becomes widely adopted in the population and the epidemic growth rate remarkably decreases. As the prevalence decreases under the threshold, the population starts to adopt again the normal behavior, producing an heavy tail in the infection dynamics.

Two key parameters characterize the timing of the behavioral response: m and ρ.

The first one describes how the perceived prevalence M is weighted in the payoff functions, i.e. in the balance of the cost associated to the risk of infection and the cost of a self-protection strategy. As a matter of fact, $1/m$ defines the threshold for the perceived

[1]It is sufficient to require that $x + q(1 - x) = \tilde{x}f + (1 - f) + \tilde{q}(1 - \tilde{x})f$.

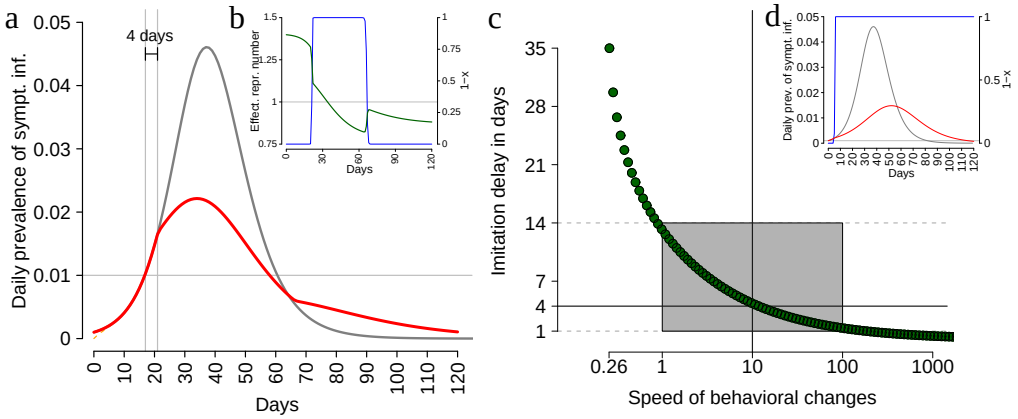

Figure 3.2: **a** Daily prevalence of symptomatic infection in the case of no response by the population, $q = 1$ (bold gray line), and in the baseline scenario, $q = 0.85$ (bold red line). Other parameters as in the baseline scenario reported in Tab.3.1. The horizontal gray line represents the prevalence threshold $1/m$. The behavioral response appears about 4 days after the perceived prevalence $M(t) = I_S(t)$ crosses the threshold $1/m$ producing a lower increase in the prevalence of infection. **b** Baseline scenario: the dynamics of $1 - x$ (blue line, scaled on the left) and the effective reproductive number over time (dark green line, scaled on the right). **c** Imitation delay as a function of ρ. Other parameters as in the baseline scenario. For each value of ρ the imitation delay is computed as the time between when the perceived prevalence crosses the prevalence threshold $1/m$ and when more than 50% of individuals have adopted the altered strategy ($x < 0.5$). The gray region represents a plausible range for the imitation delay. This, in turn, determines plausible values of ρ. For instance, if $\rho = 10$ (as assumed in the baseline scenario) the imitation delay is 4 days, compliant to that observed in **a**. **d** Daily prevalence of symptomatic infection in the case of no response by the population, $q = 1$ (bold gray line), and in the baseline scenario, $q = 0.85$ (bold red line), but for the prevalence threshold $1/m = 10^{-3}$. This example shows that, altrough the altered behaviors is (almost) always the most convenient strategy, human responsiveness takes about 4 days to spread in the population.

prevalence above which individuals reducing contacts have a larger payoff than other ones. The larger is m, the earlier the risk induced by the epidemic is (perceived) sufficiently large to make the altered behavior as the most convenient choice.

On the other hand, ρ represents the speed of the imitation process with respect to the disease transmission time–scale. As a matter of fact, ρ entails the delay (embedded in the imitation dynamics) between the time at which a strategy becomes more convenient and the time at which the majority of population adopt this strategy. For instance, when $1/m < I_s(0)$, the altered behavior is more convenient than the normal one since the beginning of the epidemic. Nonetheless, if $x \neq 0$, the altered behavior takes some time to spread in the population as well (see Fig.3.2d). We define the duration of this transition as the *imitation delay*. We mesure the imitation delay as the time between

when the perceived prevalence crosses the threshold $1/m$, and when more than 50% of the population has changed the strategy. The relation between the imitation delay and ρ is depicted in Fig.3.2c. Our analysis highlights that the larger is ρ, the erlier the most convenient strategy spreads in the population.

It is worth of noticing that if $\rho = 10$ (as assumed in the baseline scenario) the imitation delay is 4 days. This delay is compliant to that observed in the dynamics of the daily prevalence of symptomatic infections in Fig.3.2a. The computation of imitation delay is roboust under different assumptions (e.g., for different values of m), as shown in Fig.3.2d. Moreover, defining a plausible range for the imitation delay allows determining a correspondent plausible range for ρ (gray region in Fig.3.2c).

In sum, the time at which the transition between two possible behaviors occurs is driven by m, while the duration of this transition is driven by ρ. Therefore, m and ρ are the main parameters determining the *responsiveness* of the population to an epidemic outbreak.

Effectiveness of human self-protection

The effectiveness of human self-protection is analyzed in term of: **i)** final epidemic size (here defined as the total number of infection at the end of the epidemic); **ii)** daily peak prevalence; **iii)** peak day.

As mentioned above, a major responsiveness of the population to an infection corresponds to a small prevalence threshold (large values of m) and to a low imitation delay (large values of ρ). As the responsiveness of population increases, a larger reduction in the final epidemic size and in the daily peak prevalence is observed (see Fig.3.3a and Fig.3.3b). The responsiveness of the population is related to when the behavioral response becomes effective. In fact, if the prevalence threshold or the imitation delay are too large the human response never takes places and the epidemic spreads following the dynamics of an SIR model driven by R_0^n. If an epidemic is not perceived sufficiently severe to trigger a behavioral response[2], this corresponds to an unreachable level of the prevalence threshold.

The size of reduction in contagious contacts associated to the altered behavior (q) has a strong impact on epidemic dynamics. As q decreases, a larger protection by the infection is performed by individuals adopting the altered behavior. This leads a decrease in both the final epidemic size and the daily peak prevalence of the epidemic (see Fig.3.3c). The peak day is remarkably anticipated as q increases; however the burden for health care centers at the epidemic peak decreases (see daily prevalence dynamics over time in Fig.3.3c). Moreover, Fig.3.3c shows that, as ρ becomes large, for small value of q the daily peak prevalence corresponds to the threshold value $1/m$.

Three interesting aspects raise from our analysis: **(i)** a large reduction in the number of contagious contacts is not necessary to affect the epidemic dynamics; in particular, a small behavioral response performed by the population can remarkably alter the spread of

[2]From a mathematical point of view, this happens when $1/m$ is larger than $I^p = 1 - \frac{1}{R_0^n} + \frac{1}{R_0^n} \log \frac{1}{R_0^n}$, i.e. the largest possible daily peak prevalence, obtained when all individuals adopt the normal behavior for the whole course of the epidemic.

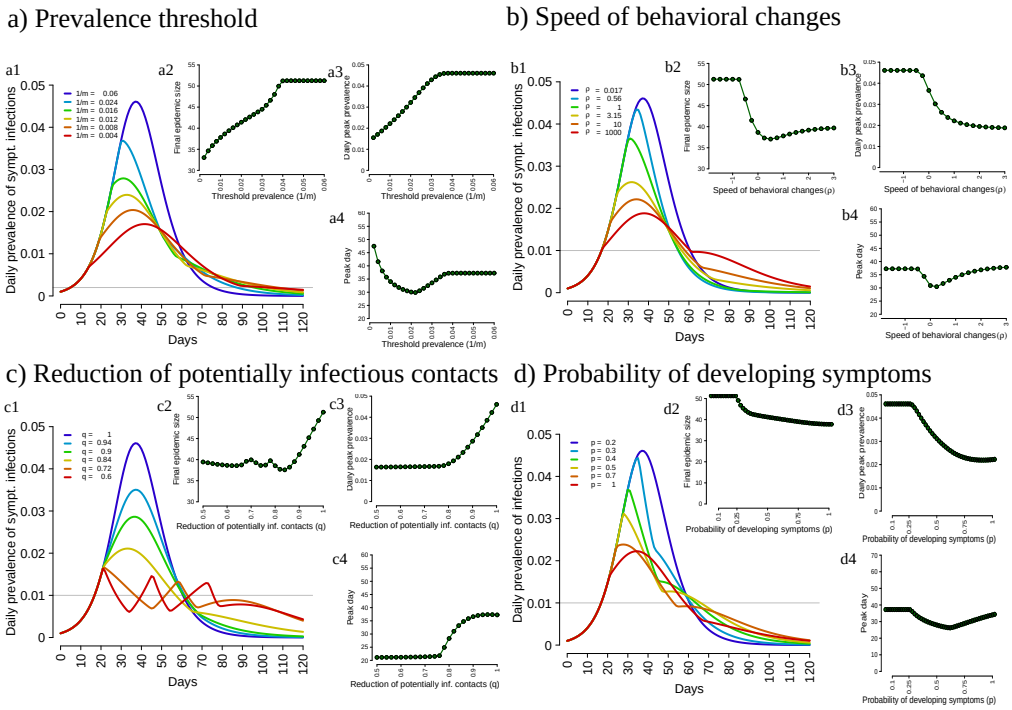

Figure 3.3: **a** Daily prevalencee of symptomatic infections (*a1*), final epidemic size (*a2*), daily peak prevalence of symptomatic infections (*a3*) and peak day (*a4*) as obtained for different values of the prevalence threshold $1/m$. Other parameters as in the baseline scenario (see Tab.3.1). **b** As **a** but for different values of the speed of behavioral changes ρ. **c** As **a** but for different values of the reduction in potentially infectious contacts q. **d** As **a** but for different values of the probability of developing symptoms p.

the epidemic; **(ii)** it exists a threshold for q, such that a further increase in the reduction q does not determine a larger impact of behavioral changes on the final epidemic size, the daily peak prevalence and the peak day; **(iii)** for small values of q multiple epidemic waves can occur. Indeed, a reduction of 100% in the number of potentially infectious contacts (corresponding to $q = 0$, i.e. assuming total isolation) results in a similar final epidemic size, daily peak prevalence and peak day to that observed by considering a reduction of 25% ($q = 0.75$). On the other hand, large values of q can trigger multiple epidemic waves. The conditions for observing multiple epidemic waves has been already discussed in [53, 127]. Briefly, the chance of observing multiple epidemic waves increase as the human responsiveness to the epidemic increases, i.e. for large values of ρ or m.

When considering the possibility of asymptomatic infections ($p < 1$, but still assuming $\beta_S = \beta_A$), asymptomatic infectives can adopt the altered behavior as well. Since they are not aware of their infection, they have no reason to behave differently from susceptibles. As the fraction of asymptomatic infections increases (i.e. as p decreases), the fraction of individuals adopting a self-protection strategy increases as well. On the other hand, a larger symptomaticity produces a larger number of observable infections and, in turn, a

larger perceived prevalence and risk. Numerical simulations show that, in this tradeoff, the latter phenomenon prevails against the former. Indeed, spontaneous behavioral changes have a larger impact on epidemic dynamics when the probability of developing symptoms is large (see Fig.3.3d).

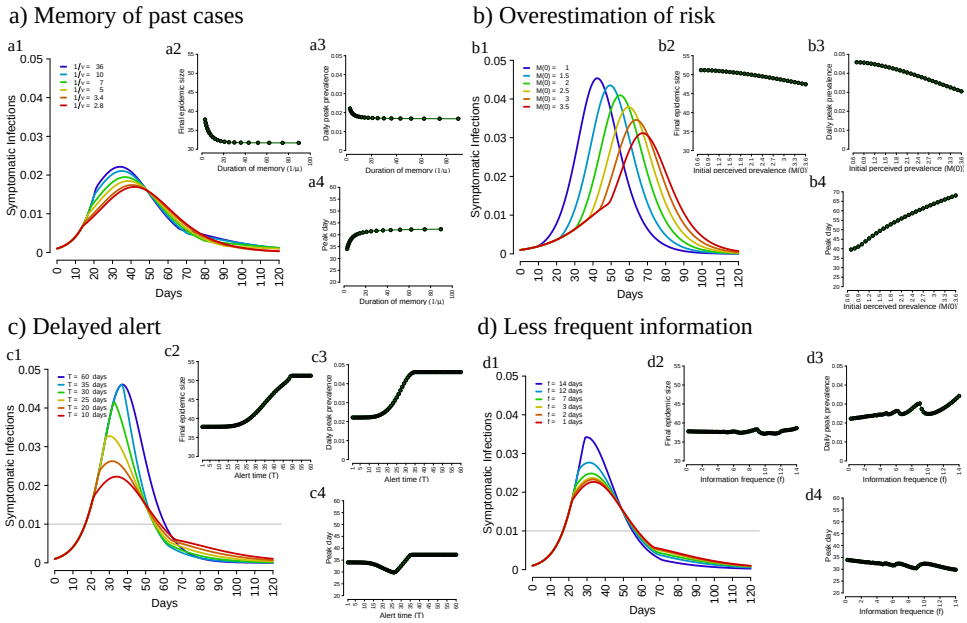

Figure 3.4: **a** Daily prevalencee of symptomatic infections (*a1*), final epidemic size (*a2*), daily peak prevalence of symptomatic infections (*a3*) and peak day (*a4*) as obtained for different values of the average memory length $1/\nu$. Other parameters as in the baseline scenario (see Tab.3.1). **b** As **a** but for different values of $M(0)$, assuming $1/\nu = 30$ and $m = 1$. **c** As **a** but for different values of the alarm times T. **d** As **a** but for different frequencies of information update: the perceived risk is updated every f days.

Risk perception and information diffusion

Different assumptions on the risk perception, the information diffusion and, more in general, the effect of the misperception of the risk of infection are analyzed. Up to now, we have assumed that the perceived prevalence M at time t is exactly the symptomatic prevalence I_S at time t (i.e. $\nu = \gamma$). Several alternative assumptions can be considered.

First of all, to determine which behavior is the most convenient to adopt, individuals can take into account infections occurred over a certain (past) period of time. This case corresponds to assume $1/\nu$ larger than $1/\gamma$. As a matter of fact, assuming $1/\nu > 1/\gamma$ results in a larger perceived risk of infection associated to every single new infection. Therefore, it is not surprising that a longer memory duration results in a larger diffusion of the altered behavior, which results in decreasing the daily peak prevalence and the final epidemic size and in delaying the epidemic peak (see Fig.3.4a).

The role of memory becomes more relevant when the population overestimates the risk of infection during the early phases of the epidemic. For instance, such kind of overestimation may happen as a consequence of the concern raised after a mass media campaign (as could have happened during 2009 H1N1 pandemic [90, 136]). An initial overestimation of the risk of infection can result an initial perceived risk above the threshold, even when the threshold is too large for supporting the altered behavior as the most convenient one. In fact, if the number of new cases produced by the epidemic is not sufficient to support the altered behavior as more convenient, the effect of misperception can vanish. On the other hand, when the initial misperception of prevalence is supported by a long lasting memory the altered behavior can result as the most convenient one for a relevant period of time. This essentially results in an initial reduced growth rate of the epidemic, which delays the epidemic (see Fig.3.4b). Moreover, if the initial overestimation of risk is supported for a sufficiently large period of time, both the daily peak prevalence and the final epidemic size decrease as well.

The misperception of risk can also occur when the population becomes aware of a new epidemic outbreak after a certain period of time, since the emergence of the epidemic. This phenomenon can be investigated by assuming that the perceived prevalence is initially equal to zero for a period of time T. Numerical simulation show that the larger is the delay T, the lower the effectiveness of human response becomes. In particular, the daily peak prevalence and the final epidemic size increase as T increases (see Fig.3.4c) and, if the alert takes place late in the course of the epidemic no relevant effects on the outbreak can be detected (see Fig.3.4c).

Finally, regardless of misperceptions or misjudgments of the risk of infection, it is fairy reasonable to assume that individuals may acquire information about the status of the epidemic only once in a while, e.g. f days, rather than in real time[3]. Our investigation highlights that less frequent information does not clearly reduce the effectiveness of the behavioral response of the population, unless very rare information is considered (see Fig.3.4d).

The main results presented in this manuscript are summarized in Fig.3.5. Specifically, we found that, if perceived risk associated to an epidemic is sufficiently large (i.e. for large values of m), even small behavioral changes can remarkably reduce the impact of the epidemic (e.g. for $q = 0.9$ the final epidemic size can decrease from about 52% to about 38%). Moreover, if the imitation delay is not too large (lower than 2 weeks), the response of the population is always effective. On the other hand, the population responsiveness increases as the symptomaticity increases, while memory of past cases and an initial overestimation of the risk of infection essentially delay the epidemic spread.

[3]However, driven by the balance based on the last information acquired by the individuals, behavioral changes may occur continuously over time.

3.5 Discussion

Human response to the perceived risk of infection can remarkably affect the epidemic spread both qualitatively and quantitatively. Nonetheless, human behavior cannot be merely considered as an independent background process of the infection dynamics. The introduced model provides a promising approach, based on evolutionary game theory, to investigate the complex interaction between human behavior and diseases transmission process. Moreover, the model is fairy general to be applied for describing any kind of disease (e.g. influenza, smallpox, SARS and endemic diseases as well).

This study represents a further step to assess quantitative and qualitative effects of spontaneous behavioral response to the perceived risk of infection. Key features of a human self-protection are captured as well as how and when behavioral responses are effective. Our results are consistent to those obtained by previous works through different assumptions. Specifically, as shown in [42], the disease spread results highly sensitive to how rapidly people adopt a self-reduction in their contact activity rates. Moreover, if behavioral changes are fast enough, they can have a remarkable effect in reducing the daily prevalence of infection [93] and the final epidemic size [67]. For suitable parameter configurations, the epidemic dynamics becomes quite rich and can account for multiple epidemic waves, as shown in [53, 127].

Spontaneous behavioral changes have detected to be occurred in recent epidemics. For instance, during the 2009 H1N1 pandemic, high levels of concern have been detected among individuals exposed to the infection [90, 136]. Moreover, spontaneous behavioral changes performed as response to an emerging epidemic have been detected during past epidemics. On 2003 this was the case of the SARS epidemic when individuals changed their behavioral patters in order to reduce their susceptibility to the infection by limiting travels [98, 59], wearing face masks and performing other self-prophylaxis measures [98].

Therefore, accounting for spontaneous behavioral changes would be helpful for giving insight to public health policy makers, for planning control strategies and for better estimating the burden for health care centers over time. However, at the current stage, the proposed model could hardly be used for real time predictions. In fact, a deep investigation on plausible values of model parameters related to human behavior is required. In order to gain a major consciousness on how such mechanisms work Further investigations may be devoted to the investigation of real epidemic outbreaks where behavioral changes have observed.

Table 3.1: *Parameters employed and initial conditions*

EPIDEMIOLOGICAL PARAMETERS*

Parameter	Interpretation	Investigation range	Baseline value
$1/\gamma$	Average length of the infectivity period (days)	-	2.8
β_S	Transmission rate for symptomatic individuals (days^{-1})	-	0.5
β_A	Transmission rate for asymptomatic individuals (days^{-1})	-	0.5
p	Probability of developing symptoms	$[0, 1]$	1
$S(0)$	Initial fraction of susceptible individuals	-	$1 - 10^{-3}$
$I_A(0)$	Initial fraction of asymptomatic infective individuals	-	0
$I_S(0)$	Initial fraction of symptomatic infective individuals	-	10^{-3}
$R_A(0)$	Initial fraction of asymptomatic recovered individuals	-	0
$R_S(0)$	Initial fraction of symptomatic recovered individuals	-	0

BEHAVIORAL PARAMETERS

Parameter	Interpretation	Investigation range	Baseline value
q	Reduction in the number of potentially infectious contacts	$[0.5, 1]$	0.85
$1/m$	Prevalence threshold/risk	$[0, 0.05]$	0.01
ρ	Speed of the behavioral changes (days^{-1})	$[10^{-1}, 10^3]$	10
$1/\nu$	Average memory length	$[1, 30]$	2.8
μ	Rate of irrational exploration	$[0, 10^{-2}]$	10^{-8}
$x(0)$	Initial fraction of individuals adopting the normal strategy	-	$1 - 10^{-6}$
$M(0)$	Initial perceived prevalence	$[0, 0.05]^\dagger$	0

$\star$ The epidemiological parameter lead to a baseline configuration with generation time 2.8 days and basic reproductive number $R_0^n = 1.4$ (assuming that all individuals adopt the normal behavior).

$\dagger$ The perceived prevalence can also be considered larger when the initial risk of the epidemic is overestimated.

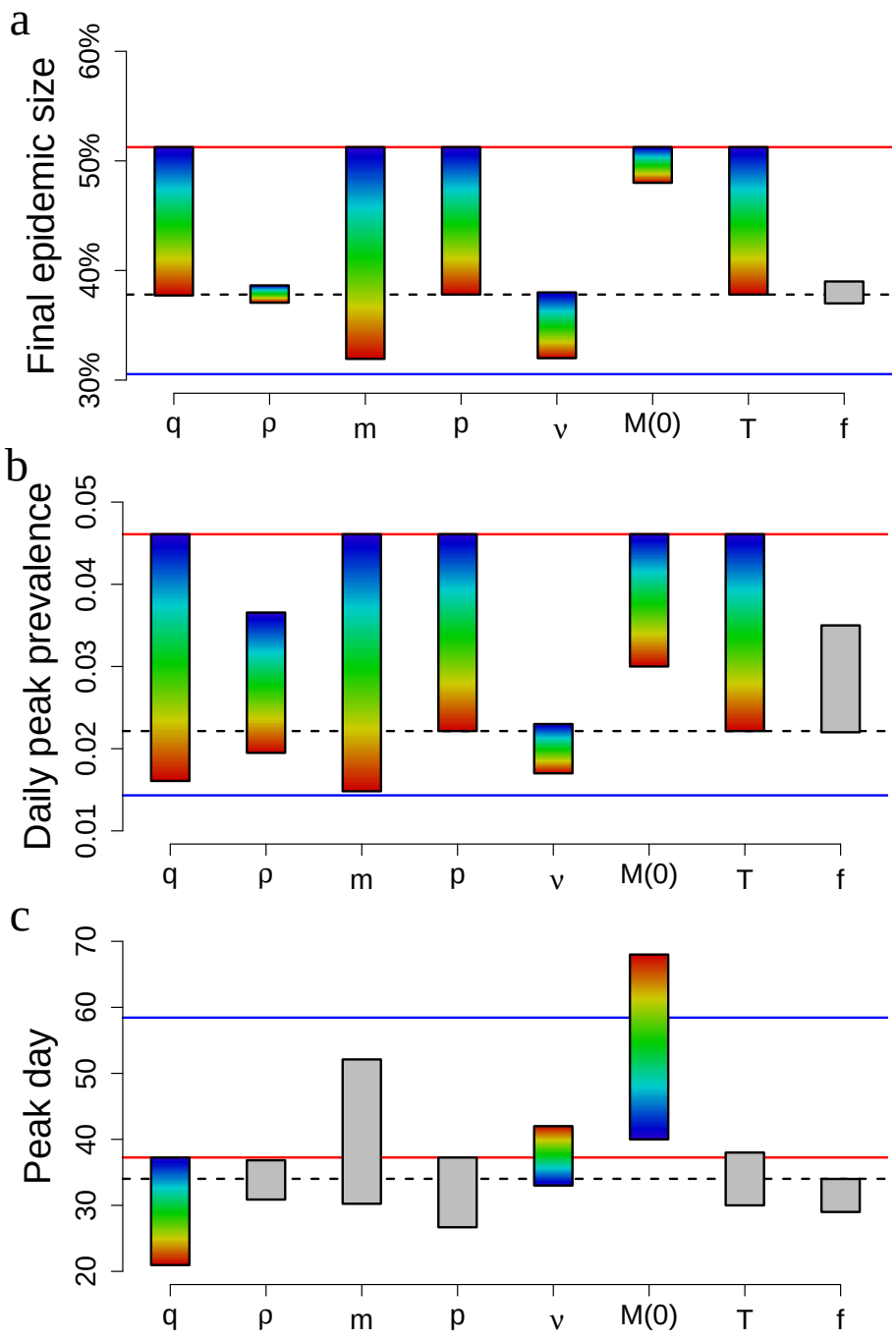

Figure 3.5: **Results summary** The influence of different key features of human behavioral responses on: **a** final epidemic size, **b** daily peak prevalence and **c** peak day. Different parameters have been investigated in the ranges defined in Tab.3.1. Colors represent the responsiveness of the population: warmer colors correspond to higher responsive population. Gray boxes have been used where no specific patterns were observed. The dashed line represents the baseline scenario, the red line represents a fully not responsive population (i.e., it corresponds to a "simple" SIR model driven by R_0^n) and the blue line represents a fully responsive population (i.e., it corresponds to a "simple" SIR model driven by R_0^a.

Chapter 4

The effect of risk perception on the 2009 H1N1 pandemic influenza dyanmics

4.1 Introduction

Among the many factors known to influence the spread of epidemics across human populations, a central role is played by the characteristics of the pathogen responsible for the infections [6, 19], human mobility patterns [84, 38, 151, 11, 112], the sociodemographic structure of the population [112] and intervention measures [6, 92]. Changes in human behaviors are largely suspected to play a crucial role as well [42, 53, 127, 67, 130]. As mathematical modeling becomes a powerful tool for decision making both in pre-planning [103, 104, 57, 58, 73, 164, 33, 41, 78, 113] and in real-time situations [12, 75, 4, 99], knowing in advance how to account for spontaneous behavioral changes would greatly improve the predictive power of epidemic transmission models and the evaluation of the effectiveness of control strategies.

In March 2009 a new influenza virus emerged in Mexico [162]. Early in the course of the pandemic the population was very concerned about the event [136, 90]. Did this affect the behavior of the population and, consequently, alter the dynamics of the epidemic? By analyzing the 2009-2010 Influenza-Like Illness (ILI) incidence in Italy, as reported to the national surveillance system, the hypothesis appears plausible that spontaneous behavioral changes have played a role in the pandemic, contributing to change the timing of spread and the transmissibility potential. In fact, after an initial period (September – mid-October 2009) characterized by a slow exponential increase in the weekly ILI incidence, a sudden and sharp increase of the growth rate was observed by mid-October. Over the whole period schools remained open [54] and only moderate mitigation measures were enacted (e.g., antiviral treatment of severe cases) [86]. However, during the initial phases of the epidemic the Italian population has been exposed to a massive information campaign on the risks of an emerging influenza pandemic, which can have contributed to alter the perceived risk. The aim of this study is to investigate the effects of the perceived

risk of infection during the course of the 2009 H1N1 pandemic in Italy. In particular, we propose a new modeling framework, based on evolutionary game theory, accounting explicitly for the dynamics of behavioral patterns adopted across the population.

4.2 Materials and Methods

4.2.1 Data description

In Italy, influenza surveillance system INFLUNET (accessible at: *http://www.iss.it/iflu/*) is based on a nationwide voluntary sentinel network of general practitioners and pediatricians. The aim is to monitor ILI incidence and to collect information on circulating strains. Incidence rates are based on the population served by each reporting physician each week.

As most European countries, Italy has experienced one single pandemic wave during fall-winter 2009 and no substantial activity has been detected during the summer [4]. The pandemic has mainly spread starting since the reopening of schools in mid-September until mid-December. During the whole period schools remained open, in fact neither regular holidays were scheduled [54] nor mitigation strategies were performed, except for a moderate vaccination program started on mid-October, and involving only a small fraction of at-risk patients and essential workers (the fraction of individuals vaccinated during the whole course of the pandemic is less than 1.5% of the population) and treatment of severe cases with antiviral drugs [86]. In this study, we consider total ILI incidence from week 38 (corresponding to the reopening of schools after the summer break, when influenza activity started to be detected by the surveillance system) to 50, 2009. This allows us to investigate an "uncontrolled" epidemic, not affected by heavy public health interventions or by school closure. The number of practitioners involved in the surveillance system over the considered period varies from 561 to 1,165; consequently, the served population varies from 767,154 and 1,509,971. These values guarantee the reliability of the number of weekly reported cases.

4.2.2 The model

The transmission process is based on a SIR model where susceptible individuals may adopt two mutually exclusive behaviors, *"normal"* and *"altered"*, on the basis of the perceived risk of infection. Individuals adopting *altered* behavior are supposed to be able to reduce the risk of infection by reducing the force of infection to which they are exposed. This defensive response takes into account both reduction in physical contacts and, more in general, all self-prophylaxis measures which can reduce the transmission probability during these contacts. For instance, a self reduction in the number of contacts can occur through the avoidance of crowded environments or by limiting travels, whereas a reduction in transmission probability can be achieved by increasing wariness in usual activities involving other individuals (e.g., the behavioral goals recommended by the

WHO for reducing influenza transmission, such as washing hands frequently or respecting cough/respiratory etiquette [161]).

In the model, individuals can change their behavior spontaneously, on the basis of cost/benefit considerations. This phenomenon perfectly fits to the language of evolutionary game theory, in which behaviors adopted by individuals correspond to strategies played in a suitable game, with certain expected payoffs: *altered* behavior takes the advantage of reducing the risk of infection, but it is more costly (e.g., because individuals have to limit their activities). Which behavior is more convenient to adopt clearly depends on the state of the epidemic. The balance of the payoff between the two possible behaviors is determined by the perceived risk of infection, which depends on the cost associated to the risk of infection and on the perceived prevalence of infections in the population. The latter is modeled by assuming a fading memory mechanism (such in [48, 3]) altering the perception of the risk of infection on the basis of the number of cases occurred over a certain (past) period of time. The diffusion of strategies in the population is modeled as an imitation process [81, 15] based on the idea that individuals change strategy as they become aware that their payoff can increase by adopting another behavior. Denoting by S, I, R the fraction of susceptible, infective and recovered individuals respectively and by introducing the variables x, describing the fraction of individuals adopting *normal* behavior, and M, describing the perceived prevalence of infection in the population, the system of ordinary differential equations regulating this process can be written as follows:

$$\begin{cases} \dot{S} &= -\beta I S\left[x + q(1-x)\right] \\ \dot{I} &= \beta I S\left[x + q(1-x)\right] - \gamma I \\ \dot{R} &= \gamma I \\ \dot{M} &= \beta I S\left[x + q(1-x)\right] - \theta M \\ \dot{x} &= x(1-x)(q-1)\beta I + \rho x(1-x)(1-mM)S \end{cases}$$

where β is the transmission rate; $1/\gamma$ is the average duration of infectivity period (corresponding to the generation time); q represents the reduction of the risk of infection to which individuals adopting *altered* behavior are exposed; θ weighs the decay of the perceived prevalence; ρ essentially represents the speed of the imitation process with respect to the pathogen transmission dynamics; m defines the risk threshold for determining which behavior would represent the most convenient choice.

Briefly, the last equation of the system models the diffusion of the two different behaviors in the population driven by an imitation/natural selection process. The first term of the equation accounts for a natural selection embedded into the transmission process that favors individuals reducing the risk of infection, while the second one accounts for an imitation process modeling spontaneous changes in individual behaviors. These changes occur on the basis of the difference between the payoffs of the two possible behaviors, the perceived prevalence, the level of the risk threshold and the speed of the imitation process which, in general, is different from the speed of the disease transmission process (as imitation is based on the diffusion of information rather than on physical contacts between individuals). Model details are presented in the Supporting Text 8.2.

The basic reproductive number R_0, which is essentially the average number of secondary infections that results from a single infectious individual in a fully susceptible population [6], can be computed by using next generation technique [44]. The resulting basic reproductive number is $R_0 = \frac{\beta}{\gamma}[x + q(1-x)]$, which can be interpreted as a weighted sum of two basic reproductive numbers: $R_0^n = \frac{\beta}{\gamma}$, the reproductive number for individuals adopting the *normal* behavior (namely the fraction x) and $R_0^a = q\frac{\beta}{\gamma}$, the reproductive number for individuals adopting the *altered* behavior (namely the fraction $1-x$). Therefore, R_0 depends on the fraction of individuals in the population who are currently adopting either *normal* or *altered* behavior.

4.3 Results

The ILI incidence as reported to the surveillance system during the 2009 H1N1 pandemic shows two different phases characterized by two distinct exponential growth rates, especially appreciable when data are plotted in a logarithmic scale (see Fig. 1a and its sub-panel). The "classical" SIR model is not able to catch this phenomenon (see Fig. 1b) unless by considering a time-dependent transmission rate, switching from a low transmission level during the first four weeks to a higher level for the rest of the epidemic (see Fig. 1c). However, this model is not able to explain the motivation underlying this sudden change in the transmissibility potential.

On the contrary, the model introduced here perfectly fits the observed ILI incidence (see Fig. 1a) providing a plausible explanation of the mechanisms responsible for the observed pattern. Specifically, the estimated parameter configuration obtained by fitting ILI incidence entails an initial overestimation of the perceived risk that decreases over time, along with an initial diffusion of the *altered* behavior in the population which becomes replaced by the *normal* behavior during the course of the epidemic. In fact, a high level of perceived risk of infection at the beginning of the pandemic leads the simulated population to adopt the *altered* behavior (as in the presence of a well sustained circulation of the virus) resulting in a growth rate of the epidemic lower than what would have been observed in a population adopting the *normal* behavior. Along with a slow increase in the number of cases, a decrease in the perceived risk of infection is observed. In fact, the latter depends on the combination of these two opposite phenomena: the increase of new infections and the decline of the perceived prevalence (slowed by the memory mechanism), which was overestimated in the early phases of the epidemic. As the perceived prevalence goes below the risk threshold $1/m$, the *normal* behavior starts to spread quickly in the population as the most convenient strategy to be adopted through the subsequent course of the epidemic. This induces an increase of R_0 which leads to a sudden change in the growth rate of the epidemic. Thus, these two distinct exponential growth phases in the observed ILI incidence correspond to two phases in the model: the first one characterized by the diffusion of the *altered* behavior in the population and thus driven by R_0^a, and the

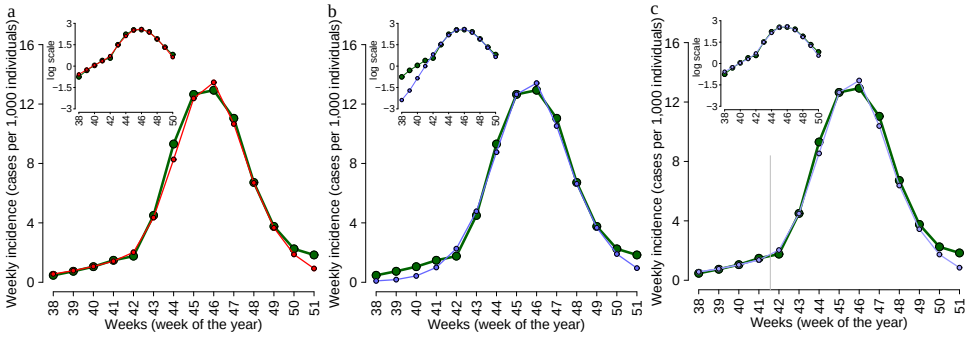

Figure 4.1: **Comparing observed ILI incidence and model simulations. a** Weekly ILI incidence as reported to the surveillance system (green) and weekly incidence simulated by the model (red). Sub-panel shows the same curves in a logarithmic scale. Parameter values used in the simulation are set as follows. The generation time $1/\gamma$ is assumed 2.5 days according to [63, 165, 74] (a sensitivity analysis on the length of the generation time is presented in the Supporting Text 8.2); $S(0) = 0.9$ according to a serological survey on the Italian population [134]; $x(0) = 10^{-8}$, assumed; $M(0) = 10.5$, $I(0) = 0.001243$, $\rho = 66$, $q = 0.84$, $m = 0.1$, $\nu = 0.005$, $\beta = 0.59$, fitted; the estimated underreporting factor is 16.9%, in good agreement with the range 18%-20.2% previously estimated in [4]. **b** Weekly ILI incidence as reported to the surveillance system (green) and weekly incidence simulated by a "simple" SIR model (blue). Sub-panel shows the same curves in a logarithmic scale. Parameter values used in the simulation are set as follows. The generation time $1/\gamma$ is assumed 2.5 days; $S(0) = 0.9$ according to [134]; $I(0) = 0.000176$, $\beta = 0.58$, fitted; the estimated underreporting factor is 17.4%. **c** Weekly ILI incidence as reported to the surveillance system (green) and weekly incidence simulated by a SIR model assuming a time-dependent transmission rate (blue). Sub-panel shows the same curves in a logarithmic scale. Parameter values used in the simulation are set as follows. The generation time $1/\gamma$ is assumed 2.5 days; $S(0) = 0.9$ according to [134]; $I(0) = 0.00126$, $\beta(t) = 0.496$ for weeks 38-41.58 and $\beta(t) = 0.596$ for weeks 41.58-51, fitted; the estimated underreporting factor is 16.7%.

second one characterized by the diffusion of the *normal* behavior and thus driven by R_0^n. The best estimate for R_0^a is 1.24 and for R_0^n is 1.48 (which correspond to two effective reproductive numbers of 1.12 and 1.33 respectively, given a 10% initial natural immunity to the 2009 H1N1pdm strain in the Italian population [134]). The basic reproductive number estimated in the phase of the epidemic characterized by the *normal* behavior, namely R_0^n, is in good agreement with the estimates previously obtained for the 2009 pandemic in Italy [4] and in several regions of the world [63, 118, 165, 74, 10].

The analysis of the sensibility of the model to changes in parameter values highlights that the model complies with observed ILI incidence only if an initial (persistent) diffusion of the *altered* behavior in the population is considered (see Supporting Text 8.2). Specifically, an initial perceived risk of infection above the risk threshold, a long-lasting memory

mechanism (able to maintain the *altered* behavior as more convenient over a relevant period of time) and a fast imitation process (enough to produce a sudden change in the force of infection) are required. Moreover, model predictions are robust in terms of final epidemic size (with absolute differences of the order of 3%), while they are more sensible in terms of timing of the epidemic. Specifically, small variations in the reduction of the risk of infection in individuals adopting the *altered* behavior result in changing R_0^a and thus the timing of the epidemic. The same holds if the initial perceived prevalence and the risk threshold determining which behavior is more convenient to adopt are perturbed. On the other hand, no relevant differences appear by increasing either the average duration of the perceived risk of infection (i.e., the length of the long-lasting memory mechanism) or the speed of the imitation process. A further analysis (shown in the Supporting Text 8.2) has revealed that, if the risk of infection is overestimated during the early phases of the epidemic, the diffusion of the virus would be slowed down (thus gaining time for vaccine production). On the other hand, if such overestimation occurs during the outbreak, a lower peak incidence (and thus a lower burden for health care centers) and a relevant decline of the final epidemic size would be observed.

Results reported above support the hypothesis that the mass media campaign on the risks of an emerging influenza pandemic performed in the early phases of the epidemic might have induced a high perceived risk of infection at the beginning of the pandemic, as it has been highlighted by specific survey studies [136, 90]. In order to investigate if such phenomenon could have been a peculiarity of the 2009 pandemic, we also analyzed the last three influenza seasons in Italy. Our analysis, reported in the Supporting Text 8.2, reveals that during the 2006-2007, 2007-2008 and 2008-2009 influenza seasons behavioral changes would not have played a relevant role in the early phases of the epidemics.

Beyond the previous analysis, the hypothesis of an overestimation of the risk is supported by the temporal pattern of drug purchases and by sporadic self-imposed school closures. Specifically, during the 2008-2009 influenza season the maximum weekly number of antiviral drugs sold was under 2 doses per $100,000$ individuals per week, while when the 2009 pandemic arrived in Europe (end of April) antiviral drug purchases immediately jumped to more than 12 doses per $100,000$ individuals per week [85]. Despite no substantial ILI activity has been detected in Italy during the summer, the purchase of antiviral drugs reached a peak of about 35 doses per 100,000 individuals per week at the end of July. As shown in Fig. 2a and 2b, during fall the purchase of antiviral drugs complies with the observed ILI temporal dynamics, while until mid-October an excess of antiviral drug purchase can be observed, supporting the hypothesis of an initial overestimation of the risk of infection. On the contrary, the sales of pain killers (which are commonly used to relieve pain due to mild symptoms) have followed a completely different pattern: during the summer the sales have been (nearly) constant, then they started to increase from the middle of September [85]. The purchase of antiviral drugs might have been amplified by the concern about the pandemic possibly thanks to the information campaign about the use of antivirals for treating H1N1 infections. Moreover, from the end of September to the beginning of October, a few examples of reactive school closure have been documented [94, 97, 96, 95]. Such school closures were "self-imposed" by the scholastic board or sug-

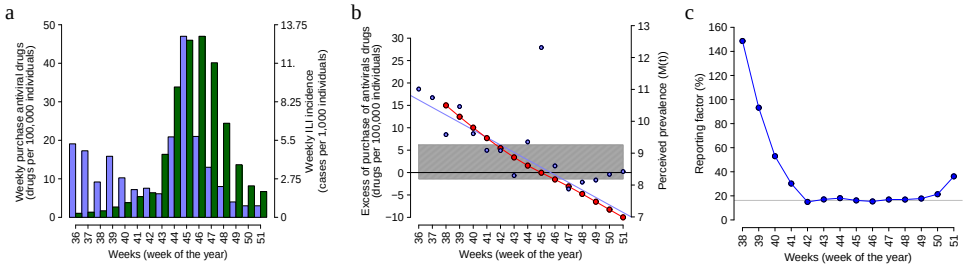

Figure 4.2: **Risk perception, antivirals purchase and reporting factor. a** Weekly purchase of antiviral drugs (light blue, scale on the left axis) and weekly ILI incidence as reported to the surveillance system (green, scale on the right axis) during the 2009-2010 pandemic in Italy. **b** Light blue points (scale on the left axis) represent the weekly excess of the purchase of antiviral drugs. The latter is defined as the difference between the actual and the expected amount of antiviral drugs purchased (which is assumed to be proportional to ILI incidence, and the proportionality constant is computed as the number of antivirals purchased divided by the ILI incidence averaged over weeks 43-51, i.e. in the period of sustained transmission). Light blue line represents the best linear model fit to the excess of purchased antivirals. Horizontal black line represents the threshold over which the number of antivirals purchased is larger than the expected one. Grey area represents the maximum and the minimum excess of antiviral drugs purchased over the weeks 43-51. Red points (scale on the right axis) represent the perceived prevalence of infection simulated by the model parameterized as in Fig. 1a. **c** Weekly reporting factor estimates that enable the simple SIR model (parameters as in Fig. 1b) to exactly fit the reported ILI incidence. The horizontal grey line represents the average reporting factor as computed over the weeks 42-50.

gested by local authorities (at municipality level). However, these sporadic closures can hardly be thought as the only responsible for the low transmission observed during the early phases of the epidemic. These two examples, however, provide empirical evidence that a high risk for the ongoing pandemic influenza has been perceived by the Italian population and that individuals have actively performed spontaneous defensive response measures aimed to reduce the risk of infection.

Behavioral changes, though not directly affecting the transmission process, can also be relevant from an epidemiological perspective. For example, as well known by epidemiologists, a high perceived risk during an epidemic can increase the notification rate, especially if the surveillance system is based on consultations. However, such phenomenon does not seem to be able to explain (alone) the observed pattern. In fact, a simple SIR model, with a time dependent reporting factor, can capture ILI incidence during the initial phase of H1N1 pandemic only by considering extremely large values of the reporting factor (even above 100%, see Fig. 2c). Similar results have been obtained by investigating a dataset combining results from the virological and epidemiological surveillance systems which allowed the estimation of a theoretic lower bound of the number of H1N1pdm infections in

Italy (see in Supporting Text 8.2).

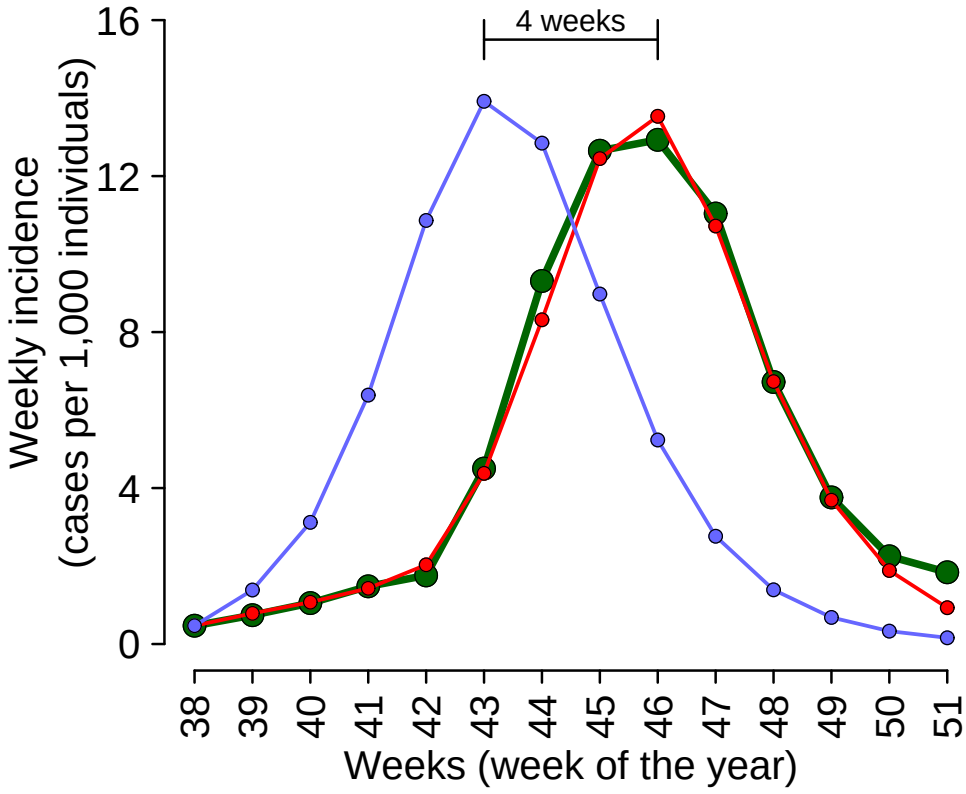

Figure 4.3: **The impact of risk perception.** Weekly ILI incidence as reported to the surveillance system (green) and incidence simulated by the model (red; parameter values as in Fig 1a). Weekly incidence simulated by the "classical" SIR model (blue; parameter values as in Fig. 1b but for $I(0) = 0.001243$).

As a matter of fact, if changes in human behavioral patterns (such as self-protection) are not taken into account, two opposite outcomes can be observed. Firstly, estimates of the growth rate based on the observations during the early phases of the epidemic may lead to an underestimation of the transmissibility potential of the disease and thus to underrate the impact of the epidemic. Secondly, predictions based on robust available estimates of the reproductive number (e.g., taken from the analysis in countries where the epidemic is already well sustained) would lead to overestimate the growth rate of the epidemic during its early phases, resulting in turn in predicting a faster spread than the actual one. For instance, by using a SIR model, accounting for the best parameter estimates as obtained by fitting the entire epidemic but initializing the system with the actual number of cases at the beginning of autumn 2009 (namely on week 38), the simulations reach the epidemic peak four weeks in advance with respect to the actual pandemic (see Fig. 3). A similar result has been observed also in [4], where - using a model not accounting for behavioral

changes in the population - the epidemic peak has been predicted two weeks in advance with respect to the actual value.

4.4 Discussion

A high level of the perceived risk at the beginning of the 2009-10 pandemic is largely suspected, as well as its effect in slowing the epidemic spread. Our aim here is to validate this hypothesis by showing that spontaneous behavioral changes in the population might have played a central role in the early phases of the pandemic in Italy. Specifically, ILI incidence shows a low (though exponential) growth, followed by a sudden change in its growth rate starting from week 42. Such pattern can hardly be captured by classical models. On the contrary, the proposed approach is able to reproduce it by explicitly modeling spontaneous behavioral changes in the population. Our analysis is supported by some empirical evidence (e.g., the purchase of antiviral drugs) and reveals that a high perceived initial risk of infection could be a plausible explanation for such phenomenon.

This study represents a first step for the estimation of the quantitative and qualitative effects of spontaneous behavioral changes in the population on the spread of epidemics. We believe it provides a promising approach, based on evolutionary game theory, for including the behavior dynamics into epidemic transmission models. The proposed approach is general enough to be used for describing any kind of disease where spontaneous behavioral changes could play a relevant role. Similar approaches have been previously used to investigate individual choices in non-compulsory vaccination programs [48, 15, 17, 69, 108].

As shown in this study, behavioral changes (e.g. induced by mass media information campaigns) can significantly affect the epidemic spread both qualitatively (e.g., by altering the epidemic dynamics) and quantitatively (e.g., by substantially slowing the epidemic spread or by determining different final epidemic sizes). Therefore, considering an approach accounting for spontaneous behavioral changes would be helpful for giving insight to public health policy makers, for planning public health control strategies (e.g., vaccination) and better estimating the burden for health care centers over time. Moreover, this study highlights that the estimation of fundamental epidemiological parameters (and in particular the reproductive number) could be largely affected by human behaviors.

At the current stage, the proposed model could hardly be used for real time predictions since our knowledge on plausible values of model parameters related to human behavior is only preliminary. Further investigations on the 2009-2010 pandemic dynamics in other countries or on other epidemics where behavioral changes have been suspected (e.g., the 2002-03 SARS outbreak) have to be performed in order to gain a major consciousness on how such mechanisms work.

Chapter 5

Optimal vaccination choice, (static) vaccination games, and rational exemption

5.1 Introduction

Despite the fundamental role played in history by vaccines, second only to potable water in the reduction of mortality and morbidity, various forms of exemption to vaccination (conscientious, religious, philosophical) have always been documented [139]. In more recent times episodes of decline in vaccine uptake have been associated to vaccine scares, e.g. the cases of the whole-cell pertussis vaccine [70], of thimerosal and HBV vaccine [107], up to the MMR scare [64, 142, 163]. In such cases a significant role of anti-vaccinators movements in raising and spreading concerns about vaccine safety was also documented [70, 126].

Today, developed countries are increasingly facing the challenge of rational exemption (RE). By RE we mean, in regimes of voluntary vaccination, the parents decision not to immunize children after a seemingly rational comparison between the perceived utility of vaccination, i.e. protection from the risk of infection perceived as very low as a consequence of the high herd immunity due to decades of successful vaccination policies - with its disutility, i.e. the risk of vaccine associated side effects. RE is often considered as a form of *free riding* [145]. Such a behavior, resulting from the optimization performed by rational agents, might well turn out to be *myopically* rational, since it considers only the current perceived risk of disease, and not the risk of its future resurgence due to declining coverage. Some evidence of rational exemption behavior is documented by surveys of vaccination lifestyles [8, 107, 163, 64].

Theoretical papers based on traditional epidemiological models have investigated the implications of RE for the dynamics and control of vaccine preventable diseases [72, 48, 49]. This literature, which has pointed out the critical interplay between information and vaccinating as well as other disease-related behavior [45], has shown that RE might make elimination a *mission impossible* unless the fraction of those who practice RE is small, i.e.

below the susceptibility threshold ensuring endemic persistence. Moreover it has shown that if the information set used by individuals includes past information then the disease dynamics might yield epidemic waves with very long period. The negative implications for rubella control of a free vaccines market have also been investigated by more realistic epidemiological models [155].

These results call for explanations of vaccination choices by behavioral variables, e.g. economic and psychological, typically neglected in epidemiological models [56]. Besides some old pioneering work [23, 61], a series of recent intriguing works by Bauch and coworkers have attempted to explain RE in its most appropriate framework, i.e. game theory [16, 15, 36, 131]. These papers have provided the first game-theoretic proof of the *elimination impossible* result, and various dynamic implications of RE. These implications suggest potential difficulties, both at the national and international level, for global eradication plans [13, 55]. In [124] it was suggested that elimination might become possible when more realistic contact network structures including local information are considered. Various applications to influenza control by vaccination, e.g. the role of adaptive behavior [150], and the interplay between perceived and real costs in vaccination choices [69], have also been considered. A two-population epidemic game related to that studied here was analyzed in [129].

In this paper we discuss RE in developed countries by simple static models of voluntary vaccination behavior. In this case the actual coverage p is the sum of the vaccination choices of the individual families. Families make their choices *rationally*, by minimizing a loss function taking into account both the perceived risk of infection and the perceived risk of vaccine associated side effects (VSE).

We first consider the simple optimization problem where homogeneous *representative* families make their choice without taking into account other families' choices. We distinguish two cases, i.e. informed families who know the principle of herd immunity, and not-fully informed ones, who believe that 100% coverage is necessary to avoid any risk of infection. We prove that the *elimination impossible* result arises as soon as informed families perceive any, however small, cost of VSE. From the case of not-fully informed families we give a possible answer on how patterns of universal vaccination might emerge. This seems to be more likely when lack of knowledge on herd immunity concur with low perceived costs of VSE.

Next we model vaccination choices as a game where families interact *strategically* by incorporating the other family choices in their loss function [110, 140]. We assume, as in the theoretical paper [36], the coexistence of two groups of social actors (labeled as pro- and anti-vaccinators) having widely different perceived costs of infection and of VSE. This is broadly consistent with the current situation of developed countries.

Unlike [16] where only the Nash equilibrium in a simultaneous game was considered, we discuss the implications of all the three classical *types* of agents' interaction, i.e. also the cases of non-simultaneous (Stackelberg) and *social planner* games [110]. In the Nash case agents play simultaneously, and take each other's action as given. In the Stackelberg (or sequential) case, a few active agents *lead* the game. This seems to be the case of anti-vaccination groups which appear to be very active in the acquisition of information,

and optimize their action by taking into account pro-vaccinators actions [8]. In the *social planner* case a *Deus ex machina* (*social planner*) seeks an agreed solution between the two groups by minimizing a *social* loss function given by an *average* of the two groups' loss functions. We prove that under informed families, the *elimination impossible* result continues to hold in both Nash and Stackelberg cases. The only case where elimination is feasible occurs when pro-vaccinators do not perceive any cost from vaccine side effects, and moreover their group is large enough to allow elimination even if the other group does not vaccinate at all. In particular the Stackelberg case with anti-vaccinators leadership always leads to a lower coverage compared to Nash behavior. Finally, we show that even in the *social planner* case elimination is possible only when, provided the *pro-vaccination* group is large enough, the social planner assigns to anti-vaccinators preferences the 100% of the weight in the social loss function. This allows a nice interpretation of the current Italian situation.

The paper is organized as follows. Section 2 deals with the basic model of vaccination choice. Section 3 discusses models of strategic interaction. Concluding remarks follow.

5.2 A simple model of optimal family behavior without strategic interaction

We consider a common Susceptible-Infective-Removed (SIR) vaccine preventable infection, such as measles or mumps, in a stationary homogeneously mixing population [5]. Infection can give rise to serious but non-fatal sequelae. The vaccine is perfect, i.e. providing 100% effective lifelong immunity. Vaccination is voluntary, and it is administered at birth. No *recuperation* strategy, such as vaccination at a later date during epochs of higher perceived risk, is allowed [48]. The infection is characterized by a basic reproduction number $R_0 > 1$ [5]. This ensures endemic circulation as far as the vaccine uptake is below the critical threshold $p_c = 1 - 1/R_0$ allowing disease elimination [5].

In this section we assume that families behave non-strategically (i.e. we rule out any game-theoretic consideration). Families are fully homogeneous in their preferences toward vaccination, i.e. we consider a single representative family [110]. This implies identical individual decisions, which in turn straightforwardly imply the equality between the individual propensity to vaccinate p and the collective coverage. Real world families have only two options: to vaccinate or not their children at birth. In our formulation each family determines its optimal propensity to vaccinate p, i.e. its vaccine demand, as the quantity that minimizes its loss function L. The propensity to vaccinate represents the agent's probability (i.e. $0 \leq p \leq 1$) to take the decision to vaccinate. The loss function summarizes the cost families will suffer as a consequence of their decisions. As loss function we take a quadratic additive function, which is the commonest type of loss function in economics [110], increasing in the perceived risk of infection $\rho_I(p)$, and in the perceived risk of vaccine associated side effect $\rho_V(p)$:

$$L = \rho_I^2(p) + \beta\rho_V^2(p) \tag{5.1}$$

In (5.1) $\beta > 0$ is the relative cost of vaccine side effects, which is given by the ratio between the cost of VSE and the cost of infection. These parameters summaries the whole set of costs (economic, psychological etc) following from serious episodes of disease or of VSE. The ideas underlying the simple quadratic additive loss (5.1) are that: (a) agents have two objective variables, i.e. the two perceived risks (from infection and from VSE); (b) there are target values ($\rho_I = \rho_V = 0$) such that any deviation from such targets results in a loss for the agent. The case $\rho_I = \rho_V = 0$ corresponds to the situation where the disease has been eliminated, so that the risk of infection has been forced to zero, but also the need to vaccinate has been eventually removed, as it has been the case of smallpox, so that also the risk of VSE is driven to zero; (c) deviations of the objective variable from the target are penalized in a more than proportional way; (d) simple additivity straightforwardly reflects the trade-off between the two objectives, e.g. the fact that if agent A increases his/her propensity to vaccinate (for example as a consequence of an external rumor which increases his perceived risk of infection), then A expects to observe a reduction in the risk of disease, but at the cost of increasing the risk of VSE.

A major problem is to what extent families are informed about the disease and the vaccine, and therefore how they evaluate risks. Families hardly know *technical* quantities as R_0 . Nonetheless it seems reasonable to assume that they are aware that (a) more transmissible diseases need a stronger vaccination effort to be controlled; (b) a higher collective coverage implies a lower individual risk of infection; (c) a coverage of 100% by a perfect vaccine is certainly sufficient to eliminate the disease. What is unclear is whether families know the existence of the critical coverage , i.e. the herd immunity principle, based on the intuitive concept that *if everyone vaccinates I do not need to* [5], ch.4). Though this does not seem to be true in general, it might be in some cases [8]. Knowledge of herd immunity was postulated in [16]. For generality we therefore consider two cases: in the first case families are *informed*, i.e. they do know herd immunity; in the second one they do not, and therefore believe universal vaccination to be the only strategy to surely avoid infection.

5.2.1 The case of *informed* families

Informed families are assumed to exactly know the critical threshold p_c, and to estimate the risk of infection as a decreasing function of collective coverage p, for p below the critical threshold p_c, and zero above it, since in this case the disease is eliminated. The simpler form is:

$$\rho_I(p) = \begin{cases} H(p_c - p) & \text{if} \quad p < p_c \\ 0 & \text{if} \quad p_c \leq p \leq 1 \end{cases} \tag{5.2}$$

Where $H > 0$ is a constant. In particular $\rho_I(0) = Hp_c$ represents the family's perceived risk of infection in absence of any immunization at the population level. In [16] perfectly informed agents were postulated to know in detail the underlying epidemiological model,

in particular the functional form $\pi(p) = (p_c - p)/(1-p)$ of the lifetime risk of infection at equilibrium, and to estimate $\rho_I(p)$ by $\pi(p)$. This choice and ours are qualitatively equivalent (both predict a vanishing risk of infection for $p = p_c$), but ours has the advantage of being simpler, and also less demanding in terms of abstraction. Though (5.2) is formally equivalent to the equilibrium force of infection in the SIR model [5], we prefer to interpret (5.2) as a coarse qualitative estimate of the lifetime risk of infection, consistently with the above made assumption that agents do not know *technical* quantities,.

The perceived risk ρ_V of a VSE is modeled as the product αp of the family propensity p to vaccinate children, times the conditional probability $\alpha > 0$ (exogenously given) of suffering a side effect given vaccination relative to the corresponding probability of suffering serious disease following infection.

The informed representative family aims therefore at choosing the value of p which minimizes the loss function [1]:

$$L(p) = \begin{cases} H^2(p_c - p)^2 + \beta\alpha^2 p^2 & \text{if} \quad p < p_c \\ \\ \beta\alpha^2 p^2 & \text{if} \quad p \geq p_c \end{cases} \tag{5.3}$$

Note that $L(p)$ has a continuous first derivative. The idea underlying the quadratic loss, as (5.3), is that families perceive two type of costs, one arising from the risk of infection, the other one from the risk of VSE, and want make both them as low as possible. In [16] the expected loss $L(p) = \rho_I(p)(1-p) + \beta\rho_V(p)$ was used [2].

Note first that if $\beta = 0$, i.e. if no cost is perceived from VSE, then (5.3) becomes:

$$L(p) = \begin{cases} H^2(p_c - p)^2 & \text{if} \quad p < p_c \\ \\ 0 & \text{if} \quad p \geq p_c \end{cases} \tag{5.4}$$

One immediately notes that for $p < p_c$, the graph of $L(p)$ is an arc of parabola decreasing to zero as p tends to p_c, implying that any choice p equal to, or above the critical coverage p_c is optimal for the individual. In other words if no costs arise from VSE it is optimal for the individual to achieve the elimination threshold.

For $\beta > 0$ the loss function is decreasing for small p and increasing for $p \geq p_c$, implying that the optimal solution can never exceed p_c. This means that policies in excess of the critical level are more costly also at the individual level, as they expose people to

[1] More general results can be obtained by more general formulations allowing interpolation between the linear and quadratic loss formulations, as suggested by an anonymous referee for these suggestions.

[2] It is possible to see that eventually the two formulations yield the same conclusions. The only difference is that the expected loss allows a dichotomy result, i.e. no one will vaccinate if the cost of VSE is always higher than the cost of infection, while in the opposite case some will vaccinate. Though the former case is of theoretical interest as it yields a *no vaccination* equilibrium, it does not seem to have practical relevance.

unnecessarily high risks of VSE. By focusing on the case $p < p_c$, differentiating the loss with respect to p, and equating to zero, we get a unique global solution of *minimum loss*

$$p_{opt} = \frac{H^2}{\beta\alpha^2 + H^2} p_c = \epsilon p_c \tag{5.5}$$

where $0 < \epsilon < 1$. Expression (5.5) shows that the optimal propensity to vaccinate p_{opt} is strictly lower than the critical coverage for any, however small, risk of VSE α. In particular p_{opt} is decreasing in both the risk, and the cost of VSE. This is the simplest proof that the family's optimal solution always implies a collective coverage below the elimination threshold, and therefore that elimination is not possible in a free vaccination market. We illustrate this (Fig.5.1) for a measles-like disease with $R_0 = 10$, implying a critical coverage $p_c = 0.9$. We consider distinct values ($\beta = 0, \beta = 0.5, \beta = 2.5$) of the relative cost of VSE; $\beta = 2.5$ means that the cost attributed to a damage from VSE is 2.5 times higher than that attributed to disease. In correspondence of the *low* relative cost of VSE ($\beta = 0.5$) the optimal propensity to vaccinate p_{opt} is about 88%, i.e. very close to p_c, whereas for the *high* value of β ($\beta = 0.25$) p_{opt} declines to about 80%, i.e. substantially less than p_c. In other words if the cost families attribute to VSE largely exceeds the cost of infection, the vaccine demand might become quite low. In the real world families will then have to implement these *theoretical* propensities into a binary decision (*vaccinate* or *not vaccinate*). If families vaccinate independently then, unless in very small communities, the actual *realized* coverage, i.e. the average of families' realized decisions, will differ little from p_{opt}. It is to be noted that p_{opt} could vary significantly among different diseases because individuals naturally tend to rank both the costs of diseases and VSE [18].

5.2.2 Not fully-informed families

By analogy with the case of informed families we use the following simple form for the perceived risk of infection:

$$\rho_I = K(1 - p) \tag{5.6}$$

where $K > 0$. This amounts to assuming that families do not know the critical threshold and believe instead that universal vaccination is the only strategy surely avoiding infection. In this case the representative family minimizes:

$$L = (K(1 - p))^2 + \beta\alpha^2 p^2 \qquad 0 \leq p \leq 1 \tag{5.7}$$

yielding the optimal solution (the graph of the loss function is again an arc of parabola):

$$p_{opt} = \frac{K^2}{K^2 + \beta\alpha^2} \tag{5.8}$$

If, for comparison purposes, we keep $K = H$, as in the case of informed families, then $p_{opt} = \epsilon$, i.e. this case allows to achieve coverages that are systematically higher compared

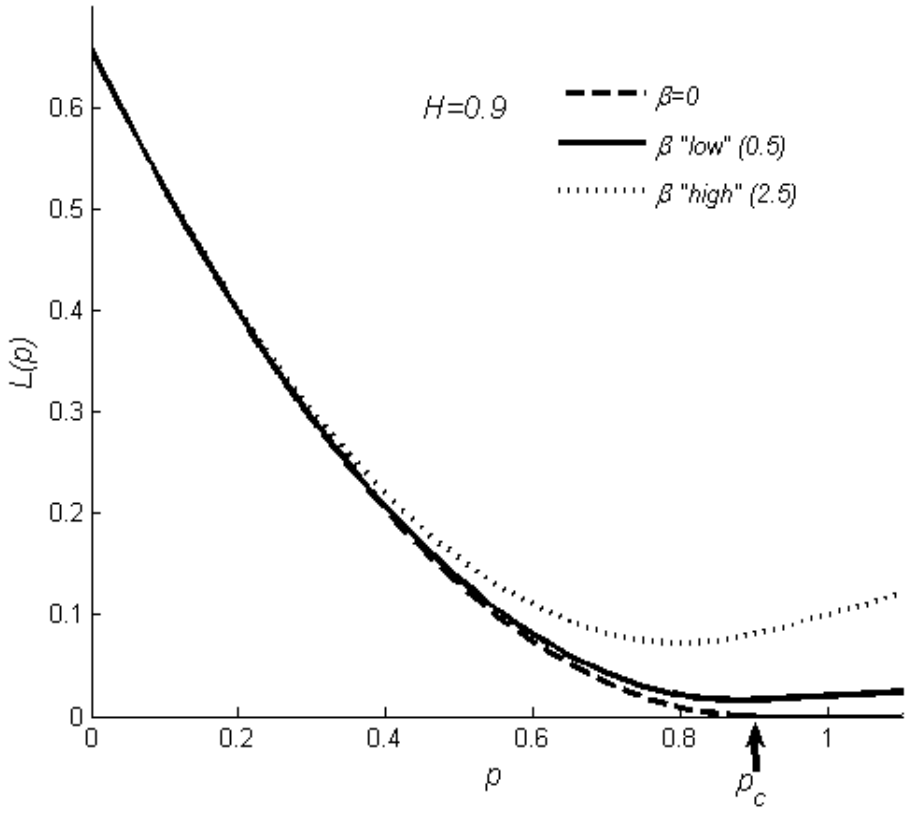

Figure 5.1: Shapes of the individual family loss as a function of the level p of vaccine *demanded* by the family for different costs of vaccine side effects β ($\beta = 0, \beta = 0.5, \beta = 2.5$). The point where the graph achieves its minimum is the optimal individual solution p_{opt}. For $\beta = 0$ the loss is minimal (i.e. zero) for any choice equal or in excess of the critical coverage p_c. Other parameters values are: $H = 0.9$, and $\alpha = 0.2$.

to the case of informed families, and in particular close to 100% if the cost of VSE is negligible. Under the same parameters assignments of the example above we find that for $\beta = 0.5$, the optimal coverage is near 98%, and even for $\beta = 2.5$ it is about 89%, i.e. still quite close to p_c. It follows that lack of information on the existence of the infection threshold seems therefore to provide a simple explanation of how patterns of universal vaccination might emerge in actual circumstances.

5.2.3 Only a fraction of the population is eligible

An interesting case is when only a fraction f_1 of the population is eligible for vaccination, for example because of the presence of a group practicing conscientious exemption. In this case the overall vaccination coverage is defined as $p_1 = pf_1$, and the critical coverage that needs to be achieved in the eligible population is $p_c^\star = p_c/f_1 > p_c$, which might be greater than one if the eligible fraction is small. In the case of informed families we get

$$p_{opt} \begin{cases} \dfrac{H^2 f_1^2}{\beta\alpha^2 + H^2 f_1^2} \dfrac{p_c}{f_1} = \epsilon_1 p_c^\star & \text{if } \epsilon_1 p_c^\star < 1 \\ \\ 1 & \text{elsewhere} \end{cases} \tag{5.9}$$

This result will be useful in the next section.

5.3 Implications of strategic behavior: the game-theoretic approach

5.3.1 A preliminary: the critical elimination line for multigroup populations

Let us now consider a SIR-type disease in a population subdivided into two groups with frequencies f_1, f_2, and heterogeneous coverages p_1, p_2. If the population is homogeneously mixing the collective coverage is $p = p_1 f_1 + p_2 f_2$ and the elimination rule ($p \geq p_c$) for vaccination at birth becomes:

$$p_1 f_1 + p_2 f_2 \geq p_c \tag{5.10}$$

showing that the possibility of elimination depends not only on groups' actual coverages but also on their frequencies. Taking the frequencies as given, (5.10) states that elimination requires coverages p_1, p_2 in the two groups lying above a critical line (CL). The CL is the portion lying in the unit vaccination square $[0,1] \times [0,1]$ (i.e. the space of admissible vaccination policies), of the straight line $p_1 f_1 + p_2 f_2 = p_c$, which can be written as:

$$p_1 = p_{1,c}^\star - \frac{f_2}{f_1} p_2 \tag{5.11}$$

where $p^{\star}_{1,c} = p_c/f_1$. Any pair (p_1, p_2) lying above the CL would eliminate the infection. The CL has negative slope (*an increase in critical coverage in group 2 allows a reduction in group 1 without compromising elimination*) $m = -f_2/f_1$, reflecting the relative size of the two groups. The intercept $p^{\star}_{1,c}$ and the foot $p^{\star}_{2,c} = p_c/f_2$ represent the vaccination effort that would be required to either group to eliminate infection when the other group does not vaccinate. If either $p^{\star}_{1,c}, p^{\star}_{2,c}$ exceeds 1 elimination is unfeasible without some *cooperation*.

By means of the CL we may answer useful questions related to the containment of the impact of anti-vaccinators on control programs, e.g. if group 2 vaccinates above threshold, to what extent can group 1 vaccinate below threshold without compromising elimination? Let us consider (Fig.5.2a) a disease with $R_0 = 5$ (sometimes adequate for rubella) implying $p_c = 0.8$, in a community where group 2 represents 90% of the population ($f_2 = 0.9$). The foot $p^{\star}_{2,c} \simeq 0.89$ indicates that group 2 can achieve elimination *alone*. However the steepness of the CL ($m = -9$) indicates that small departures from this level make it necessary to vaccinate also in group 1. If coverage in group 2 is 85%, then elimination requires at least 35% coverage in group 1.

To sum up, the shape of the CL reflects both the difficulty to eliminate the disease, summarized by p_c (which in turns reflects transmissibility through the increasing relation $p_c = 1 - 1/R_0$), shifting upward when, other things being equal, p_c increases, and the relative size of the two groups. Fig.5.2b illustrates the possible forms of the CL. These forms correspond to distinct socio-epidemiological *types*: (a) the CL entirely lies within the vaccination square: this is characterized by the condition $p_c < min\{f_1, f_2\}$ and implies the case of a *moderately* transmissible infection, i.e. such that $p_c < 1/2 \Leftrightarrow R_0 < 2$, with groups of not too dissimilar size ($p_c < f_1 < 1 - p_c$); (b) both the intercept and the foot of the CL lie outside the vaccination square: this corresponds to a *highly* transmissible infection ($p_c > 1/2 \Leftrightarrow R_0 > 2$) and groups of not too dissimilar size; (c) the intercept lies outside and the foot inside: this is expressed by the condition $f_1 < p_c < f_2$. This case is compatible with very large differences in size between the two groups when R_0 approaches 1 or when it is very large ($R_0 >> 2$); (d) the intercept lies inside the and the foot outside; this is just the symmetric of (c) when the roles of the two groups are interchanged (not reported in the figure).

Given our focus on the possibility to eliminate a highly transmissible disease in presence of a small group with low vaccine uptake, the *type* of major interest for our discussion is (c). It is important to remind that in this case group 2 is large enough to eliminate without cooperation from group 1, i.e. $p^{\star}_{2,c} < 1$. This means that if for instance $R_0 = 15$, so that $p_c = 0.93$, the maximal *affordable* size of the anti-vaccine group is less than 7%.

5.3.2 The vaccination game

In a game-theoretic framework, unlike the individual optimization of section 2, families (*players*) make their choices by taking into considerations other families' decisions. We assume that families are subdivided into two groups of fixed (no migration between the groups is allowed) sizes f_1 and f_2. Families are characterized by homogeneous preferences

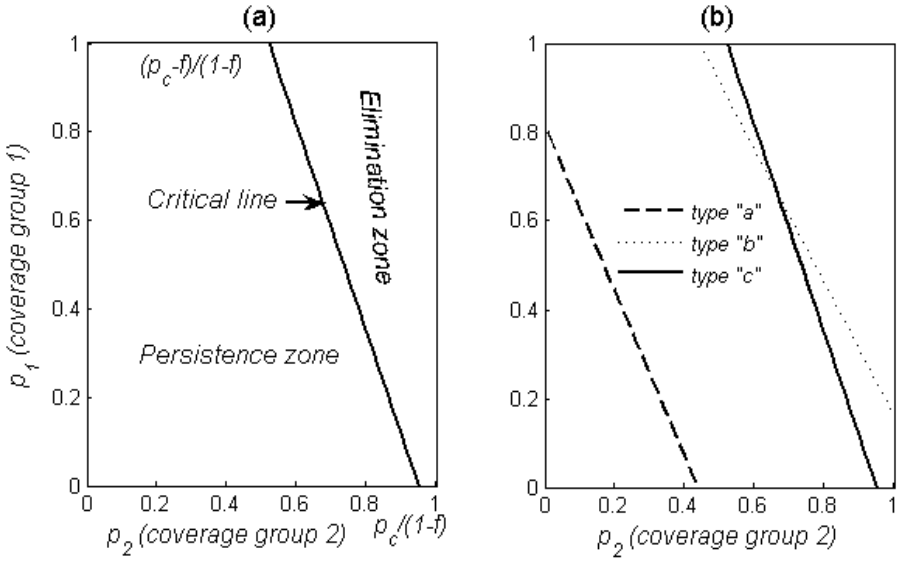

Figure 5.2: (a) Vaccination square, critical line, and *elimination zone* for a disease with $R_0 = 5$ ($p_c = 0.8$) in a community where group 2 is majority ($f_2 = 0.9$); (b) Different shapes of the CL corresponding to the three different socio-epidemiological *types*: type *a*: $R_0 = 1.4, f_1 = 0.35$; type *b*: $R_0 = 3, f_1 = 0.4$; type *c*: $R_0 = 3, f_1 = 0.3$

within the group they belong to, but heterogeneous preferences between groups. This allows to refer to a representative agent for each group. Group 1 (*anti-vaccinators*)[3] has a higher relative cost of VSE ($\beta_1 > \beta_2 \geq 0$) as in [36], and it is smaller ($f_1 < 1/2$). We focus on the case of informed families, but the extension to non fully informed families is straightforward. The informed representative family of each group determines its vaccination propensity p_j ($j = 1, 2$) by solving the problem:

$$Min_{p_j} L_j = (\rho_I(p))^2 + \beta_j \alpha^2 p_j^2 \qquad j = 1, 2; \quad 0 \leq p_1, p_2 \leq 1 \tag{5.12}$$

where the perceived risk of infection is, as before, given by:

$$\rho_I(p) = \begin{cases} H(p_c - p) & \text{if } p < p_c \\ \\ 0 & \text{elsewhere} \end{cases} \tag{5.13}$$

In particular $p = p_1 f_1 + p_2 f_2$ (the constraint $0 \leq p_1 f_1 + p_2 f_2 \leq 1$ is always fulfilled as $0 \leq p_1, p_2 \leq 1, 0 \leq f_1, f_2 \leq 1$) represents the overall coverage that would follow from

[3]We have made the distinction between *pro* and *anti*-vaccinators just for labeling the two groups. The only difference between the two types of agents lies in the different perceived costs following from their decisions (as a consequence perhaps of using distinct information sources), and neither imply distinct apriori propensities to vaccinate nor a larger apriori cooperative attitude. However we will see that these different costs imply that a posteriori one group will be more inclined to vaccinate than the other. This results from the competition within groups as a Nash strategy within group.

choices (p_1, p_2) of families of the two groups. In other words families know that the overall coverage depends on their choices (i.e. from people of their group) but also on the other group choices. Given that choices made by either group produces some effects also on the other group, solving (5.12) and (5.13) requires to make assumptions as to the type of strategic game families play. We will consider simultaneous games, non simultaneous games (also termed Stackelberg games), and *social planner* games [110].

5.3.3 The basic strategic competition

In this case the two groups decide their action simultaneously by taking as given the action of the other group. The Nash solution to (5.12) and (5.13) uses the concept of vaccination reaction function. The reaction function $M_1(p_2)$ ($M_2(p_1)$) of players of group 1 (2) defines the optimal vaccination choice of player 1 (2) corresponding to any feasible vaccination choice $0 \leq p_2 \leq 1$ of players from group 2 (1). The points where the two reaction functions intersect are Nash Equilibria [110]. The algebraic determination of the reaction functions, though elementary, requires a tedious computation to consider all the possible cases, depending on the *type* of the Critical Line, and on the values of the costs β_i. For sake of simplicity we just summarize the main graphic features of $M_1(p_2)$ (which hold mutatis mutandis for $M_2(p_1)$):

1 since the risk of infection is positive only in the region below the CL (see (5.13)), it is intuitive that the reaction functions will be positive only in such a region;

2 if group 2 is able to eliminate without cooperation from group 1 (f_2 large enough that $p^\star_{2,c}$), then every p_2 choice in excess of $p^\star_{2,c}$ is a feasible elimination choice. In this case $M_1(p_2)$ is identically zero for $p^\star_{2,c} \leq p_2 \leq 1$;

3 if group 2 is not large enough to eliminate alone ($p^\star_{2,c} > 1$), then $M_1(p_2)$ is positive for all $0 \leq p_2 \leq 1$;

4 if the value p_1^{opt} determined in section 2.3, which represents the intercept $M_1(0)$, exceeds 1 (this can happen if $p^\star_{1,c} > 1$), a portion of $M_1(p_2)$ will lie *flat* on the upper boundary of the vaccination square;

5 the positive portion of $M_1(p_2)$, will be decreasing in p_2 to mirror that as group 2 increases its demand for vaccines, group 1 will find it convenient to vaccinate less (and symmetrically for $M_2(p_1)$). This is found by optimizing L_1 in the region below the CL, yielding:

$$p_1^{opt}(p_2) = \frac{f_1^2 H^2}{\beta_1 \alpha^2 + f_1^2 H^2}(p^\star_{1,c} + \frac{f_2}{f_1} p_2) = \epsilon_1 (p^\star_{1,c} + \frac{f_2}{f_1} p_2) \tag{5.14}$$

with $0 < \epsilon_1 < 1$. The line (5.14) is always flatter than the Critical Line, and it has the same foot. By finally relating the possible shapes of $M_1(p_2)$ to the underlying *types* of the CL (Fig.5.2b) we obtain the forms represented in Fig.5.3.

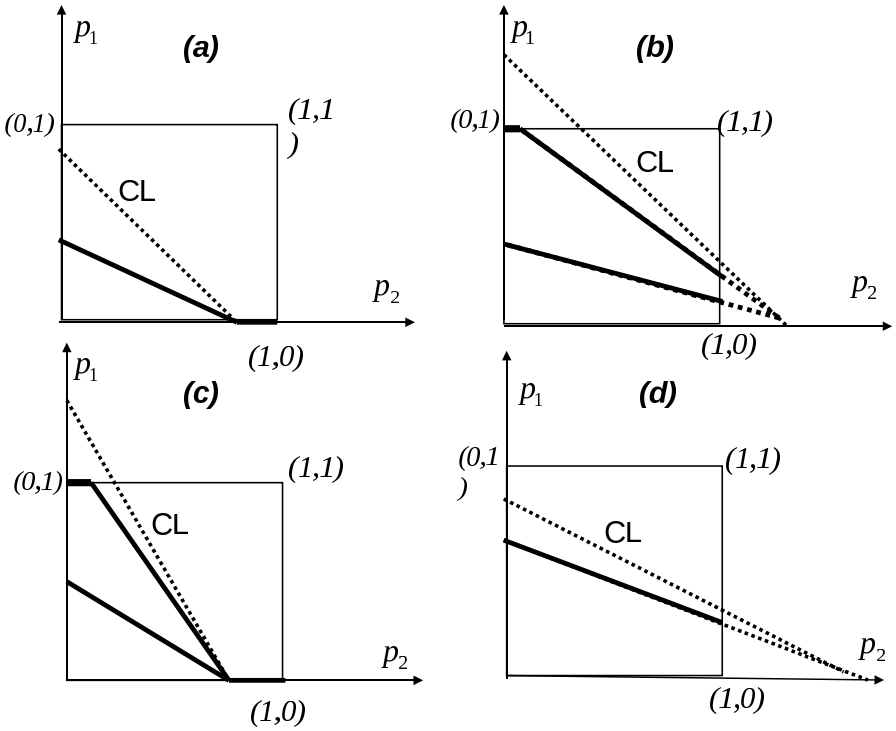

Figure 5.3: Possible shapes of the reaction function $M_1(p_2)$ of group 1 in relation to the underlying *types* of the Critical Line.

A special but important case occurs when families of group 2 assign a zero cost to vaccine side effects ($\beta_2 = 0$). In this case the internal portion of the reaction function $M_2(p_1)$ will always coincide with the Critical Line.

Finally, as for the case of not-fully informed families, it seems natural to assume that at least families of group 2 are not aware of herd immunity, and therefore obey (5.5)-(5.6). This will imply, other things being equal, a reaction function M_2 having a higher intercept and the same slope.

We can now collect our results. They are summarized in Fig.5.4 for a variety of different circumstances. For brevity we only discuss the case of type (c), that is the most important for our purposes. For generality we consider two distinct possibilities as for the relative cost of VSE in group 1: $\beta_{1,\text{low}} = 1, \beta_{1,\text{high}} = 2.5$ and take $\beta_2 < \beta_{1,\text{low}}$. The case $\beta_{1,\text{high}}$ corresponds to a very *low* reaction function of group 1, which vaccinates little even if group 2 does not vaccinate, whereas in the case $\beta_{1,\text{low}}$ group 1 vaccinates 100% at very low vaccination choices of group 2. In particular Fig.5.4a, 5.4b, 5.4c deal with the case of informed families, while Fig.5.4d with the case of non-fully informed agents. If the relative cost of VSE in group 2 is positive, however small (Fig.5.4a), then the Nash equilibrium, i.e. the intersection between the reaction functions, will lie strictly below the Critical Line, indicating that the families' behavior is not compatible with elimination. When group 2 does not suffer costs from VSE ($\beta_2 = 0$) then (Fig.5.4b) the internal portion of the reaction function of group 2 coincides with the CL, and the Nash equilibrium is located at the foot $p^\star_{2,c}$ of the CL. In this case elimination is feasible because group 2 is large enough to support the whole elimination effort without any cooperation from group 1. Note however that if group 2 is not sufficiently large, then elimination becomes impossible even in the favorable case $\beta_2 = 0$ (Fig.5.4c). Indeed a larger anti-vaccine group make the CL (and M_2) flatter, so that the Nash equilibrium is *pushed* out of the vaccination square. If families of group 2 do not know herd immunity then, other things being equal, M_2 moves upward (Fig.5.4d) and can therefore always lie above the CL. In this case the Nash equilibrium locates above the elimination threshold. Therefore lack of knowledge of the elimination threshold make elimination possible even when this was not the case under fully informed agents. The previous results therefore prove the following:

Result 1 (*Elimination is impossible under* informed families). As long as both groups assign a positive value to the cost of VSE ($\beta_1, \beta_2 > 0$) elimination is never possible. Elimination is possible if pro-vaccinators do not suffer costs from VSE (i.e. $\beta_2 = 0$) and their group size is large enough to sustain elimination without the cooperation of the other group.

Summarizing, in presence of informed families, the forces operating in the Nash case are never able to promote a coverage above the critical one. This provides the main rationale for compulsory vaccination as the rule to avoid non-cooperative Nash behavior.

When families are not aware of herd immunity, then, as noted in section 2, circumstances are more favorable to elimination (as in Fig.5.4d). Nonetheless high costs of VSE and increases in the size of the anti-vaccine group can obviously lead to a community coverage below the critical threshold in this case as well.

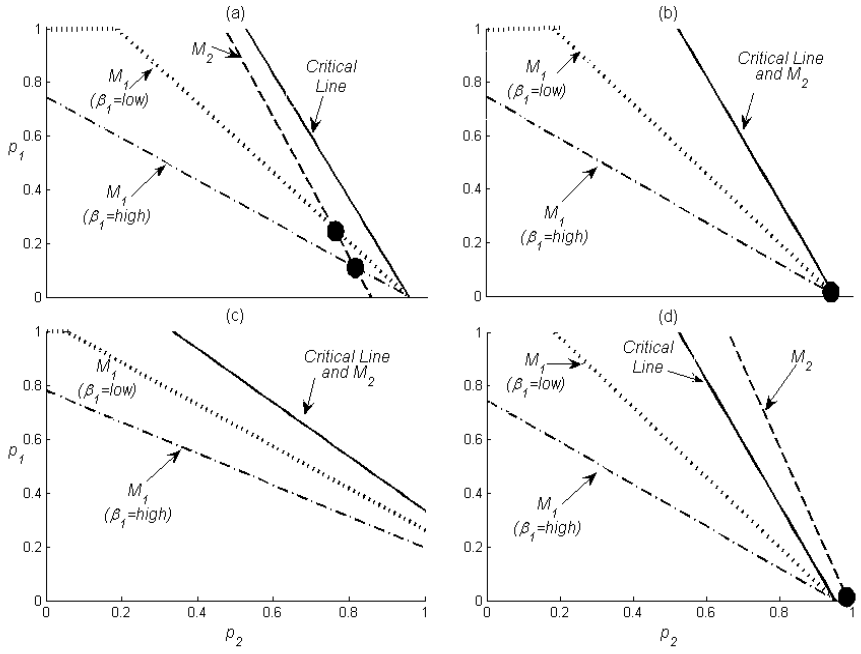

Figure 5.4: Critical Line, reaction functions, and Nash equilibrium points (represented by bold points) under socio-epidemiological *type* c. Graphs (a), (b), (c) deal with informed families, (d) with non-fully informed families. H, R_0, p_c, α are the same throughout the graphs: $H = 0.9, R_0 = 3, p_c = 0.66, \alpha = 0.2$. Moreover: (a) $f_2 = 0.7$ implying $p^{\star}_{2,c} = 0.952, \beta_2 = 0.75$ (b) $f_2 = 0.7, \beta_2 = 0$ (c) $f_2 = 0.55, \beta_2 = 0$ (d) $f_2 = 0.7, \beta_2 = 0.75$ as in (a).

We finally note that the coordinates of the Nash equilibrium can be computed explicitly:

$$
\begin{aligned}
p_1^{Nash} &= \frac{H^2 f_1 \beta_2}{H^2(f_1^2\beta_2 + f_2^2\beta_1) + \alpha^2\beta_1\beta_2} p_c \\
p_1^{Nash} &= \frac{H^2 f_2 \beta_1}{H^2(f_1^2\beta_2 + f_2^2\beta_1) + \alpha^2\beta_1\beta_2} p_c
\end{aligned}
\tag{5.15}
$$

so that the corresponding overall coverage is:

$$
p^{Nash} = p_1^{Nash} f_1 + p_2^{Nash} f_2 = \frac{H^2(f_1^2\beta_2 + f_2^2\beta_1)}{H^2(f_1^2\beta_2 + f_2^2\beta_1) + \alpha^2\beta_1\beta_2} p_c \tag{5.16}
$$

which immediately shows our main result: $p^{Nash} \leq p_c$.

5.3.4 The Stackelberg case with anti-vaccinators leadership

In Stackelberg games[4] there is a *leader* who minimizes its loss function by taking into account the reaction function of the *follower*, rather than by taking it as given, as in the previous section. This implies therefore a behavioral asymmetry, that might be consistent with the vaccination game in developed countries where anti-vaccinator groups tend to be very active in the information acquisition and decision processes. To model this anti-vaccinators leadership in our framework we assume that anti-vaccinators have an *information advantage*, i.e. they know pro-vaccinators behavior (i.e. their reaction function) and incorporate it into their loss function.

We therefore assume that families from group 2 play as before, thereby computing their reaction function $M_2(p_1)$, whereas families from group 1 know $M_2(p_1)$, and incorporate it into their own loss function. Thus group 1 determines its optimal vaccination choice p_1^{Stack}, and group 2 will as a consequence *follow* by just recomputing its choice as $M_2(p_1^{Stack})$. In the case of informed families it holds:

$$
p_1^{Stack} = \frac{f_1^2 H^2 (1-\epsilon_2)^2}{f_1^2 H^2 (1-\epsilon_2)^2 + \alpha^2\beta_1} p_c \tag{5.17}
$$

where

$$
\epsilon_2 = \frac{f_2^2 H^2}{\alpha^2\beta_2 + f_2^2 H^2}
$$

It is thus easy to see that when both groups have positive costs of VSE, the *elimination impossible* result continues to hold. In addition it is possible to prove that in the Stackelberg equilibrium $(p_1^{Stack}, M_2(p_1^{Stack}))$ the demand for vaccines by group 1 will

[4]Stackelberg games are usually compared with Cournot games when distinguishing sequential and simultaneous play. Both types of games can have strategies satisfying Nash's criteria [140].

be lower compared to the basic simultaneous game of section 3.2, while that of group 2 will be consequently higher. The intuition for such a result is that when group 1 acts as Stackelberg leader it has the advantage to decide its optimal policy by considering the entire reaction of group 2 to its own behavior. For instance group 1 knows that if it decides not to vaccinate, group 2 will entirely bear the burden of the (whole) community immunization (included the cost of VSE). No surprise, then, that in such a case the vaccination effort of group 1 will be lower than in the case in which the two groups play simultaneously.

5.3.5 The social planner case

The *elimination impossible* trap under Nash or Stackelberg rules suggests to look at the possibility that a social planner may attempt to find an *agreed* solution. To this end, we consider a social loss function $L = L(p_1, p_2)$ of a utilitarian type [110], defined as a weighted average of the loss functions of the two groups. The social planner will find a socially optimal solution by minimizing the social loss function and then will seek appropriate policy tools to actually implement the optimal solution among the two groups. He will solve:

$$Min_{p_1,p_2} \quad xL_1 + (1-x)L_2 \qquad 0 \leq x \leq 1 \tag{5.18}$$

where x is the weight that he assigns to the loss of group 1. This case requires some elaboration (see appendix in [109]), but its results are easy to understand. We only consider the case of fully informed families. In this case no solution can lie above the CL ($p \geq p_c$): in fact the partial derivatives of the social loss function L are always non negative and do not vanish simultaneously. Looking for solutions lying below the CL, standard computations yield the following optimum point, i.e. the so called Nash equilibrium in the social planner case:

$$p_1^{Soc} = \begin{cases} \hat{p}_2 & \text{if } \hat{p}_1 < 1 \\ 1 & \text{elsewhere} \end{cases} \tag{5.19}$$

$$p_2^{Soc} = \begin{cases} \hat{p}_2 & \text{if } \hat{p}_1 < 1 \\ \dfrac{H^2 f_2^2 (p^{\star}_{2,c} - f_1/f_2)}{H^2 f_2^2 + (1-x)\beta_2 \alpha^2} & \text{elsewhere} \end{cases}$$

where

$$\begin{aligned} \hat{p}_1 &= \frac{(1-x) f_1 H^2 \beta_2}{H^2((1-x) f_1^2 \beta_2 + x \beta_1 f_2^2) + x(1-x)\alpha^2 \beta_1 \beta_2} p_c \\ \hat{p}_2 &= \frac{(1-x) f_2 H^2 \beta_1}{H^2((1-x) f_1^2 \beta_2 + x \beta_1 f_2^2) + x(1-x)\alpha^2 \beta_1 \beta_2} p_c \end{aligned} \tag{5.20}$$

One thus immediately notes that for values of the weight x belonging to $(0,1)$ it holds: $p^{Soc} = p_1^{Soc} f_1 + p_2^{Soc} f_2 < p_c$. This means that when both groups concur to form the social loss function, and in presence of informed families with positive costs from VSE, elimination is impossible even under social planning.[5] Nonetheless, the present case yields, in most situations, a higher coverage compared to both Stackelberg and Nash cases. This can be better understood from the limit cases where the social planner assigns a unit weight to either groups. These cases are discussed easily. Note instead that if $x = 1$ then:

$$p_1^{Soc} = \hat{p}_1 = 0; \qquad p_2^{Soc} = \hat{p}_2 = p_{2,c}^{\star} \tag{5.21}$$

Therefore under *type* c, there exists an optimal social planning solution which allows elimination. On the other hand, if $x = 0$ then: $\hat{p}_1 = p_{1,c}^{\star} > 1$ and $\hat{p}_2 = 0$. Therefore

$$p_1^{Soc} = 1; \qquad p_2^{Soc} = \frac{f_2^2 H^2}{f_2^2 H^2 + \beta_2 \alpha^2} \left(p_{2,c}^{\star} - \frac{f_1}{f_2} \right) \tag{5.22}$$

It is easy to see that this solution does not allow elimination since it yields an overall coverage lower than p_c:

$$\begin{aligned} p^{Soc} &= p_1^{Soc} f_1 + p_2^{Soc} f_2 \\ &= f_1 \left(1 - \frac{f_2 H^2}{f_2 H^2 + \beta_2 \alpha^2} \right) + p_c \frac{f_2 H^2}{f_2 H^2 + \beta_2 \alpha^2} < p_c \end{aligned} \tag{5.23}$$

To sum up, for $x = 1$ social planning yields a feasible elimination policy if group 2 is large enough to eliminate *alone*.

The overall implications of different weights given by the social planner to the two groups in the social loss functions are illustrated (Fig.5.5) for a highly transmissible disease with $R_0 = 10$ ($p_c = 0.9$) and $f_2 = 0.9$. This means $p_{c2}^{\star} = 1.0$, i.e. that a vaccine demand of 100% in group 2 would be required to achieve elimination when group 1 does not vaccinate. In addition we assume that group 2 has a cost of VSE smaller than the cost of infection ($\beta_2 = 0.75$) whereas for group 1 this cost is much higher ($\beta_2 = 2.5$). It happens (Fig.5.5a) that the vaccine demand in group 1 is constant at 100% ($p_1^{Soc} = 1$) for very small x values, but as x exceeds a threshold value it starts to fast decline up to zero. Similarly, the vaccine demand in group 2 is initially constant at a level around 76%, but when the vaccine demand of group 1 starts declining it starts increasing and reaches universal coverage for $x = 1$. As regards the overall coverage (Fig.5.5b) this is initially constant around the level of 78%, but when coverage in group 2 starts increasing it starts increasing as well, achieving the elimination threshold $p_c = 0.9$ for $x = 1$. All this is consistent with our theoretical findings. It is interesting to note that social planning does not necessarily yields an improvement of the Nash solution (the flat line in Fig.5.5b): this happens only when the vaccine demand in group 2 becomes sufficiently high, which does

[5] It is possible to envisage other social planner functions, based on very different perspectives, that might lead to elimination.

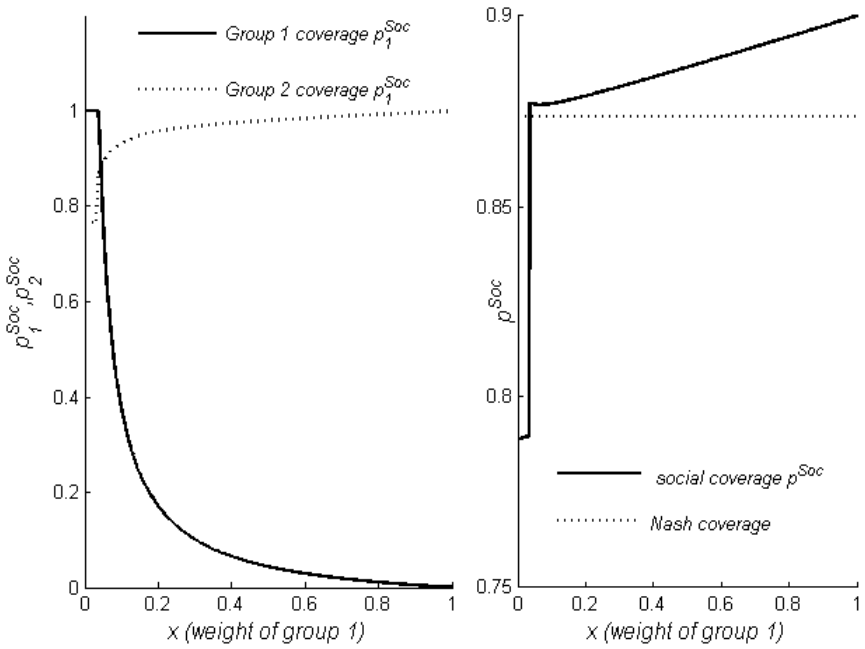

Figure 5.5: The social planner case. (a) the optimal vaccine demand in groups 1,2 (p_1^{Soc}, p_2^{Soc}) as functions of the weight x attributed to group 1 in the social loss function; (b) Overall vaccine demand (p^{Soc}) versus the corresponding quantity in the Nash case. Parameter values: $R_0 = 10, \beta_1 = 2.5, \beta_2 = 0.5, \alpha = 0.2, f_1 = 0.1$.

not occur if x is close to zero.[6] Note also that if the social planner assigns to group 1 a weight proportional to its demographic frequency ($x = 0.1$), which *a priori* could appear a reasonable choice, an overall coverage of 87.7% follows, which is better than the Nash coverage.

The results for $x = 1$ and $x = 0$ lead to interesting remarks. Note that for $x = 1$ elimination does not require that $\beta_2 = 0$, as in the Nash and Stackelberg cases. The explanation is that for $x = 1$ the preferences (i.e. the costs) of group 2 are not taken into consideration by the social planner (whereas those of group 1 fully are), so that group 1 achieves its optimum (not vaccinating at all), and then group 2 needs to supply residually the amount of vaccination needed to minimize the social loss function. It happens that this amount is, consistently with the frequencies of the two groups, the one required to eliminate the disease. In more concrete terms, for $x = 1$ the social planner gives whole weight to the preferences of anti-vaccinators, and no weight to the preferences of vaccinators, on the assumption that this is a good way to achieve the social optimum i.e. disease elimination. This means that *vaccinators* contribute fully altruistically to the

[6]We note that the Nash solution results slightly better than the Stackelberg one (not reported in the figure). Moreover under not-fully informed families an increase in the overall coverage will follow, in line with our previous findings.

social optimum, since they entirely supply the elimination effort. It is also interesting to note that the opposite case ($x = 0$), i.e. *full weight* to the pro-vaccinators preferences, is the one yielding the worse result in terms of coverage, even worse of the non-cooperative Nash outcome.

5.4 Discussion: can we get off the no-elimination trap?

A variety of models of vaccination choice, both without and with strategic behavior, have been investigated, under both informed, and not-fully informed agents.

The analysis of the non-strategic choice indicates that informed families knowing the herd immunity principle will always vaccinate below the critical threshold as soon as they suffer any, however small, cost of VSE, while a high collective coverage is much more likely to be achieved if families are not aware of herd immunity. The analysis of the strategic case, carried out on the assumption of the existence of a vast (fixed) majority of agents having a small perceived cost of VSE (labeled as *pro-vaccinators*) versus a minority having a high perceived cost of VSE (*anti-vaccinators*), confirms that in presence of fully informed families disease elimination continues to be impossible unless pro-vaccinators do not associate any cost to vaccine side effects, and moreover their frequency is in excess of the critical elimination coverage. If anti-vaccinators *lead* the game, i.e. in the Stackelberg case, the outcome in terms of coverage will be worse compared to the Nash case. Even if the State aims at favoring *cooperative* behavior through social planning, elimination is possible only when the State takes into account in the social loss functions the preferences of anti-vaccinators only[7]. This scenario seems to be representative of the current Italian situation, where the possibility to switch from a compulsory to a voluntary vaccination system is actively debated, and one region, Veneto, has recently *made the step* [60]. In this context, under the pressure of anti-vaccinators, the Italian government has gradually accepted an increasing number of right claims by anti-vaccinators, for example it has removed the parents' duty to vaccinate their children in order to enroll them to compulsory school grades. This can be interpreted as a massive increase of the weight of anti-vaccinators in the social loss function. Our results indicate that a social planning policy of this sort, i.e. paying more weight to anti-vaccinators, seems to be *technically* correct (in fact in the opposite case, where the State takes into account the preferences of pro-vaccinators only, dramatically low coverage would follow, even worse than the Stackelberg outcome.). However such static results figure out the possible dynamic unsustainability of such a policy. Indeed, how to prevent migrations towards the anti-vaccine choice, if this starts to be more generally perceived as more protective of children's health? Though the consideration of migration between groups would require a dynamic model (as [15]),

[7]Clearly this result relies upon the adopted form of the social loss function. This does not exclude that other social planner functions, based on different perspectives, for example including the Government loss, could allow to achieve elimination under weaker conditions. We thank an anonymous referee for this remark.

we note that global socio-economic trends are not favorable in this sense: empirical studies indicate that often those vaccinating less are the more educated, or the richer, ones [18, 142]. One can certainly invoke the economic argument that no free-rider groups can expand above a certain threshold. In epidemiological terms this means that any further expansion in the anti-vaccinator group will decrease the degree of herd immunity and will therefore be stopped by the necessary re-emergence of the disease. The public health dangerousness of such a situation, think for instance to slow declines in herd immunity due to slow migrations toward the anti-vaccinator group, call for a careful monitoring of such processes.

The case of not fully informed families produces, as a rule, better outcomes. However it also raises substantive questions. Which information mechanisms cause real communities to polarize into a majority who usually vaccinates universally, and a very active minority who is strongly reluctant to vaccinate? Our model static is not capable of explaining polarization (it just postulates it) it strongly suggests that universal vaccination in the majority follows from: a) a very small cost associated to VSE, b) the lack of knowledge of the critical threshold, i.e. parents believing that a propensity to vaccinate of 100% is necessary to fully protect children against disease. This wrong perception (mathematics tells indeed that the critical threshold for disease elimination is always less, sometimes substantially less, than 100%) is the likely cause of the asymmetry of the *real world* vaccination game. Asymmetry stems from the fact that certain group of agents might instead have a correct knowledge of herd immunity. But this asymmetry is dangerous for the public health system since it implies the uneven situation where someone takes the risks of vaccine side effects to protect all, as a consequence of limited information. This further enhances the danger that people improve their information set, and as a consequence rationally *migrate* towards the anti-vaccinator group.

In conclusion, do we need to fear RE? Mathematics shows that RE can be devastating for immunization programs [16, 15, 36, 48, 49], [131]. This is especially true when rumors, e.g. the MMR scare [135], contribute to disproportionately increase perceived risks of vaccine associated side effects compared to the perceived risk of infection [142]. As regards remedies against RE, first economic papers on the subject [23, 72] suggested that the free-rider problem might partly be overcome through e.g. taxes and subsidies. A recent modeling effort [124] has shown that the free-rider effect may be amplified by the assumption of homogeneous mixing, and that the problem can be largely reduced when more realistic contact networks are considered. Be things as they may, the actual impact of vaccination free-riding is hard to predict: RE is human behavior, which, as recently pointed out, is a *missing factor* of our epidemiological explanation [56].

However, better mathematical models could help to improve our understanding of such phenomena, and to design more informative studies of vaccination behavior, possibly aimed to also capture *strategic* parameters. On the other hand we believe that for those public health systems that have already initiated a *roadmap* towards voluntary vaccination, as in Italy is the case of Veneto region [60], investment in education to the social role of vaccination will be an unavoidable task in the future.

Chapter 6

The impact of vaccine side effects on the natural history of immunization programs: an imitation-game approach

6.1 Introduction

Although forms of exemption to vaccination have always existed [139], the "natural history" of vaccination programmes, as part of the historical pathway through which humankind progressive rids itself of infectious diseases, has always been pervaded by a high degree of optimism [30]. However, recently this optimistic view has increasingly been challenged: for example, opposition to the whole-cell pertussis vaccine [70], the thimerosal case [106], and the MMR scare [135] can be considered evidence that in industrialized countries, the success story of vaccination is feeding back on itself. This is the consequence of two different processes. On the one hand, the high degree of herd immunity achieved by decades of successful immunization programmes has reduced the incidence of many infections to negligible levels. On the other hand the large, and increasing, number of vaccines routinely administered every year yields steady flows of vaccine-associated side effects [160], [159]. In the US approximately 30,000 reports of Vaccine Adverse Events are notified annually, with 10–15% classified as serious [62]. In such circumstances the perception of the public will likely rank the perceived risk of suffering a vaccine side effect (VSE) as much higher than the corresponding risk of infection [16, 15, 48, 49]. A common example is poliomyelitis in industrialized countries. For example in Italy during 1980-2000 the number of vaccine-induced polio cases was three times higher than wild polio cases [43]. Under voluntary vaccination high degrees of herd immunity might therefore incentivise vaccination free riding [23],[131], i.e. the parents' decision not to vaccinate children after comparing the perceived risk of disease and the perceived risk of vaccine side effects [16, 15, 48]. Vaccination free riding [23, 61, 72, 16, 15, 48, 49, 46, 131, 129, 69] makes eradication impossible (unless special contact structures are considered [124]) and

triggers stable oscillations in the infection prevalence.
Previous studies on the impact of vaccination free riding on endemic infections have focused on scenarios where the vaccine demand is driven by the time changes in the perceived risk of disease, measured through the current (or past) infection prevalence. Based on the above-cited literature on VSEs we instead suggest that in industrialized countries, where the incidence of common vaccine preventable infections is very low, the available information on vaccine side effects might become the main driving force of vaccine demand. The only paper devoted to this issue is [46], where, however, vaccine demand was phenomenologically modelled as a decreasing function of the perceived risk of suffering a vaccine-associated side effect. The perceived risk of VSEs was in its turn evaluated by the public from available information on current and past trends of side effects attributed to the vaccine. In this paper we shift the focus onto the impact of VSEs on the dynamics of immunization programmes for endemic infections, using an SIR transmission model with voluntary vaccination choice. Vaccination choices are described by an evolutionary game as in [15], where the vaccine uptake $p(t)$ is determined by an imitation process between agents (the parents of the children to be vaccinated) who are divided into "vaccinators" and "non-vaccinators". However, in [15] the perceived payoff of the "non-vaccinators" is proportional to the prevalence of the disease, whereas the payoff of "vaccinators" is constant, i.e. independent of VSEs).
The novelty of the present work is that the payoff of "vaccinators" is proportional to the incidence of vaccine-associated side effects. In turn, this incidence is proportional to the actual vaccine uptake. We believe that this model represents a more appropriate description of the future evolution of immunization programmes in voluntary vaccination regimes. Indeed, the fact that available information on vaccine side effects might become the main driving force of vaccine demand is strongly supported by the empirical evidence, e.g. the case of England and Wales, where due to the MMR scare[135], first dose measles uptake fell for several years from 94% to about 75%. Compared to [15] we also expand our basic model to include (a) nonlinear perceived costs of infection; (b) the possibility that the perceived costs of infection and vaccination are evaluated by the public using past values of state variables, for example due to information delay [49] or of the perception of long-term vaccine side effects [46].

6.2 Materials and Methods

6.2.1 Dynamic vaccine demand and vaccine side effects

We consider a family of models of the spread of a non-fatal SIR infection controlled by voluntary vaccination with a "perfect" vaccine administered in a single dose at birth and

giving life-long immunity:

$$S' = \mu(1-p) - \mu S - \beta SI \tag{6.1}$$

$$I' = \beta SI - (\mu+\nu)I \tag{6.2}$$

$$p' = k_1 \Delta E p(1-p) \tag{6.3}$$

where: S, I are the susceptible and infective fractions, and p the vaccinated proportion among newborn children; $\beta > 0$, $\mu > 0$, $\nu > 0$ denote the transmission, the mortality and the recovery rates. We assume that, in absence of vaccination, the disease is endemic, i.e. $R_0 = \beta/(\mu+\nu) > 1$.
The dynamics of p obeys a *learning by imitation* [81] process where k_1 is the "imitation" coefficient and switching between the decisions to vaccinate or not to vaccinate, is determined by the payoff gain $\Delta E(t)$. The latter is given by the difference between the perceived payoff of vaccinators $-\rho_V(t)$, where $\rho_V(t)$ is the perceived risk of suffering a VSE, and the perceived payoff of non-vaccinators: $-\rho_I(t)$, where $\rho_I(t)$ is the perceived risk of suffering serious illness due to infection.
We note that, irrespective of the specific forms of $\Delta E(t)$, the family of models (6.1-6.2-6.3) has the following three equilibria: (i) an unstable disease-free equilibrium with no vaccinators $A = (1,0,0)$; (ii) a pure-vaccinator disease-free equilibrium $B = (0,0,1)$; (iii) the pre-vaccination equilibrium $C = \left(S_{SIR} = R_0^{-1}, I_{SIR} = \mu(1-R_0^{-1})/(\mu+\nu), 0\right)$.
The stability of B and C and the existence of further equilibria depend on the specific types of the payoff gain.
Modelling of the dynamics of p by an imitation game was introduced in the seminal paper [15], where a specific model of the family (6.1-6.2-6.3) was proposed, where: *i)* the perceived payoff of vaccinators is constant:$-\rho_V = -r_V$; and *ii)* the perceived payoff of non-vaccinators is proportional to the infective prevalence $I(t)$: $-\rho_I(t) = -r_I m I(t)$, where $mI(t)$ is an estimate of the current risk of infection, and r_I is the risk of serious disease as a consequence of infection. Hence:

$$\Delta E(t) = r_I m I(t) - r_V = r_V\left(\vartheta I(t) - 1\right),$$

where $\vartheta = m r_I / r_V$ is proportional to the relative cost of the non-vaccinator strategy.
In Bauch's model the B equilibrium is unstable and there is a fourth equilibrium: the post-vaccination equilibrium $D = \left(R_0^{-1}, \vartheta^{-1}, \widehat{p}\right)$ where: $\widehat{p} = (1+\nu/\mu)\left(I_{SIR} - \vartheta^{-1}\right)$. At $\vartheta = \vartheta_0 = I_{SIR}^{-1}$ there is a transcritical bifurcation between C and D. In turn, the stability/instability of D depends on the product $k_1(\vartheta - \vartheta_0)$.
The assumption in [15] that the perceived risk of vaccination $\rho_V(t)$ is constant can be justified if the public correctly evaluates this risk as the ratio between total VSEs per unit time, given by $\alpha\left(\mu N\right) p(t)$ $(\alpha \in (0,1))$ where N is the total population size (so that μN is the yearly number of births), and α the per-capita probability of incurring a VSE during a single vaccine administration, and the total number of vaccinations administered for that specific disease $\mu N p(t)$. We instead suppose that the public evaluates the risk of VSEs by using the available information on the total number of vaccine-associated side

effects, or, which is equivalent, on the ratio between the total number of vaccine associated side effects and the total number of newborn children per unit of time. We therefore set:

$$\rho_V(t) = \alpha p(t) \tag{6.4}$$

The implication of (6.4) is that periods of large vaccine uptake negatively feed back, through an increase in the incidence of VSEs, into the proportion of parents favourable to vaccination.
We model the perceived risk of infection as an increasing function $h_1(\cdot) \geq 0$ of the information index M, introduced in [48, 49], that summarizes the publicly available information on the infection:

$$\rho_I(t) = h_1(M(t)). \tag{6.5}$$

The index M, used by agents to evaluate the risk of infection, may model not only current, but also past information. The case $h_1(0) > 0$ accounts for the scenario where the disease is locally eliminated but disease re-emergence by external reintroduction is feared. In the simplest case, the information index $M(t)$ is related to the current $I(t)$ as follows:

$$M(t) = h_2\left(I(t)\right), \tag{6.6}$$

where $h_2(\cdot) > 0$ and $h_2'(\cdot) > 0$. Using (6.4)-(6.5)-(6.6) the dynamics of p can be written as follows:

$$p' = k\left(h(I) - p\right) p\left(1 - p\right) \tag{6.7}$$

where $h(I) = \alpha^{-1} h_1(h_2(I))$, $k = \alpha k_1$.
First, note that from: $p' \geq k\left(h(0) - p\right) p\left(1 - p\right)$ it follows that $h(0) \geq 1 \Rightarrow p(t) \to 1$, so that we shall not consider this trivial case. On the contrary, if $h(0) < 1$ then $p(t) \geq h(0)$ holds asymptotically, i.e. the collective coverage will at least reach the minimal level $h(0)$. Symmetrically, inequality $p' \leq k h^{Max} p\left(1 - p\right)$ means that $p(t)$ is bounded by a logistic dynamics with kinetics constant $k h^{Max}$. Finally, if imitation dynamics is faster than the infection time scale: $k >> (\mu + \nu)^{-1}$, then $p(t)$ is at quasi-equilibrium:

$$p(t) \approx \min\left(h\left(M(t)\right), 1\right), \tag{6.8}$$

which is the phenomenological relationship first proposed in [48].

6.2.2 The importance of time delays

The assumption that ΔE depends only on current values of I and p is an approximation. For example agents might perceive that vaccines are responsible for VSEs arising with long time delays [46], as might be the case with auto-immune diseases [116]. Moreover, delays of different nature, concerning the information on the spread of the disease, may involve

both $p(t)$ and $M(t)$ [48]. Thus in the case in which the perceived risk of vaccination is evaluated on past VSEs:

$$\rho_V(t) = \int_{-\infty}^{t} Q_H(T_v)\alpha p(t - T_v)dT_v \tag{6.9}$$

where Q_H is a delay kernel. An important kernel is the *exponentially fading memory*: $Q_H(x) = bExp\left(-bx\right),\ b > 0$, which allows reduction to ODE since it holds that:

$$\rho_V' = b\left(\alpha p(t) - \rho_V\right). \tag{6.10}$$

Scenarios such as long-term VSEs may require different kernels, more concentrated on past periods, such as the Erlang functions: $A_n x^{n-1} Exp(-bx)$, also allowing reduction to ODEs.

6.3 Results

6.3.1 Endemic equilibria and their stability

In this section we shall investigate the model (6.1)-(6.2)-(6.7) where no delays are present. Considering a generic $h(I)$, the system (6.1)-(6.2)-(6.7) has three equilibrium points A (unstable), B (unstable) and C, which, unlike [15], is always unstable since the linearized equation for p reads $\eta' = kh\left(I_{SIR}\right)\eta$. Moreover, two further equilibria are induced by the specific ΔE we introduced:

- A disease-free equilibrium with positive vaccine uptake $E_{dfe} = (1 - h(0), 0, h(0))$.
- A new behaviour-related endemic equilibrium:

  $$E_{beh} = \left(R_0^{-1}, I_e, h\left(I_e\right)\right),$$

  where I_e is the unique solution of the equation:

$$h(I) = 1 - R_0^{-1} - \frac{\mu + \nu}{\mu} I. \tag{6.11}$$

Remark 6.3.1. *The equilibrium E_{beh} is equal to the endemic equilibrium of the model studied in [46], where, however, p is not a state variable.*

Since all equilibria are independent of k, this makes it natural to choose k as a bifurcation parameter. Our main results (demonstrated in the *Appendix* 8.3) are as follows:

A) If

$$\beta I_e \mu h'\left(I_e\right) < (\mu + \beta I_e)\left((\mu + \beta I_e) + 2\sqrt{\beta I_e(\mu + \nu)}\right) \tag{6.12}$$

then E_{beh} is locally asymptotically stable (LAS) irrespective of the imitation speed k;

B) On the contrary, if

$$\beta I_e \mu h'(I_e) > (\mu + \beta I_e)\left((\mu + \beta I_e) + 2\sqrt{\beta I_e(\mu+\nu)}\right) \tag{6.13}$$

holds then there are two positive values k_1 and $k_2 > k_1$ such that:

1. If $0 < k < k_1$ or $k > k_2$ then E_{beh} is LAS;
2. At $k = k_1$ and at $k = k_2$ there are Hopf bifurcations;
3. If $k \in (k_1, k_2)$ then E_{beh} is unstable.

C) In the case $k \in (k_1, k_2)$ the orbits $x(t) = (S(t), I(t), p(t))$ are oscillatory in the sense of Yabucovich. This intuitively means that for sufficiently large t all state variables are permanently oscillating, with regular or irregular oscillations. Formally, for $j = 1, 2, 3$ it holds that:

$$minlim_{t\to+\infty} x_j(t) < maxlim_{t\to+\infty} x_j(t).$$

D) If $h_0 > p_c$ then E_{dfe} is globally asymptotically stable (GAS); if $h_0 < p_c$ then E_{dfe} is unstable.

Remark 6.3.2. *Note that the r.h.s. of (6.13) is $O(\mu^{3/2})$, whereas $\mu\beta I_e$ is $O(\mu^2)$, implying that to have Hopf bifurcation at E_{beh} the derivative of h there has to be at least of order $O(\mu^{-1/2})$*

Remark 6.3.3. *Property **D** shows that, unlike [15], elimination is possible in our model, although only if in absence of the disease the vaccinator payoff is so large as to yield a vaccine uptake greater than the elimination threshold.*

To better understand the phenomenon of epidemic oscillations driven by vaccination choice we compare the above results with the recent literature on this subject. Unlike [15] where large values of $k(\vartheta - \vartheta_0)$ induce sustained oscillations around the endemic state, in our model oscillations are possible in an intermediate window of values of the imitation coefficient k. This means that both slow and fast imitation are stabilizing forces. Moreover, we note that the stability condition (6.12) has the same formal structure as that of the *delayed* model in [48], where dependence of the current vaccine uptake on past incidence was required to obtain oscillations. Indeed, imitation is a (nonlinear) adjustment process introducing a delay, whose characteristic time scales are determined by the speed with which the vaccine uptake reacts to changes in the payoff gain. Heuristically, close to the equilibrium eq. (6.7) becomes:

$$p' \approx kh(I_e)(1 - h(I_e))(h(I) - p) = \Psi(h(I) - p) \tag{6.14}$$

which may be read as an exponentially fading memory mechanism with average delay $1/\Psi$. This suggests a route to estimate the elusive imitation coefficient k, by preliminarily estimating the average delay $1/\Psi$.

Finally, we note that the Yabucovitch oscillatority is a global result, unlike the Hopf bifurcation theorem, which is local. Although the nature (periodic, quasi-periodic or chaotic) of Yabucovitch oscillations cannot be determined a priori, this makes the predictions of our model very general.
Finally, it is easy to show that the inclusion of time delays does not affect the location and stability of equilibria A, B, C and E_e, whereas the stability of E_{beh} may be affected, as seen in the numerical simulations below (see also the *Appendix* 8.3).

6.3.2 Analysis of selected subcases

We report numerical illustrations of noteworthy sub-cases of epidemiological interest. The basic reproduction number R_0 is set to 10; the recovery rate is set to either $\nu = 0.1\text{day}^{-1}$ (pertussis) or $\nu = (1/7)\text{day}^{-1}$ (measles), which correspond to an average duration of respectively 10 days (pertussis) and one week (measles). Finally the life expectancy $L = 1/\mu$ is fixed either at $L = 50$ years (used in [15] to more closely reproduce UK pertussis data) or at $L = 75$ years, which is more representative of mortality in modern industrialized countries.

The basic unlagged model: the case of linear $h(I)$

Letting $h(I) = \vartheta I$, the infection prevalence at E_{beh} is:

$$I_e = I_e(\vartheta) = \frac{1 - \frac{1}{R_0}}{1 + \frac{\nu}{\mu} + \vartheta} = I_{SIR}\frac{1 + \frac{\nu}{\mu}}{1 + \frac{\nu}{\mu} + \vartheta}$$

and the vaccine uptake is:

$$p_e(\vartheta) = \vartheta I_e(\vartheta) = p_c\frac{\theta}{1 + \frac{\nu}{\mu} + \vartheta} \tag{6.15}$$

As regards the stability of E_{beh}, it is of interest to assess the relative role of the two main behavioral parameters introduced by our model: ϑ and k. By applying (6.13) it is easy to show that a ϑ^* exists such that for $\vartheta > \vartheta^*$ then (6.13) is fulfilled and the two branches $k_1(\vartheta)$ and $k_2(\vartheta)$ of the bifurcation curve in the space (k, ϑ) exist and are analytically computable. Below ϑ^* the equilibrium E_{beh} is (at least) locally stable.
For example in the case $\nu = 0.1$ day^{-1}, $\mu = 1/50\text{year}day^{-1}$ it is $(\vartheta^*, k^*) \approx (280, 0.042)$, from which the two branches $k_1(\vartheta)$ and $k_2(\vartheta)$ of the Hopf curve depart. For $\vartheta = 1000$ (implying $I_e = 3.18 \times 10^{-4}$ and $p_e = 0.32$) we obtain $k_2^{-1} = 4.75$ days and $k_1^{-1} = 312$ days a range difficult to interpret. However, the heuristic average imitation delay $1/\Psi$ correspondingly ranges between three weeks and about four years, close to the values found in [48]. The bifurcation curve in the (k, ϑ) and (k^{-1}, ϑ) parametric spaces are shown in Fig. 6.1.

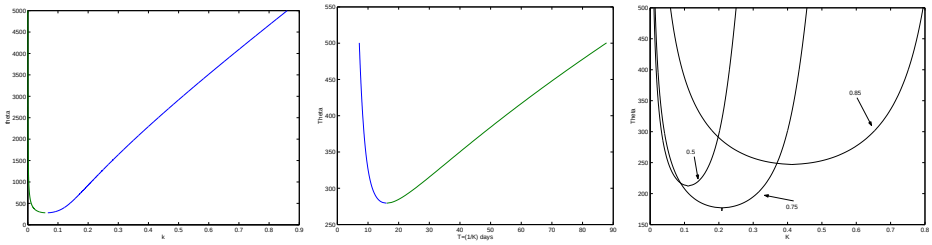

Figure 6.1: Bifurcation curve for linear and linear affine $h(I)$, in the case $R_0 = 10$, $\nu = 1/10$ day^{-1}, , $\mu = 1/50$ year^{-1}. (left-hand panel) Bifurcation curve for linear $h(I) = \vartheta I$ in the parameter space (k, ϑ). (Central panel) Bifurcation curve for linear $h(I) = \vartheta I$ in the parameter space (k^{-1}, ϑ) emphasizing patterns for small imitation-related delays. (Right-hand panel) Bifurcation curve for linear affine $h(I) = p_0 + \vartheta I$ plotted for three values of p_0. As p_0 increases the minimal threshold of ϑ is non-monotone.

The basic unlagged model: the case of linear-affine $h\,(I)$

The case $h(I) = \vartheta_0 + \vartheta I$ is of interest since it assumes that even in scenarios of zero prevalence agents perceive a positive risk ϑ_0 of infection re-emergence. We get:

$$I_e(\vartheta) = \frac{1 - R_0^{-1} - \vartheta_0}{1 + \frac{\nu}{\mu} + \vartheta},\ p_e(\vartheta) = \vartheta_0 + \vartheta \frac{1 - R_0^{-1} - \vartheta_0}{1 + \frac{\nu}{\mu} + \vartheta}$$

Thus the perception of such a risk has a positive effect on equilibrium uptake. The dependence of the bifurcation curve on ϑ_0 may be non-monotone, as in the right-hand panel of Fig. 6.1.

6.4 Substantive implications of vaccine side effects for vaccination programmes

6.4.1 The epidemiological transition and vaccination payoff

We use equilibrium results from the simple case of linear $h(I)$ to explore the impact of human progress on the natural history of vaccination programmes. Note that in the parametric set we are considering the quantity ν/μ ranges from about 1826 (pertussis in a population with low life-expectancy) up to about 3913 (measles in a population with high life-expectancy). Thus, achieving a large equilibrium uptake requires very large ϑ, i.e. of the order of ν/μ. Since $\vartheta = r_I m/\alpha$, it follows that to achieve large equilibrium uptakes for measles or pertussis, the perceived cost of serious disease has to be at least three order of magnitude higher than the perceived cost of VSE. Though this seems surprising, we feel it is consistent with what was still observed at the beginning of the 20th century, when the risk of serious sequelae following measles or scarlet fever was extremely large (100-250 deaths per 100000 cases of disease), and the absence of vaccines was keeping the risk of infection very high. In such circumstances even a large probability of suffering a

VSE from a vaccine could have been tolerated by the community. This also suggests that in industrialized countries the recent (say after 1970-1980) 'big vaccination age' is coming to an end due to the completion of the epidemiological transition [143], i.e. the historical change in the cause composition of mortality from infectious and nutritional diseases to chronic degenerative ones. Indeed, an outcome of the transition has been the dramatic fall in the levels of serious morbidity and mortality from all infectious diseases. Finally, as regards the role played by life expectancy on the steady state E_{beh}, our results suggest that the achievement of a given equilibrium uptake in industrialized countries (i.e. with a very high life expectancy) requires a much larger value of ϑ compared to developing countries. This is consistent with the fact that in regimes with low mortality (also as a consequence of vaccinations), agents demand a vaccine only if the relative risks of suffering a VSE are very low. We stress that our predictions are equilibrium ones based on a simple deterministic model with homogeneous mixing. Nonetheless more realistic models would not substantially affect them.

6.4.2 Simulations

In our simulations we set $h(I) = \vartheta I$ and, to better emphasize our main messages, we allow immigration of infectives, according to two different hypotheses: **a)** a small constant transfer Imm from the susceptible to the infective state, representing a steady flow of infections as a consequence of international travelling; **b)** a few new infections appear at some stage once and for all, in order to mimic the possibility of infection resurgence. Indeed, in the oscillatory regime the infection prevalence $I(t)$ may reach extremely low values, which calls into question the appropriateness of a deterministic model. This drawback is avoided by assumption **a**, also used in [15]. Imm is set to one infective individual per week in a population of 5×10^6 individuals.

The basic unlagged model

We first assess the impact of VSEs on the transient infection dynamics triggered by a new vaccination introduced at the pre-vaccination endemic state, and under assumption **a**. The vaccine is introduced at time $t = 0$, with initial vaccine uptake set to $0.95 > p_c$. Vaccine side effects occur from the beginning of the programme. We set $\vartheta = 15000$ (implying $p_e \approx 0.71$, $k = 0.002$ day^{-1} and $1/\Psi \approx 7$ years). Note that k is small since it is the product between the natural imitation rate and the low probability α of suffering a VSE. As predicted by (6.13), the system converges, in epidemiologically reasonable time scales, to a stable limit cycle. With reference to Fig. 6.2, the vaccine uptake (right-hand panel) starts declining soon after the programme starts, due to the onset of VSEs, and falls below the critical threshold p_c in less than four years. Thus the effective reproduction number $R_E(t) = R_0 * S(t)$ (left-hand panel) initially declines but then increases and exceed the unit threshold at $t \approx 8$ years, yielding a new epidemic outbreak at $t \approx 10$ years. During this rather long 'honey-moon' period the circulation of the infection is essentially sustained by immigration. Note that $p(t) > p_c$ for a rather long period of

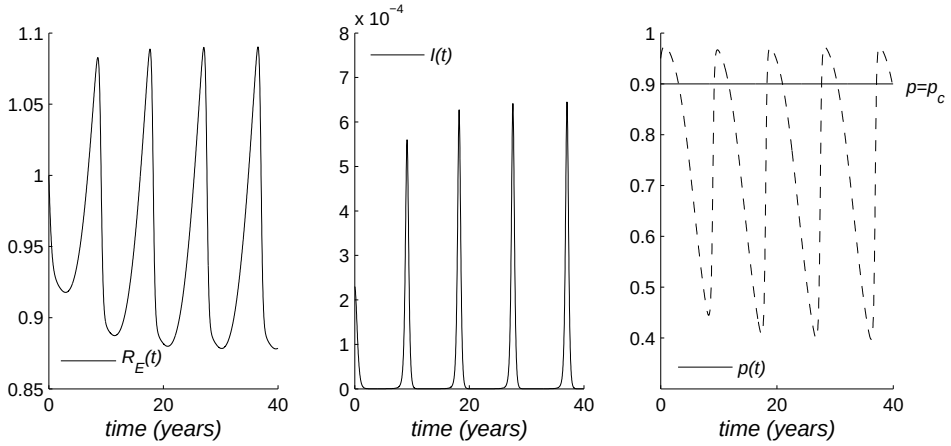

Figure 6.2: The unlagged model with linear $h(I)$: dynamics of $R_E(t)$ (left-hand panel), $I(t)$ (centre), $p(t)$ (right-hand panel), following the initiation of an immunization programme with $p(0) = 0.95$; S_0, I_0 fixed at their pre-vaccination endemic state. Parameters: $R_0 = 10$, $\nu = 1/7$ day^{-1}, , $\mu = 1/75$ year^{-1}, $\theta = 15000$,$k = 0.002$ day^{-1}.

time (about 36 per cent of total time). During such periods routine vaccination surveys would reveal a satisfactorily high coverage. Therefore they could not explain the endemic persistence of infection.

The role played by k is illustrated in Fig. 6.3, which considers the values: $k = 0.0005$, $k = 0.002$ (as before), $k = 0.0035$, and which shows that: *i)* the average uptake is not significantly affected by k and remains close to p_e; *ii)* both the amplitude of oscillations of $p(t)$ and the fraction of total time where $p(t) > p_c$ increase in k; *iii)* the duration of the period between the start of the programme and a new epidemic outbreak is decreasing in k. For example, the 'low' k value ($k = 0.0005$) yields oscillations that are of small amplitude and that for a small portion of their period are such that $p(t) > p_c$. Moreover, there is an interval of about 17 years about before a new epidemics, which is only a few years long for $k = 0.0035$. This is the consequence of the slow spread of information occurring for low k, which slows down the reactivity of the vaccine uptake to changes in the payoff gain. Note that if no external infections are introduced, then for small k the infection prevalence is close to zero. This suggests that oscillations might produce stochastic elimination of infection.

We now study the introduction of a new vaccine for which no vaccine side effects are initially known. In this case it seems reasonable to assume that an intermediate period might exist during which no perception of VSEs arises. We consider $\alpha = 0$ for $t < t_1$ where $t_1 = 10$ years, and that the starting point is the pre-vaccination steady state. Of course, the vaccine uptake start increasing since the payoff vaccination is initially positive ($\alpha = 0$). If VSEs raise after a very long time, or no VSEs are reported, then stochastic elimination is possible. By contrast, if evidence of VSEs emerges, the scenario reduces straightaway to the cases treated above. If the imitation process is very slow, VSEs appear before reaching a sufficient coverage and a sub-optimal vaccination coverage is achieved

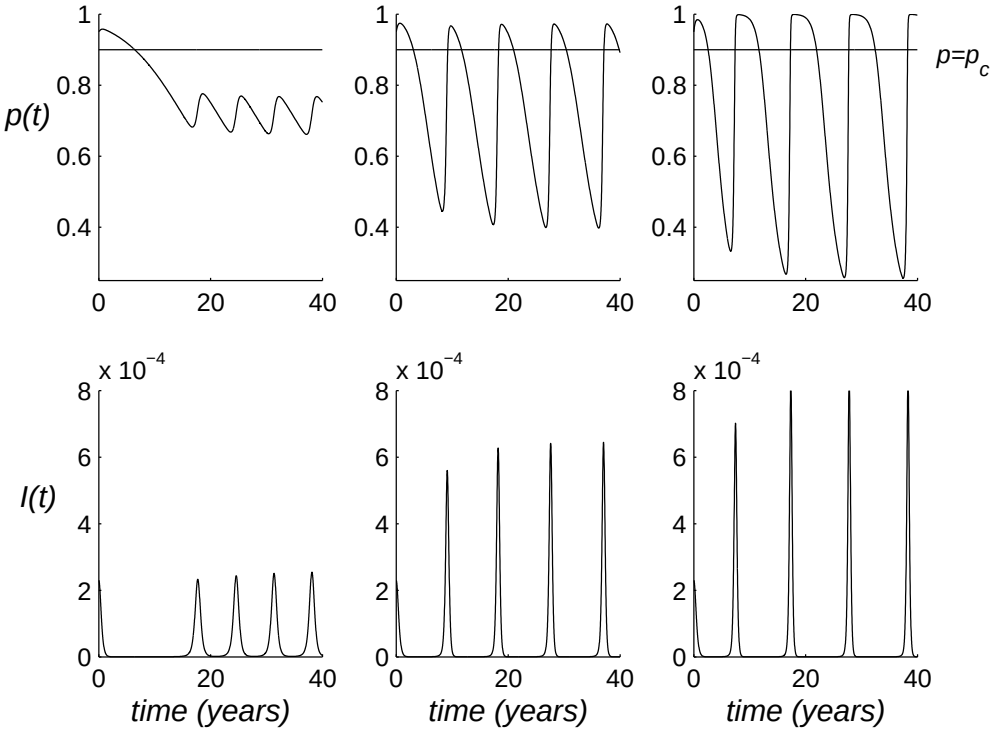

Figure 6.3: The unlagged model with linear $h(I)$: dynamics of $p(t)$ (top) and $I(t)$ (bottom), for $k = 0.0005$ (left), $k = 0.002$ (centre), $k = 0.0035$ (right) following the initiation of an immunization programme with $p(0) = 0.95$; S_0, I_0 fixed at their pre-vaccination endemic state. Other parameters: $R_0 = 10$, $\nu = 1/7$ day^{-1}, , $\mu = 1/75$ year^{-1}, $\theta = 15000$.

(left-hand panel of Fig. 6.4). Instead for a larger value of k, the infective fraction is very close to 0 such that stochastic elimination may occur (central panel of Fig. 6.4). Finally, for an intermediate range of k there is onset of oscillations, but at the end of their transitory the minimum $I(t)$ is very close to 0 and elimination can again occur (right-hand panel of Fig. 6.4).

Finally, we simulated the case where eradication was achieved thanks to a period of compulsory vaccination, after which vaccination becomes voluntary. In this case VSEs induce individuals to switch to the 'non-vaccinator' strategy, thereby producing a decrease in vaccination coverage. This in turn increases the probability of infection re-emergence from imported cases. If a few new external infections are introduced (assumption **b**) before $R_E(t) = 1$, then the occurrence or not of stochastic transient elimination depends again on k, with patterns similar to the previous case (see Fig. 6.5.a,6.5.b,6.5.c). Moreover, if individuals take into account a non zero risk of infection re-emergence from importation (the linear affine case $h(I) = \vartheta_0 + \vartheta I$), the population is more 'protected' and the impact of the external infections can be reduced also for large values of k (see Fig. 6.5.d).

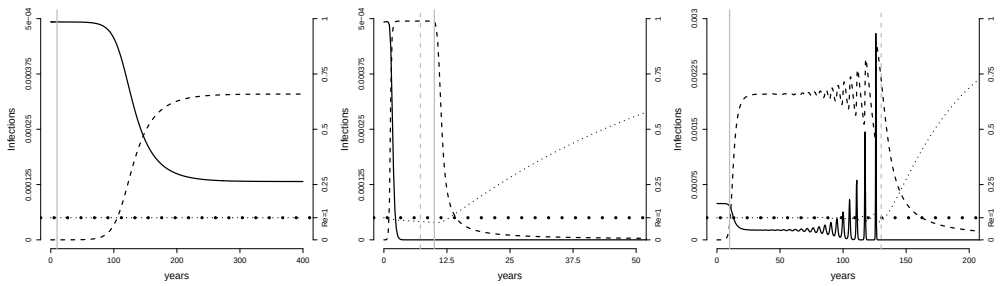

Figure 6.4: Dynamics of $I(t)$ (black line), $R_0S(t)$ (dotted black line), $p(t)$ (dashed black line) with (a), $k = 0.0001$ (b) and $k = 0.001$ (c). The vertical grey dashed line describe the time in which elimination occur. The vertical grey line describe the time in which VSE appears. Initial conditions: $S(0), I(0)$ fixed at pre-vaccination endemic state, $p(0) \simeq 0$. Other parameters: $R_0 = 10$, $\nu = 1/10$ day^{-1}, , $\mu = 1/50$ year^{-1}, $\theta = 5000$.

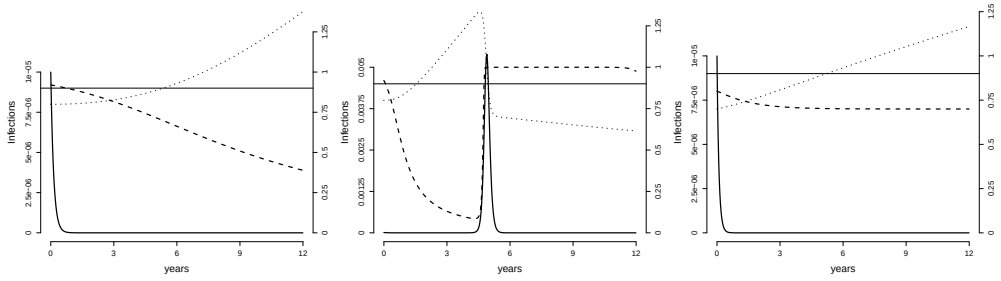

Figure 6.5: Left and central panels: dynamics of $I(t)$ (black line), $R_0S(t)$ (dotted black line), $p(t)$ (dashed black line) for $\theta = 5000$,$h0 = 0$. and $p(0) = 0.95$, $S(0) = 1 - p(0)$, $I(0) = 10^{-5}$. Left-hand panel $k = 0.001$. Central panel: $k = 0.01$. The black line is the threshold p_c. Right-hand panel: as the central panel but for $h0 = 0.7$,$p(0) = 0.80$ and $S(0) = 0.07$. Other parameters: $R_0 = 10$, $\nu = 1/10$ day^{-1}, , $\mu = 1/50$ year^{-1}, $\theta = 5000$.

Impact of information-related delays

An exponentially distributed lag in the p term yields a model given by (6.1)-(6.2) complemented by:

$$p' = k\,(h(I) - H))\,p\,(1 - p) \tag{6.16}$$

and by (6.10). Fig. 6.6 reports the stability regions in the (k, b) plane for $\vartheta = 260$, $\vartheta \approx 279.5$ (which is close to the critical value ϑ^* in absence of delays) and $\vartheta = 500$. Note that for $\vartheta = 500 > \vartheta^*$ for all b there are two values $k_l(b;\vartheta)$ and $k_r(b;\vartheta)$ such that for $k_l(b;\vartheta) < k < k_r(b;\vartheta)$ the endemic state E_e is unstable and it is also an easy matter to show that Yabucovitch oscillations can arise. Similar plots are obtained in all cases where $\vartheta > \vartheta^*$. This can be easily explained since for very large b the lagged model reduces to the unlagged one that, for $\vartheta > \vartheta^*$, has an instability interval.
Interestingly, the right panel of 6.6 for $\vartheta = 260 < \vartheta^*$ shows instability regions that are

uniquely due to the information delay, because in absence of the delay (i.e. for large b) there is no instability, as shown in the previous sub-sections. This confirms that the addition of time delays in the p term (mimicking delayed onset of VSEs or delayed information acquisition) cumulates with the imitation delay in triggering instabilities.

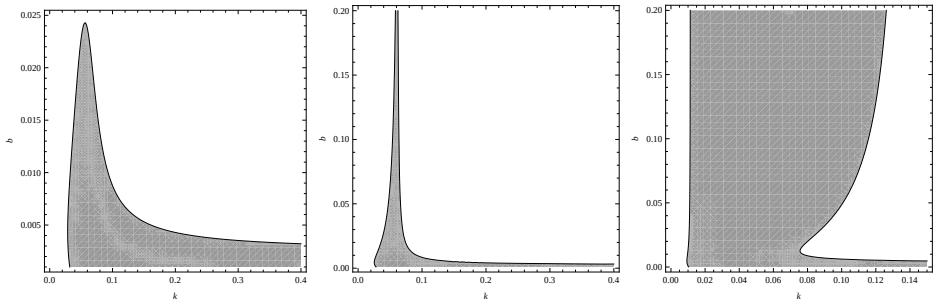

Figure 6.6: Effects of an exponentially fading memory in the perceived risk of infection: stability regions in the (k, b) plane for $\vartheta = 260$ (left), $\vartheta = 500$ (right) and $\vartheta = 279.5$ (centre), a value slightly higher than the bifurcation value. Other parameters: $R_0 = 10$, $\nu = 1/10$ day^{-1}, , $\mu = 1/50$ year^{-1}.

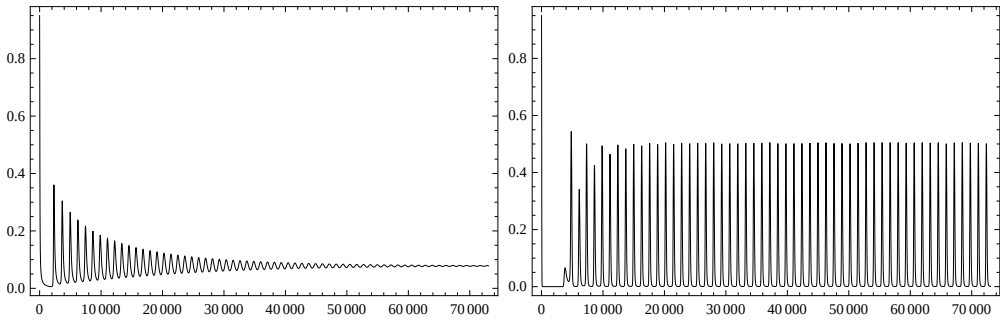

Figure 6.7: Effects of an exponential fading memory in the perceived risk of vaccination with $\vartheta = 260$. Left-hand panel: the case of no delay. Right-hand panel: the delayed case with $b = 0.004$ $days^{-1}$, corresponding to an average delay of 250 days. Other parameters: $R_0 = 10$, $\nu = 1/10$ day^{-1}, , $\mu = 1/50$ year^{-1}.

Fig. 6.7 reports the time course of vaccine uptake $p(t)$ for $\theta = 260$ for two distinct cases. In the left-hand panel the behaviour in absence of delay is reported, showing convergence to the endemic state. The right-hand panel reports the behaviour for a delay of 250 days ($b = 0.004$) in the occurrence of side effects, showing instead convergence to a limit cycle. Let us now consider an exponentially fading memory in the perceived risk of infection: let M stand for past prevalence, and a the corresponding delaying rate. We set $h_1(M) = \vartheta M$, and $h_2(I) = I$. In Fig. 6.8 we plotted the stability regions in the (k, a) plane for $\vartheta = 260$, $\vartheta \approx 279.5$ (which is close to the critical value ϑ^*) and $\vartheta = 500$.

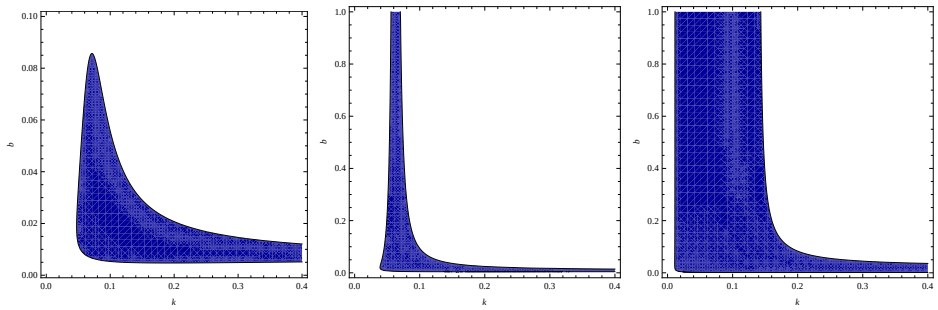

Figure 6.8: Information xdelayed case. Stability regions in the (k, a) plane for $\vartheta = 260$ x(left), $\vartheta = 500$ (right) and, in the centre, $\vartheta = 279.5$, a value slightly higher than ϑ_H. Other parameters: $R_0 = 10$, $\nu = 1/10$ day^{-1}, , $\mu = 1/50$ year^{-1}. Note that in the central sub-figure the maximum a is 100.

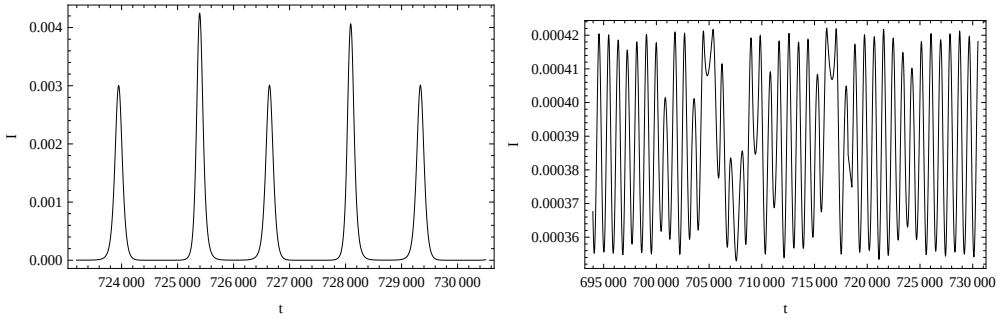

Figure 6.9: Effects on $I(t)$ of exponential fading memories in both information and side effects. In both panels $a = 20b$, $R_0 = 10$, $\nu = 1/10$ day^{-1}, $\mu = 1/50$ year^{-1}. (Left-hand panel) Periodic solution with alternating low and high peaks arising for $\vartheta = 260$, $b = 1/365.25$; (Right-hand panel) Aperiodic solutions arising for $\vartheta = 500$, $b = 0.04$.

Finally, in the case where exponentially fading memories appear both in the perceived risk of vaccination (with rate b) and the perceived risk of infection (with rate a), numerical simulations showed a wide pattern of periodic behaviour, including very long periods (an example with alternating low and high peaks is reported in the left-hand panel of Fig. 6.9), and also aperiodicity (as in the right-hand panel of Fig. 6.9)

6.5 Concluding remarks

We investigated an SIR transmission model with voluntary vaccination. Unlike [15] we consider a dynamic perceived risk of vaccination proportional to the trends of VSEs. Mathematical analysis of the model confirms already known results, such as the onset of behaviour-triggered steady oscillations about the post-vaccination endemic state. In addition it shows some noteworthy differences compared to findings elsewhere. For example global elimination may. or may not, be possible depending on the actual magnitude of

the baseline perceived risk of disease relative to the risk of vaccine side effects. As regards the pre-vaccination equilibrium, differently from [15], it is always unstable, so that any vaccination programme will initially be successful, at least partially. Moreover oscillations occur, provided the relative risk of disease is large enough, in a bounded window of the imitation parameter. In addition, we also considered the impact of time delays on the vaccination payoff gain, which is a realistic feature. Finally, the model allows noteworthy inferences on the future lifetime of vaccination voluntary programmes. It suggests that in order to achieve high equilibrium uptakes for e.g. measles, the perceived cost of the disease must be at least three orders of magnitude higher than the perceived cost of vaccine-associated side effects, and moreover that this requirement is further increased under situations with large life expectancies. Both these facts seem to be consistent with real world observations, and suggest that maximal vaccination effort by international institutions should target increasing vaccine uptake in less developed countries where the risk of serious sequelae is still high, and life expectancy is still low. Simulations finally provide further interesting insights on the effect of behavioural parameters on vaccine uptake.

Chapter 7

Conclusion

As recently pointed out, human behavior is a relevant *missing factor* of epidemiological modeling [56, 52].

In fact, organized measures such as quarantine or closure of public places are one way that behavior can change, but people may also spontaneously modify their behavior to reduce perceived risk.

Results presented in my thesis show that spontaneous behavioral response to epidemics, coming either from the concern about the infection or from possible vaccine side effects, can remarkably affect the epidemic spread both qualitatively and quantitatively and may also compromise the expected outcome of voluntary vaccination programs and other control measures. Indeed, human behavioral changes may alter timing, dynamics and overall number of cases during a (severe) epidemic outbreak while the problem of rational exception may be responsible of drops in vaccine uptake and suboptimal vaccine coverage and may trigger the resurgence of diseases for which the current prevalence is very low.

Evidences about spontaneous social distancing and other self-imposed prophylactic measures in response to emerging outbreaks, have been reported for past epidemics [98, 59, 90, 136, 144]. On the other hand, a large number of countries, whose vaccination policies are based on voluntary compliance, are increasingly facing the challenge of refusal of vaccines caused by high concerns about proclaimed risks from vaccine side effects [70, 106, 89, 135, 64, 142, 163]. Thus, spontaneous behavioral responses, not accounted by large majority of transmission models, can not be neglected to correctly inform public health decision makers.

The class of models developed in this thesis project provides a promising approach, based on evolutionary game theory, to investigate the complex interaction between human behavior and diseases transmission process, contributing to assess possible effects deriving by risk perception and individual choices.

When studying the spread of epidemics, behavior and contact patterns are typically considered as a "background" for the infection process– i.e., they are not variables of the dynamics. For mild infections such approximation is justified, as individuals rarely funda-

mentally change their behavior because of symptoms associated to diseases auch as cold. On the other hand, the evidence shows that faced with lethal or novel pathogens, people will change their behavior to try to reduce their risk [56]. In these cases, population behavior cannot be merely considered as an independent (though time-varying) parameter, but it is better modeled as a variable whose evolution influences, and is influenced by, the dynamics of the infection.

Actually, the diffusion of human beliefs can be driven by mechanism similar to those driving an epidemic; different source of information can be considered for the spread of information in a population (e.g., rumors, media, ...). Recently, models have been proposed for investigating spontaneous social distancing describing human behavioral responses as driven by the diffusion of fear, which is modeled as a parallel infection [147, 42, 53, 93, 67, 66]. However, evolutionary game theory – that is a natural framework for studying human behavior – provides an alternative way for modeling the diffusion of responsiveness in the population.

Models introduced in chapters 2, 3, 4, 6 couple the transmission dynamics with an imitation process, i.e. a learning process, in which the convenience of self-protection (e.g., the reduction of the number of potentially infectious contacts or the choice to vaccinate) is assessed trough personal encounters. Human behavior is assumed to be driven by the evaluation of prospective outcomes deriving from alternative decisions and cost-benefit considerations that depend on the perceived prevalence of infection and, in the case of voluntary vaccination choices, the incidence of vaccine side effects (possibly considering time delays and memory mechanisms).

With the introduction of explicit models for behavioral changes based on evolutionary game theory, infection and behavior both contribute to define the context for the other. Symmetry between these two key-factors is therefore restored, and no *by-principle* prevalence is given (even formally) to one over the other. Not only the infection dynamics depends on both the transmission and behavior, but also the behavior dynamics depends on behavior (and infection as well). This is what makes evolutionary game theory especially suited to this situation as compared to classical game theory. In fact, application of the latter would result in (rational) instantaneous best responses to the infection dynamics, regardless of the current distribution of behavioral strategies. On the other hand, at first sight, introduction of irrational behavior may appear unnecessary, and contrasting with models simplicity. Yet, by avoiding extinction of allowed behaviors, irrational behavior overtakes an unrealistic (and undesirable) effect of strict imitation: the pool of strategies from which an individual can choose is limited to those effectively represented in the population. On the other hand, by allowing exploration of *all possible* behaviors, irrational behaviors may account for erroneous decisions or idiosyncratic attitudes always present in human societies.

Independently of how the risk is specifically reckoned, the access to information pertaining the relative efficacy of behaviors may also be collected across more structured networks (e.g., the media). In this respect, considering different time units adds some flexibility to models developed, in that it allows for different speeds in the diffusion of infection and behavior. For example, tuning of key parameter driving the speed of behav-

ioral changes (e.g., ϵ in chapter 2, ρ in chapters 3,4 and k in chapter 6) may be obtained on the basis of empirical evidence.

More structured models, as for instance individual based models and network models, may be more appropriate for investigating actual situations and empirical data. However, it is worth of noticing that the approach proposed is fairy general to be applied for describing any kind of disease (e.g. influenza, smallpox, SARS, measles, varicella, pertussis) and, it can be easily included into more structured models in order to account for spontaneous human behavior.

The simple model introduced in chapter 2 allows the investigation of the dynamics of spontaneous reduction in the number of contacts, performed as a protective response to the state of the epidemic and the spread of a (severe) disease. That is why the behavioral change modeled here affects only susceptible individuals (infected individuals may of course change behavior as an effect of their status, regardless of the state of epidemic). The proposed model couples an SIR model with selection of behaviors driven by imitation dynamics. Therefore, infection transmission and population behavior become dynamical variables that influence each other. In particular, time scales of behavioral changes and of epidemic transmission can be different. The performed analysis provide a full qualitative characterization of the solutions when the dynamics of behavioral changes is either much faster or much slower than that of epidemic transmission. For suitable parameter configurations, the model accounts for multiple outbreaks occurring within the same epidemic episode. Moreover, the model can explain "asymmetric waves", i.e. infection waves whose rising and decaying phases differ in slope. Finally, it is proved that introduction of behavioral dynamics can lead to a reduction of the final attack rate.

In chapter 3, an extension of the model introduced in chapter 2, including a wider class of scenarios, is presented. The model of behavioral changes is extended to infected individuals subgrouped in symptomatic and asymptomatic, treating the infected asymptomatic as susceptibles for anything concerning the behavioral dynamics. The impact of key features of a human self-protection on the effectiveness of behavioral responses are discussed. The analysis of the proposed model highlights that, if the perceived risk associated to an epidemic is sufficiently large, even small behavioral changes can remarkably reduce the final epidemic size and the daily peak prevalence. Moreover, if the delay in the behavior diffusion – embedded in the imitation process – is not too large, the response of the population is always effective. The population responsiveness increases as the symptomaticity increases, while memory of past cases and initial overestimation of the risk of infection essentially delay the epidemic spread. Results of this study are consistent to those obtained by previous works through different assumptions. Specifically, as shown in [42], the disease spread results highly sensitive to how rapidly people adopt a self-reduction in their contact activity rates. Moreover, if behavioral changes are fast enough, they can have a remarkable effect in reducing the daily infection prevalence [93] and the final epidemic size [67]. Finally, as in [53], for suitable parameter configurations,

the epidemic dynamics can account for multiple epidemic waves.

In chapter 4 the approach introduced in chapter 3 is used for investigating the 2009 H1N1 pandemic influenza dynamics in Italy. As it emerges from the analysis of influenza-like illness incidence data, after an initial period characterized by a slow exponential increase in the weekly incidence, a sudden and sharp increase of the growth rate is observed. The performed investigation, based on model fit to epidemiological data and on the analysis of antiviral drugs purchase, reveals that an initial overestimation of the risk in the general population, possibly induced by the high concern for the emergence of a new influenza pandemic, can result in a pattern of spread compliant with the observed incidence. Moreover, the analysis of influenza-like illness incidence data highlights that the estimation of fundamental epidemiological parameters (and in particular of the reproductive number) may be reconsidered as well, as it could be largely affected by human behaviors.

Static models for vaccination choice introduced in chapter 5 allow getting some meaningful insights on disease elimination feasibility under voluntary vaccination policy. First, the *elimination impossible* result is proved by a simple model of individual choice in presence of informed families, i.e. families aware of herd immunity, and it is suggested that limited information might explain patterns of universal vaccination. Next, vaccination choices are investigated in a game-theoretic framework for communities stratified into two groups, *pro* and *anti* vaccinators, having widely different perceived costs of infection and of vaccine side effects. Under the assumption of informed families neither a Nash nor a Stackelberg behavior (characterized respectively by players acting simultaneously and by an asymmetric situation with a *leader* and a *follower*) allow disease elimination, unless *pro-vaccinators* assign no costs to vaccine side effects. Elimination turns out to be possible when "cooperation" is encouraged by a social planner, provided however he incorporates in the *social loss function* the preferences of anti-vaccinators only.

Finally, the model with dynamic vaccine demand, based on imitation and described in chapter 6, may represent a significant contribution for the investigation of the problem of rational exception. Here the perceived risk of vaccination is modeled as a function of the incidence of vaccine side effects, instead of using a constant. This represents the main innovative aspect of the model. The impact of time delays on the vaccination payoffs is considered as well. Mathematical analysis of the model confirms already known results, such as the onset of behavior-triggered steady oscillations about the post-vaccination endemic state. The model shows important differences compared to previous game dynamic models of vaccination. For example, global elimination may, or may not, be possible depending on the actual magnitude of the baseline perceived risk of disease relative to the risk of vaccine side effects. Differently from [15], the pre-vaccination equilibrium is always unstable, so that any vaccination program will initially be successful, at least partially. Moreover, provided the relative risk of disease is large enough, oscillations occur in a bounded window of the imitation parameter. The performed analysis suggests that, in

order to achieve high coverages, a huge disproportion between the perceived risk of disease and vaccination is necessary. This disproportion is further increased in highly industrialized countries. Both these facts seem to be consistent with "real world" observations, and suggest that maximal vaccination effort by international institutions should target increasing vaccine uptake in less developed countries where the risk of serious sequelae is still high, and life expectancy is still low.

As regards the problem of rational exception in vaccination choices, noteworthy inferences emerged in the analysis of proposed models need to be properly discussed. The possibility to switch from a compulsory to a voluntary vaccination system is actively debated, and one Italian region, Veneto, has recently *made the step* [60]. In epidemiological terms, any further expansion in the anti-vaccinator group will decrease the degree of herd immunity and will therefore be stopped by the necessary re-emergence of the disease. Though the consideration of migration between groups would require a specific dynamic model, global socio-economic trends are not favorable in this sense: empirical studies indicate that often those individuals vaccinating less are the more educated, or the richer, ones [18, 142]. The public health dangerousness of such a situation, think for instance to slow declines in herd immunity due to slow migrations toward the anti-vaccinator group, call for a careful monitoring of such processes.

Moreover, the investigation performed in chapters 5 and 6 strongly suggest that universal vaccination in the majority of the population follows from: a) a very small cost associated to vaccine side effects, b) the lack of knowledge of the critical threshold, i.e. parents believing that a propensity to vaccinate of 100% is necessary to fully protect children against disease. This wrong perception (mathematical models show that the critical threshold for disease elimination is always less, sometimes substantially less, than 100%) is dangerous for the public health system since it implies the uneven situation where someone takes the risks of vaccine side effects to protect all, as a consequence of limited information. This further enhances the danger that people improve their information set, and as a consequence, rationally *migrate* towards the anti-vaccinator group. Thus, for those public health systems that have already initiated a *road map* towards voluntary vaccination, as in Italy is the case of Veneto region [60], investment in education to the social role of vaccination will be an unavoidable task in the future.

After all, considering models accounting for spontaneous behavioral changes would be helpful for giving insight to public health policy makers for planning public health control strategies during an emerging epidemic (also providing better estimates about the burden for health care centers over time) and for evaluating the effectiveness of control measures based on voluntary compliance.

However, as regards spontaneous behavioral changes occurring during an epidemic outbreak, *"the challenge for mathematical modelers is that data are scarce, and often qualitative when they do emerge"*, as pointed out in [56]. Actually, few efforts have been

made to validate models dealing with spontaneous behavioral changes from empirical observations.

The study performed in chapter 4 may represent a further step in this direction, as the quantitative and qualitative effects of spontaneous behavioral changes in the population on the spread of an epidemic have been validated against empirical data. However, at the current stage, the proposed models could hardly be used for real time predictions since our knowledge on plausible values of model parameters related to human behavior is only preliminary. Further investigations have to be performed in order to gain a major consciousness on how such mechanisms work.

Undeniably, a lot of empirical data would be needed for models validation and parametrization. However, recent surveys on human behavioral response have started to answer questions as: where people obtain their information from, which of information available to them they trust, if and how they act upon the information [90, 82, 39, 98, 144].

On the other hand, the chance of considering reliable data on human behavior increases in the context of vaccination. Indeed, data on vaccine uptake may represent also human behavior and would allow quantitative estimation, model validation and, in turn, a better understanding of mechanisms that drive information and beliefs diffusion and the interplay between risk perception and the spreading responsiveness during epidemics.

Chapter 8

Appendix

8.1 Appendix A

8.1.1 Proofs

Proof of Proposition 2.3.2

S1 Let us consider the set $T_1 = \{0\} \cup \{\bar{t} > 0 \mid I(t) < 1/m \ \forall\, t \in (0, \bar{t})\}$. $T_1 \neq \emptyset$ and let us define $t_1 = \sup T_1$. $I(0) := I_0 < 1/m$ implies that $t_1 > 0$. Let us consider any finite time $\tilde{t} < t_1$. For any $t \in [0, \tilde{t}]$, the boundary–layer system (2.9) with $I = I(t)$ admits the asymptotically stable equilibrium $x^\star(I)$, as defined in Eq. (2.10) and $x^\star(I) \to 1$ when $\mu \to 0$ (see Prop. 2.3.1). In fact, $I(t) < 1/m$ for each $t \in [0, \tilde{t}]$. Therefore, the solution of the degenerate system (2.8) is equivalent to that of a classical SIR model with $R_0 = R_0^n$ on the whole interval $[0, \tilde{t}]$. By Tikhonov theorem [148], this is also the approximation of the solution of system (2.5). Condition $1/m < I_p$ guarantees that $t_1 < +\infty$. In fact, if $t_1 = +\infty$, system (2.5) is equivalent to an SIR model with $R_0 = R_0^n$ and thus $I(t) = I_p > 1/m$ for some finite time $t > 0$, which implies $t_1 \neq \sup T_1$. Moreover, $I(t_1) = 1/m$.

S2.1 Let us now assume that $R_0^a S(t_1) \leq 1$. As observed in the main text, the only admissible value for the fraction of infected individuals is $I(t) = 1/m + O(\epsilon)$ as long as $R_0^n S(t) > 1$. Formally, if $I(t) > 1/m$ in some interval then $x(t)$ would be very close to 0 in almost the whole interval. Thus, $\dot{I}(t)$ would be negative and $I(t)$ would decrease below $1/m$. On the other hand, if $I(t) < 1/m$ in some interval then $x(t)$ would be very close to 1. Thus, $\dot{I}(t)$ would be positive and $I(t)$ would increase over $1/m$.

This has two relevant consequences, namely

- in the slower time scale system we have $\dfrac{dI}{dt}(t) = 0$;
- in the faster time scale system we have $\dfrac{dx}{ds}(s) = 0$ since $\mu = o(\epsilon^k)$ with $k \geq 1$ (see Eq. 2.9). In particular, this implies that the under the hypotheses of

the Proposition, the dynamics of x is not faster than that of the epidemic transmission when $I(t) \approx 1/m$.

By setting $\dot{I}(t) = 0$ in the degenerate system (2.8) we obtain

$$x = \frac{\gamma - \beta^a S}{\beta^n S - \beta^a S} \ . \tag{8.1}$$

By substituting this value in the equation for $S(t)$ and by setting $I(t) = 1/m$ we obtain

$$\dot{S}(t) = -\gamma/m \ ,$$

whose explicit solution is $S(t) = S(t_1) - \frac{\gamma}{m}(t - t_1)$ as long as $R_0^n S(t) > 1$, that is for all $t \in (t_1, t_2')$ where $t_2' = t_1 + \frac{m}{\gamma}(S(t_1) - \frac{1}{R_0^n})$. Afterwards, the fraction of infected $I(t)$ decreases below $1/m$ and we can apply the line of reasoning applied in *S1* to show that the solution of system (2.5) approximates that of an SIR model in its decaying phase with $R_0 = R_0^n$.

One can iterate the procedure to compute the $O(\epsilon)$ terms. In fact, let us assume that $1 - mI = \epsilon v$. The equation for $x(t)$ allows us to estimate v. Indeed, we can rewrite the equation for $x(t)$ as:

$$\dot{x} = x(1 - x)v + \epsilon^{k-1}(1 - 2x) \ , \tag{8.2}$$

where, if $k > 1$, the second righthand term can be ignored. Both $\dot{x}$ and $x(1-x)$ can be explicitly computed from Eq. (8.1). By substituting the resulting expressions in Eq. (8.2) and considering that $1 - mI = \epsilon v$ we have:

$$1 - mI = \frac{\epsilon\gamma(R_0^n - R_0^a)}{m(SR_0^n - 1)(1 - R_0^a S)} \ .$$

If $k = 1$ we can apply the same line of reasoning, though we do not obtain such a simple expression for $1 - mI$.

Going on, one can obtain $O(\epsilon)$ corrections for $x(t)$ and $S(t)$ in (t_1, t_2), but these are not really needed.

S2.2 If $R_0^a S(t_1) > 1$ we are guaranteed that the epidemic is still in its growing phase. Let us consider the set $T_2 = \{t_2\} \cup \{\bar{t} > t_2 \mid I(t) > 1/m \forall\ t \in (t_2, \bar{t})\}$. We can now apply the same line of reasoning applied in *S1*. The only difference is that $x^\star(I) \to 0$. Note that $t_2 < +\infty$ since $I(t) \to 0$ when $t \to +\infty$ and $I(t_2) = 1/m$.

S2.2.1 Similar to *S2.1*, after having observed that $R_0^a S(t_2) < 1$.

S2.2.2 Trivial. □

Lemma 8.1.1. *If $R_0^n > 1$, the set of the solutions of the inequalities $1 < R_0^a < R_0^n \exp\{-R_0^a(1-1/R_0^n)\}$ is non empty.*

For fixed values of $R_0^n > 1$, let us consider the function

$$h_{R_0^n}(x) = x - R_0^n \exp\{-x(1-1/R_0^n)\} \ .$$

We have that $h_{R_0^n}(R_0^n) > 0$. We are interested to study the sign of the function $k(R_0^n) := h_{R_0^n}(1) = 1 - R_0^n \exp\{1/R_0^n - 1\}$. We have that $k(1) = 0$, $\lim_{R_0^n \to \infty} k(R_0^n) = -\infty$ and $\dot{k}(R_0^n) < 0$. It follows that $h_{R_0^n}(1) < 0$ for each $R_0^n > 1$. Therefore, it does exist $\bar{R}(R_0^n) \in (1, R_0^n)$ such that $h_{R_0^n}(\bar{R}) = 0$. It follows that choosing R_0^a with $1 < R_0^a < \bar{R}(R_0^n)$, we satisfy the inequality in the thesis. □

Proof of Proposition 2.3.3

Let us consider the time interval $[0, t_1]$ where t_1 is defined in the proof of Prop. 2.3.2. Since the system is equivalent to a SIR model with $R_0 = R_0^n$, we can employ the SIR invariant $S(t) + I(t) - \frac{1}{R_0^n} \log S(t) = const$ in $[0, t_1]$ to compute $S_1 := S(t_1)$. Since $S(0) = 1 - I_0$, $I(0) = I_0$ and $I(t_1) = 1/m$ it follows that S_1 is a zero of the function $f(x) = x + \frac{1}{m} - \frac{1}{R_0^n} \log x - 1 + O(I_0)$, where $O(I_0) = \frac{1}{R_0^n} \log(1 - I_0)$ can be ignored. Since $f(1) = 1/m > 0$ and $f(1/R_0^n) = 1/m - I_p < 0$ (by hypothesis) it follows that it does exist S_1 such that $f(S_1) = 0$ and

$$S_1 \in (1/R_0^n, 1) \tag{8.3}$$

with $\lim_{1/m \to 0} S_1 = 1$ and $\lim_{1/m \to I_p} S_1 = 1/R_0^n$. Since $f(x)$ is increasing for $x > 1/R_0^n$ the solution is unique.

Let us now assume that R_0^a satisfies the inequalities $1 < R_0^a < R_0^n \exp\{-R_0^a(1-1/R_0^n)\}$ (it is possible thanks to lemma 8.1.1), which in particular implies $R_0^a < R_0^n$. Since $R_0^n > 1/S_1$ (see Eq. (8.3)), we can distinguish two cases:

- *Case 1*: $R_0^a > 1/S_1$,
- *Case 2*: $R_0^a \leq 1/S_1$.

In Case 2, we have a solution of type $C1$, satisfying the thesis.

Hence, we look only at Case 1. We are guaranteed that the epidemic is still in its growing phase. Let us consider the time interval $[t_1, t_2]$ where t_2 is defined in the proof of Prop. 2.3.2. Again, we can employ the SIR invariant in $[t_1, t_2]$ to compute $S_2 := S(t_2)$. Since $S(t_1)$ and $I(t_1)$ are known and $I(t_2) = 1/m$ it follows that S_2 is a non trivial solution of the equation $g(x) = g(S_1)$ where $g(x) = x + \frac{1}{m} - \frac{1}{R_0^a} \log x$. Function g is convex, has a absolute minimum for $x = 1/R_0^a$, is strictly decreasing for $x < 1/R_0^a$ and it is strictly

increasing for $x > 1/R_0^a$, $\lim_{x\to 0} = +\infty$ and $\lim_{x\to+\infty} = +\infty$. Since $S_1 > 1/R_0^a$, a unique $S_2 \in (0, 1/R_0^a)$ exists such that $g(S_2) = g(S_1)$.

We now show that $S_2 > 1/R_0^n$. Since $R_0^a < R_0^n \exp\{-R_0^a(1 - 1/R_0^n)\}$ it follows that:

$$1 - \frac{1}{R_0^a}\log\frac{1}{R_0^a} < \frac{1}{R_0^n} - \frac{1}{R_0^a}\log\frac{1}{R_0^n} \ .$$

Since

$$1 - \frac{1}{R_0^a}\log\frac{1}{R_0^a} > S_1 - \frac{1}{R_0^a}\log S_1$$

we have that $g(S_2) = g(S_1) < g(1/R_0^n)$ and thus $S_2 > 1/R_0^n$ since g is decreasing in $(0, 1/R_0^a)$.

We have thus demonstrated that $R_0^n S_2 > 1$ which implies that we have a solution of type *C2*.

Case 2. Trivially, we have a solution of type *C1*. □

Lemma 8.1.2. *When $S(t) = 1/R_0^n$, the solution of system (2.5) satisfies $I(t) < 1 - \frac{1}{R_0^n} + \frac{1}{R_0^n}\log\frac{1}{R_0^n}$.*

Equations of system (2.5) for I and S can be written in the general form

$$\left\{\begin{array}{rcl} \dot{S} &=& -\beta(t)SI \\ \dot{I} &=& -\beta(t)SI - \gamma I \end{array}\right. \tag{8.4}$$

with $\beta(t) \in [\beta_a, \beta_n]$. It is easy to show that for system (8.4) the function

$$S(t) + I(t) - \frac{1}{R_0^n}\log S(t)$$

is decreasing in t. It follows that

$$1 = S(0) + I(0) - \frac{1}{R_0^n}\log S(0) > S(t) + I(t) - \frac{1}{R_0^n}\log S(t) \ .$$

The thesis follows by substituting $S(t) = 1/R_0^n$. □

Proof of Proposition 2.3.4

Let us define $(S^{\mathrm{SIR}}(t), I^{\mathrm{SIR}}(t))$ and $(S(t), I(t))$ as the fractions of susceptible and infected individuals for a classical SIR model and for system (2.5), respectively. In the phase plane (S, I) the solution of a classical SIR model goes through the point $(\frac{1}{R_0^n}, 1 - \frac{1}{R_0^n} + \frac{1}{R_0^n}\log\frac{1}{R_0^n})$, corresponding to the epidemic peak. The solutions of system (2.5) pass through the point $(1/R_0^n, \tilde{I})$ where $\tilde{I} < 1 - \frac{1}{R_0^n} + \frac{1}{R_0^n}\log\frac{1}{R_0^n}$ thanks to lemma 8.1.2.

Let us assume that $S_\infty < S_\infty^{\rm SIR}$. It follows that in the phase plane the trajectories of the two models must intersect at a certain point $(S^\star, I^\star)$ with $S^\star < 1/R_0^n$. Moreover, at this point both S and I are decreasing and thus we can assume that the functions $I^{\rm SIR}(S^{\rm SIR})$ and $I(S)$ are well defined, and that

$$\frac{dI^{\rm SIR}}{dS^{\rm SIR}}(S^\star) > \frac{dI}{dS}(S^\star) \ .$$

hence,

$$-1 + \frac{\gamma I^\star}{S^\star I^\star \beta_n} > -1 + \frac{\gamma I^\star}{S^\star I^\star (\beta_n x + \beta_a (1-x))}$$

which is absurd since $\beta_a < \beta_n$ and $x \in (0,1)$. □

Proof of Proposition 2.3.5

Let us consider system (2.5). We have already seen that a time t_3 exists such that $I(t_3) = 1/m$ and $S(t_3) = 1/R_0^n$ (see Prop. 2.3.2). Moreover, for $t > t_3$ system (2.5) can be approximated by an SIR model with $R_0 = R_0^n$. Thus we can employ the SIR invariant in $[t_3, +\infty)$. It follows that $S_\infty(m)$ is solution to the equation:

$$S_\infty(m) - \frac{1}{R_0^n} \log S_\infty(m) = S(t_3) + I(t_3) - \frac{1}{R_0^n} \log S(t_3) = \frac{1}{R_0^n} + \frac{1}{m} - \frac{1}{R_0^n} \log \frac{1}{R_0^n}$$

while $S_\infty^{\rm SIR}$ is solution of the equation

$$S_\infty^{\rm SIR} - \frac{1}{R_0^n} \log S_\infty^{\rm SIR} = 1 \ .$$

Therefore, we have to compare the solutions of the equations:

$$l(x) = 1 \ , l(x) = b(m)$$

where $l(x) = x - \frac{1}{R_0^n} \log x$ and $b(m) = \frac{1}{R_0^n} + \frac{1}{m} - \frac{1}{R_0^n} \log \frac{1}{R_0^n}$.

Condition $1/m < I_p$ implies that $b(m) < 1$. Function l is convex, has an absolute minimum at $x = 1/R_0^n$ with $l(1/R_0^n) < b(m)$, it is strictly decreasing for $x < 1/R_0^n$ and $\lim_{x \to 0^+} = +\infty$.

Since we are interested in solutions $x < 1/R_0^n$, we have that $b(m) < 1$ implies $S_\infty(m) > S_\infty^{\rm SIR}$. Moreover, $b(m)$ is an decreasing function of m and thus $S_\infty(m)$ is an increasing function of m.

Finally, $b(m) \searrow l(1/R_0^n)$ when $1/m \to 0$; thus $S_\infty(m) \to 1/R_0^n$ when $1/m \to 0$. □

8.2 Appendix B

8.2.1 The model

The aim here is to introduce a model for a disease transmission process, accounting for heterogeneity with respect to the behaviors adopted spontaneously by the individuals of

the host population. The diffusion of the different behaviors performed by the population is modeled through evolutionary game theory. Specifically, we introduce a simple SIR model where individuals can adopt two mutually exclusive behaviors on the basis of the perceived risk of infection through a classical imitation process. We decided to keep the transmission model as simple as possible. Therefore no latency period, age classes, different levels of symptomaticity, variable viral load over time are considered. The host population is assumed to be divided into three classes, namely susceptible (S), infective (I) and recovered (R) individuals.

We assume that individuals are able to reduce the force of infection to which they are exposed as a spontaneous defensive response to the epidemic. Actually, individuals exposed to the risk of infection are only susceptible ones. As we are considering the dynamics of a spontaneous self–protection strategy that reduces the undergoing force of infection, neither infective, nor recovered individuals can achieve any benefit through a reduction of their force of infection, unless by assuming an altruistic interaction between them and susceptible individuals. Since such investigation is beyond the scope of this work, we consider only behavioral changes among susceptible individuals. Therefore, susceptible individuals are divided in two subclasses: individuals adopting a *"normal"* behavior (S_n) and individuals adopting an *"altered"* one (S_a), assuming that the latter are able to reduce the received force of infection. From now on, let us denote as b_n and b_a the two different behaviors adopted by S_n and S_a respectively.

Let us define β as the transmission rate, $1/\gamma$ the average duration of the infectivity period and $q \in (0,1)$ the reduction of the force of infection performed by S_a (e.g., by avoiding crowded environments or by increasing wariness in usual activities involving contacts with other individuals). The epidemic flows between classes can be described as follows:

$$
\left\{
\begin{array}{rcl}
\dfrac{dS_n}{dt}(t) & = & -\beta I(t) S_n(t) \\
\dfrac{dS_a}{dt}(t) & = & -q\beta I(t) S_a(t) \\
\dfrac{dI}{dt}(t) & = & \beta I(t)[S_n(t) + qS_a(t)] - \gamma I(t) \\
\dfrac{dR}{dt}(t) & = & \gamma I(t).
\end{array}
\right. \tag{8.5}
$$

Setting $x = S_n/(S_n + S_a)$, where x represents the fraction of susceptible individuals adopting the *normal* behavior b_n, system (8.5) can be rewritten as follows

$$
(8.6) \qquad \begin{cases} \dfrac{dS}{dt}(t) &= -\beta\left[x(t)+q(1-x(t))\right]S(t)I(t) \\ \dfrac{dI}{dt}(t) &= \beta\left[x(t)+q(1-x(t))\right]S(t)I(t)-\gamma I(t) \\ \dfrac{dR}{dt}(t) &= \gamma I(t) \\ \dfrac{dx}{dt}(t) &= x(t)(1-x(t))\left[q\beta I(t)-\beta I(t)\right] \ . \end{cases}
$$

where, as mentioned above, $S = S_n + S_a$ is the whole fraction of susceptible individuals.

The latter equation of system (8.5), obtained by deriving $S_n/(S_n+S_a)$, can be read as a "natural" selection process embedded in the transmission dynamics that favors individuals reducing the force of infection.

Let us assume that individuals can also change strategy spontaneously during the course of the epidemic, through cost–benefit considerations that involve the perceived risk of infection.

This phenomenon perfectly fits to the language of evolutionary game theory, in which behaviors correspond to strategies that are adopted or not on the basis of their convenience. More specifically here we assume that behavior diffusion is driven by an imitation dynamics [81, 122, 15, 127]: a fraction of the individuals playing strategy b_n can switch to strategy b_a after having compared the payoffs of the two strategies, namely p_n and p_a, at a rate proportional to their difference $\Delta P = p_n - p_a$, with proportionality constant ω; conversely for the fraction of the individuals playing b_a. As this comparison is based on the diffusion of information and may not involve only physical contacts between individuals, the imitation process and the pathogen transmission can have two different time scales. Thus let us introduce τ as the time unit for spontaneous behavioral changes, and let us assume that $t = \alpha\tau$ with $\alpha \in \mathbb{R}$.

The convenience of two mutually exclusive behaviors is modeled through their corresponding payoff functions. We consider that all individuals pay a cost for the risk of infection, which we assume to depend linearly on the perceived prevalence, $M(\tau)$, and it is higher for b_n than for b_a. Moreover, individuals playing strategy b_a pay an extra fixed cost. Hence, the payoffs associated with b_n and b_a are respectively:

$$
\begin{aligned} p_n(\tau) &= -m_n M(\tau) \\ p_a(\tau) &= -k - m_a M(\tau) \quad , \end{aligned}
$$

with $m_n > m_a$. We may think of m_n and m_a as parameters related to the risk of developing symptoms induced by the two different behaviors b_n and b_a, while k represents the cost of any self-imposable prophylactic measure (e.g., less traveling).

The perceived prevalence M is modeled through an exponentially fading memory mechanism (such as in [48]) as follows:

$$
\frac{dM}{dt}(t) = \beta\left[x(t)+q(1-x(t))\right]S(t)I(t)-\theta I(t) \ .
$$

where θ weighs the decay of the perceived risk of infection produced by new cases and thus $1/\theta$ can be read as the average duration of the memory of new cases in the perceived prevalence.

By adding the imitation dynamics in the last equation of system (8.6), the equation for the fraction of susceptible individuals adopting *normal* behavior x becomes

(8.7)
$$\frac{dx}{dt}(t) = x(t)(1-x(t))\left[q\beta I(t) - \beta I(t)\right] + \frac{\omega}{\alpha}x(t)(1-x(t))S\left[k - (m_n - m_a)M(t)\right]$$

expressed in the time scale of infection transmission process. Equation (8.7) can be rewritten in the following form:

$$\frac{dx}{dt}(t) = x(t)(1-x(t))\beta(q-1)I(t) + \rho x(t)(1-x(t))S\left[1 - mM(t)\right] \ .$$

where $\rho = \frac{\omega k}{\alpha}$, $m = (m_n - m_a)/k$.

As a matter of fact, $1/m$ defines the threshold for the perceived prevalence $M(t)$, over which it is more convenient to adopt the *altered* behavior. Moreover ρ essentially represents the speed of the imitation process with respect to the pathogen transmission dynamics. Finally, q tunes the reduction of the force of infection for individuals adopting the *altered* behavior.

One could consider a more general model for behavior dynamics, including the possibility that individuals can also (rarely) change behavior regardless of cost–benefit considerations, as driven by an *irrational exploration*. This possibility can be modeled as a mutation dynamics [81], not favoring any strategy, by considering a mutation rate $\mu << 1$. The resulting equation for x would become

$$\frac{dx}{dt}(t) = x(t)(1-x(t))\beta(q-1)I(t) + \rho[x(t)(1-x(t))S(1-mM(t)) - \mu x + \mu(1-x)] \ .$$

Mutation dynamics might be considered to gain more realism (details have been largely discussed in [127]). Nonetheless, its effect can be neglected for the purpose of this work.

8.2.2 Sensitivity analysis

In order to assess the robustness of qualitative results shown in the main text, we investigate the sensibility of the model by changing one–by–one the values of fitted parameters starting from the estimates obtained by model fitting.

The timing of the simulated epidemics is highly sensible to changes in the parameter values, while just slightly differences in the final epidemic size can be appreciated. In general, the final size varies from 38% to 41% whereas the epidemic peak week can change of more than 3 weeks.

Results are stable for large values of ρ, representing a fast imitation process, for small $x(0)$ values, i.e. if *altered* behavior is initially widespread in the population, and for a long lasting memory (Fig. 8.1). As varying $x(0)$ in a range $10^{-6} - 10^{-12}$ does not result

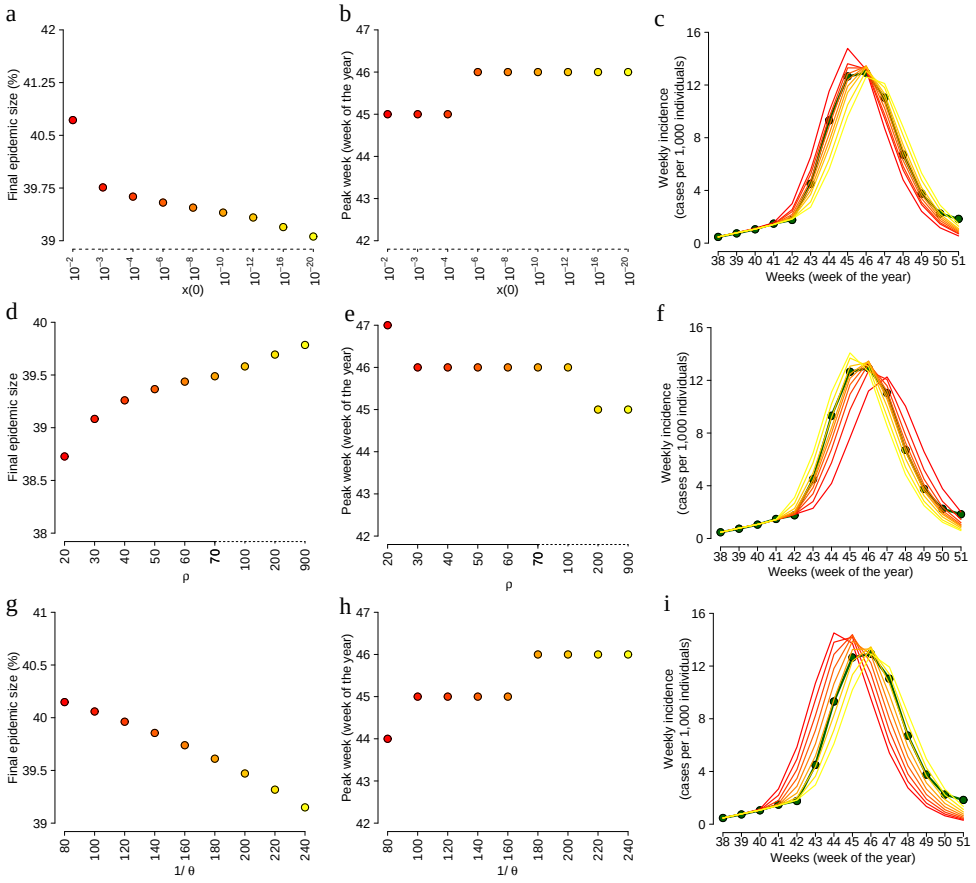

Figure 8.1: **a** Final epidemic size as simulated by the proposed model for different values of $x(0)$. Other parameters as described in the main text (see Fig. 1). **b** As is **a** but for the peak week. **c** As is **a** but for the weekly incidence. Lines colors correspond to points colors in **a** and **b**. **d**, **e** and **f** As **a**, **b** and **c** but varying ρ. **g**, **h** and **i** As **a**, **b** and **c** but varying θ.

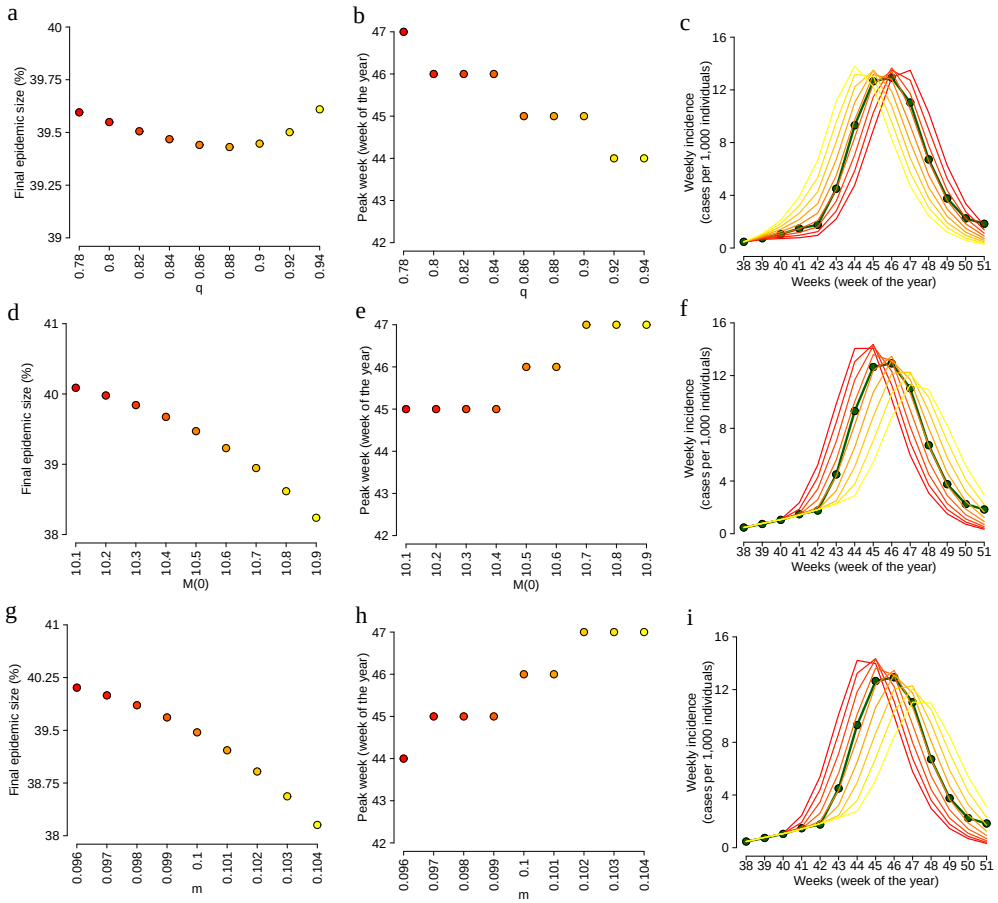

Figure 8.2: **a** Final epidemic size as simulated by the proposed model for different values of q. Other parameters as described in the main text (see Fig. 1). **b** As is **a** but for the peak week. **c** As is **a** but for the weekly incidence. Lines colors correspond to points colors in **a** and **b**. **d**, **e** and **f** As **a**, **b** and **c** but varying $M(0)$. **g**, **h** and **i** As **a**, **b** and **c** but varying m.

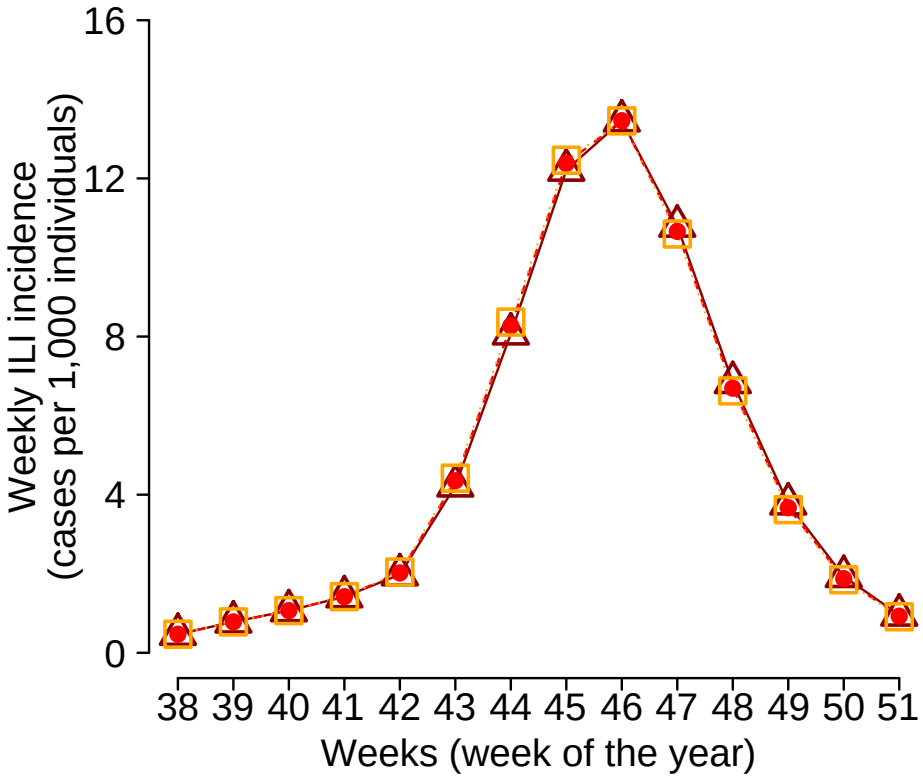

Figure 8.3: Weekly incidence as obtained by simulating the proposed model for three different sets of values of m and $M(0)$ (constrained to $m \cdot M(0) = 1.05$). Other parameters as described in the main text (see Fig. 1).

in appreciable effects in model fit, we decide to fix $x(0) = 10^{-8}$, instead of searching for an optimum $x(0)$ value.

On the other hand, small variations of q — the size of the reduction on the force of infection performed by individuals adopting the *altered* behavior — significantly influence the initial growth of the epidemic. This in turn strongly affects the peak week of the epidemic (Fig. 8.2 b, c). Specifically, for $q \in (0.78, 0.94)$, R_0^a lies in the range $1.1 - 1.4$. However, no significant differences can be appreciated in the final epidemic size (Fig. 8.2a). Indeed, a slower increase in the early phases of the epidemic would produce a lower number of cases, but would also accelerate the decrease of the perceived risk of infection, advancing the diffusion of the *normal* behavior in the population. In conclusion, the reduction of the force of infection in the early phases of an epidemic, due to an initial overestimation of the risk of infection, leads to a delay in the epidemic spread.

As for the risk threshold $1/m$ and the initial perceived prevalence $M(0)$, they both contribute to set the initial perceived risk of infection and they determine, through the memory mechanism, when it becomes more convenient to adopt the *normal* behavior. This in turn determines the period characterized by a growth rate of the epidemic lower than that expected in a population where no spontaneous behavioral changes occur. The larger is $M(0)$, the smaller is the final epidemic size and the more delayed is the epidemic

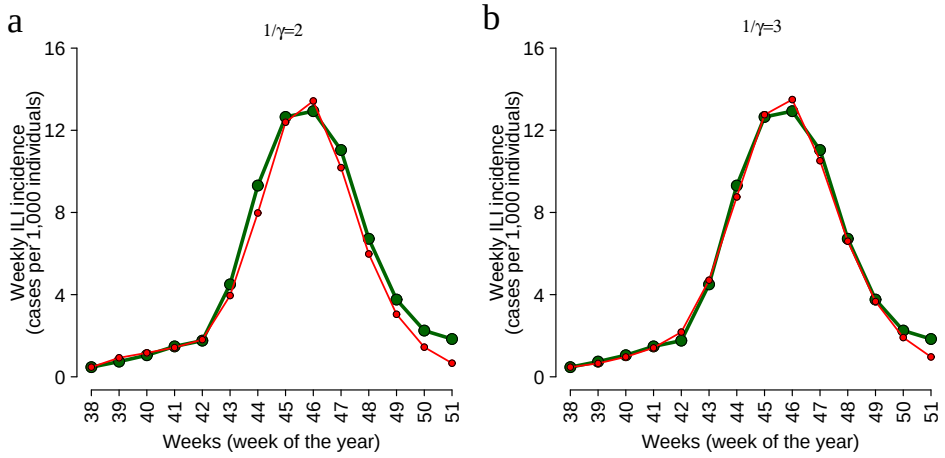

Figure 8.4: **a** Weekly ILI incidence as reported to the surveillance system (green) and weekly incidence simulated by the model by assuming $1/\gamma = 2$ days (red). Parameters values: $\beta = 0.719$, $q = 0.83$, $m = 0.1$, $\rho = 61.3$, $\mu = 0.005$, $M(0) = 10.5$, $x(0) = 10^{-8}$, $I(0) = 0.00121$ and $S(0) = 0.1$. The estimated basic reproductive number lies in the range $1.2 - 1.44$ and the reporting factor is 17.9%. **b** Weekly ILI incidence as reported to the surveillance system (green) and weekly incidence simulated by the model by assuming $1/\gamma = 3$ days (red). Parameters values: $\beta = 0.518$, $q = 0.84$, $m = 0.1$, $\rho = 64.9$, $\mu = 0.005$, $M(0) = 10.5$, $x(0) = 10^{-8}$, $I(0) = 0.00124$ and $S(0) = 0.1$. The estimated basic reproductive number lies in the range $1.31 - 1.55$ and the reporting factor is 15.4%.

peak (see Fig. 8.2 d, e and f). The same is observed for m (see Fig. 8.2 g, h and i). Specifically, variations of the order of 10% in $M(0)$ or in m result in absolute differences in the epidemic size of about 2% and, most remarkably, in variations of 3-4 weeks of the epidemic peak week.

Actually, the investigated situation is characterized by: *(i)* a risk of infection unable to sustain the *altered* behavior as a convenient choice; *(ii)* an initial overestimation of this risk of infection. In this specific case, the product $m \cdot M(0)$ is the crucial factor (rather than the values of the single parameters). In fact, as shown in Fig. 8.3, by varying values of m and $M(0)$ under the constraint that their product is kept constant, no appreciable differences in model trajectories can be detected.

In our investigation we have assumed a fixed generation time of 2.5 days, according to recent estimates [63, 165]. As shown in Fig. 8.4, predictions are not very sensitive to the length of the generation time (for $1/\gamma = 2$ and $1/\gamma = 3$).

In short, the model is able to account for the notable observed pattern, characterized by a sudden change in the slope of the incidence, if:

I an initial large diffusion of the *altered* behavior, due to a perceived risk of infection over the threshold, occurs;

II the *altered* behavior results as more convenient for a relevant period of time thanks to a long-lasting memory;

III the imitation process is fast enough to allow a sudden change in the distribution of the behaviors adopted by the population, which in turn results in a sudden change of the growth of the epidemic.

In conclusion, $m \cdot M(0) > 1$ represents an overestimation of the initial risk of infection. The closer is the product $m \cdot M(0)$ to one and the larger is ρ, the smaller are the effects of the overestimation of the risk and thus the shorter is the period characterized by the diffusion of the *altered* behavior. As a consequence, as this period becomes smaller, the dynamics of the model becomes similar to the one predicted by a "simple" *SIR* model.

8.2.3 Alert time

Our analysis has revealed that a central role for determining epidemic dynamics has been played by the initial concern about the spread of a new influenza pandemic. Here we investigate what would happen if the overestimation of risks occurs at different times (here considered as "alert" times), for example driven by different timing in the mass media information campaign. Specifically, as shown in Fig. 8.5, if the alert takes place during the early phases of the epidemic, no relevant effects are observed in terms of final epidemic size nor in the peak incidence, while the diffusion of the virus can be slowed down allowing public health agencies to gain time to perform control strategies such as vaccination (which requires time for the preparation and the distribution of doses). Alerts performed during the course of the outbreak have limited effects in slowing the epidemic spread and thus they do not allow gaining time for the interventions. However, these alerts can result in lower peak incidence (and thus in a lower burden for health care centers) and in a relevant decline of the final epidemic size. Clearly, alerts performed at the end of the epidemic have no effects on the timing and on the peak incidence of the epidemics but may result only in a reduction of the final size as they can contribute to accelerate the decline of the epidemic.

8.2.4 Analysis of past influenza seasons

As shown in the main text, the proposed model perfectly fits the ILI incidence reported to the Italian surveillance system during the 2009 H1N1pdm influenza. Specifically, our analysis has shown that a self-protection behavior, spontaneously performed by the population in response to a high initial perceived risk of infection, represents a plausible explanation for the notable observed pattern. As discussed in the main text, this could have been induced by the mass media information campaign on the risks of an emerging influenza pandemic; such hypothesis is also supported by empirical evidence (such as the trend of antivirals drugs sales and the sporadic self-imposed school closures during October 2009). Our aim in this section is to investigate if behavioral changes spontaneously performed by the population have been a peculiarity of the 2009 pandemic or if (and possibly how) they could have played a central role during past influenza seasons.

Our analysis focuses on the last three influenza seasons (namely, the 2006-2007, the 2007-2008 and the 2008-2009) in Italy and, exactly as for the analysis shown in the main

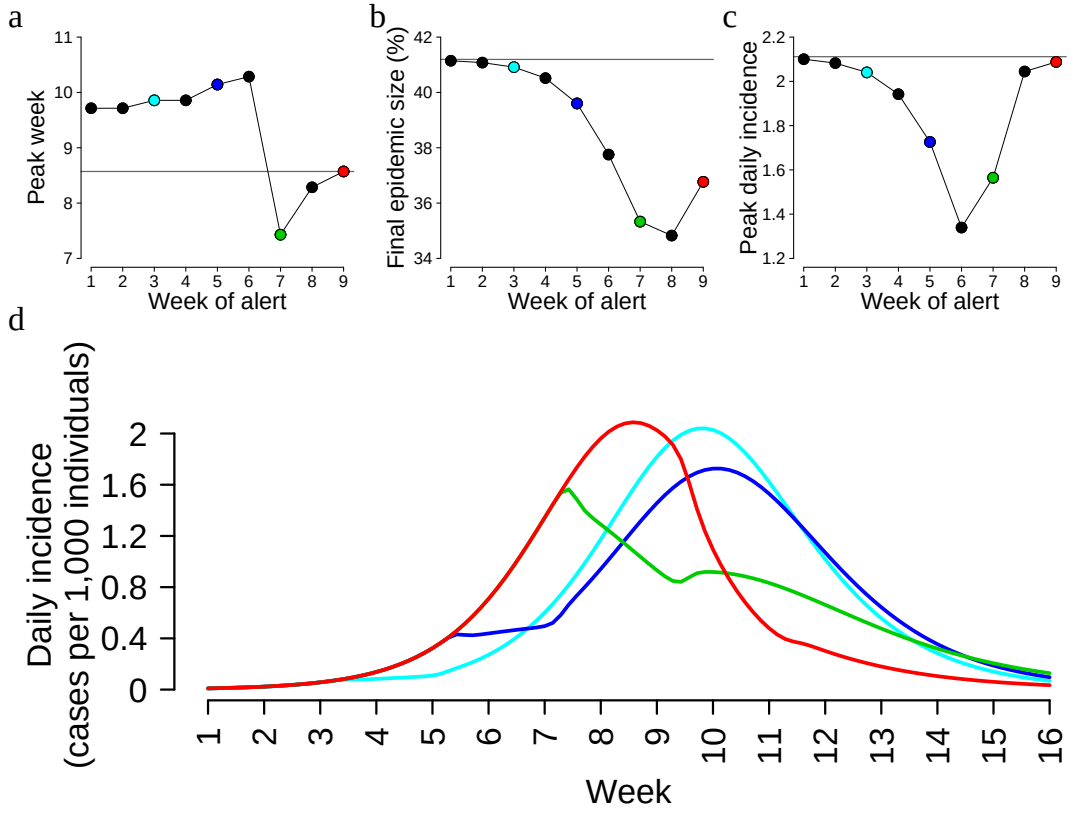

Figure 8.5: **a** Peak week as predicted by the model for different times of the alert. Parameters as in Fig. 1a of the main text, but for M, which is set to 10.5 at the time of the alert (same value as in Fig. 1a of the main text but different time). Horizontal black line represents the peak week as predicted by the "classical" SIR model. **b** Final epidemic size as predicted by the model for different times of the alert. Horizontal black line represents the final epidemic size as predicted by the "classical" SIR model. Parameters as in **a**. **c** Peak daily incidence (cases per 1,000 individuals) as predicted by the model for different times of the alert. Horizontal black line represents the peak daily incidence as predicted by the "classical" SIR model. Parameters as in **a**. **d** Daily incidence as predicted by the model for different times of the alert. Colors of the lines correspond to colors of the points in **a**, **b** and **c**.

text, it is based on model fit to ILI incidence reported to the Italian surveillance system (data available at *http://www.iss.it/iflu/*).

We found that considering behavioral dynamics does not improve the accuracy of the fit with respect to a "simple" SIR model for the 2006-2007 and the 2008-2009 influenza seasons. Specifically, the best parameter sets estimated by using a least square fitting procedure for both 2006-2007 and 2008-2009 seasons force the system to a configuration characterized by the diffusion of a single strategy adopted by the population over the whole course of the epidemic (i.e., $x(t) = 0 \forall t$ or $x(t) = 1 \forall t$). Therefore, the proposed

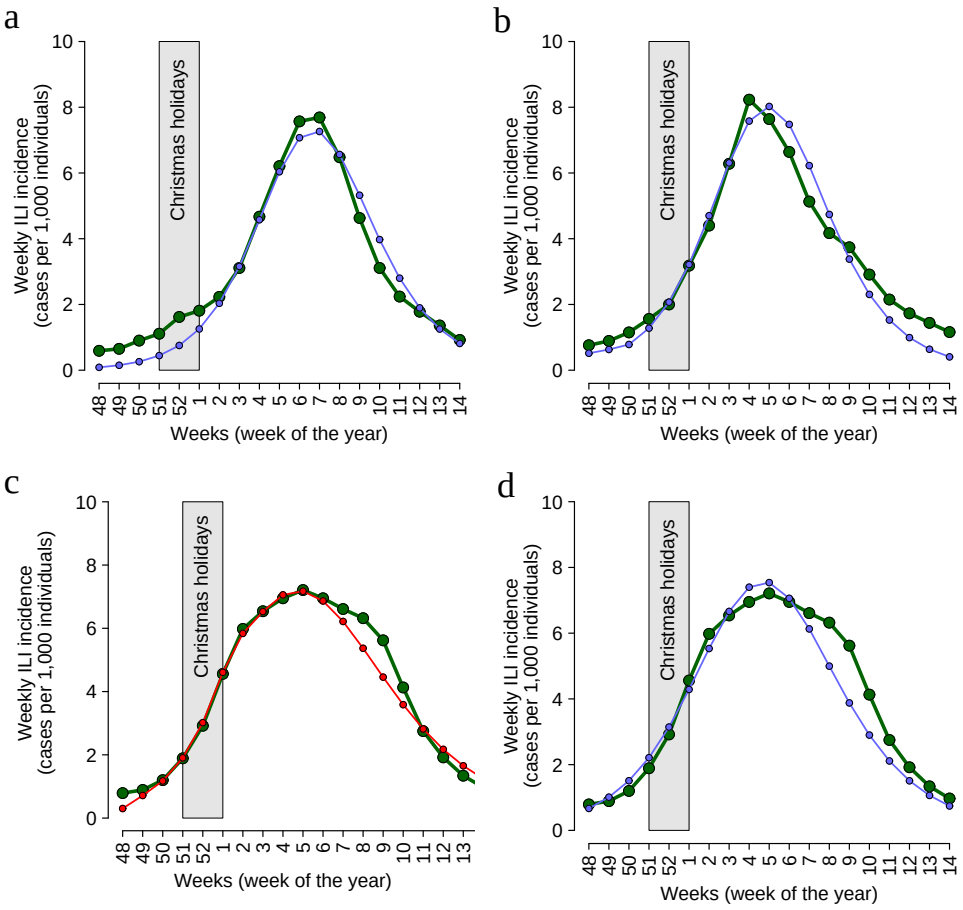

Figure 8.6: Analysis of the 2006-2007, the 2007-2008 and the 2008-2009 influenza seasons. **a** Weekly ILI incidence as reported to the Italian surveillance system (green) in the 2006-2007 season and weekly incidence as simulated by the "classical" SIR model (blue). Parameters values: $\beta = 0.49$, $\gamma = 0.26$, $I(0) = 0.001$. Since serological analysis on those influenza seasons are not available to us, the initial fraction of susceptible individuals in the population is $S(0) = 0.73$ as assumed in literature (e.g., in [105, 28]). The estimated effective reproductive number results to be 1.38 and the reporting factor is 15%. **b** Weekly ILI incidence as reported to the Italian surveillance system (green) in the 2008-2009 season and weekly incidence as simulated by the "classical" SIR model (blue). Parameters values: $\beta = 0.46$, $\gamma = 0.27$, $I(0) = 0.001$ and $S(0) = 0.73$. The estimated effective reproductive number results to be 1.24 and the reporting factor is 23%. **c** Weekly ILI incidence as reported to the Italian surveillance system (green) in the 2007-2008 season and weekly incidence as simulated by the proposed model (red). Parameters values: $\beta = 0.35$, $\gamma = 0.18$, $q = 0.89$, $m = 30$, $\rho = 400$, $\mu = 0.03$, $M(0) = 0$, $x(0) = 0.99$, $I(0) = 0.001$ and $S(0) = 0.73$. The estimated effective reproductive number lies in the range $1.26 - 1.42$ and the reporting factor is 26%. **d** Weekly ILI incidence as reported to the Italian surveillance system (green) in the 2007-2008 season and weekly incidence as simulated by the "classical" SIR model (blue). Parameters values: $\beta = 0.44$, $\gamma = 0.26$, $I(0) = 0.0001$ and $S(0) = 0.73$. The estimated effective reproductive number results to be 1.24 and the reporting factor is 27%.

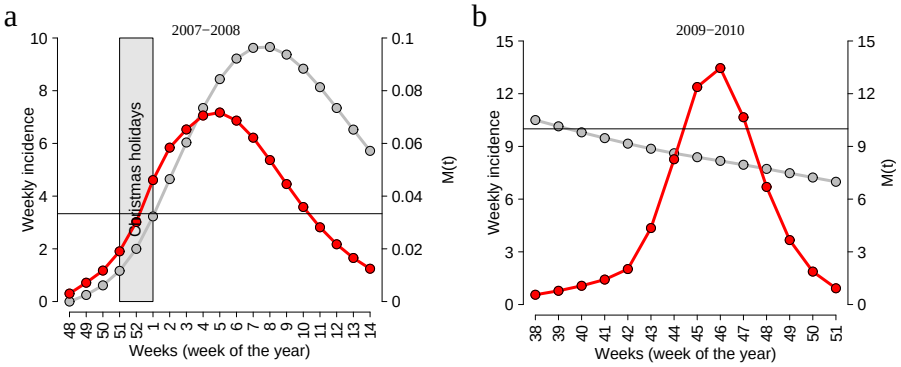

Figure 8.7: **a** Weekly incidence (cases per 1,000 individuals) as simulated by the proposed model (red) for the 2007-2008 season. Dynamics of the perceived prevalence (gray, scale on the right axis). Horizontal gray line represents the risk threshold. **b** As **a** but for the 2009-2010 pandemic season.

model and the "classical" SIR model coincide. Best model fits to the weekly ILI incidence in 2006-2007 and 2008-2009 influenza seasons are shown in Fig. 8.6 a and b.

As regards the 2007-2008 influenza season, we found that the proposed model, accounting for behavioral changes in the population, fits the weekly ILI incidence better than the "classical" SIR model (see Fig. 8.6 c and d). However, our parameters estimate suggests no initial overestimation of the perceived prevalence. The diffusion of an "altered" behavior could possibly have occurred during the most acute phase of the epidemic, close to the epidemic peak, i.e. when the risk of infection was "really" higher. Hence, even in this case, no overestimation of the perceived risk of infection at the beginning of the epidemic has been detected by our analysis, as opposed to that observed for the 2009-2010 season. Fig. 8.7 show the dynamics of the ILI incidence and of the perceived prevalence, as obtained by fitting the 2009-2010 and the 2007-2008 influenza seasons.

In conclusion, this analysis suggests that behavioral changes would not have played a relevant role in past influenza seasons, at least in the early stages of the epidemic. The initial overestimation of the risk of infection seems to be a peculiarity of the 2009 pandemic.

8.2.5 Analysis of epidemiological and virological surveillance data

By combining virological [88] and epidemiological [87] surveillance data on the 2009–2010 season, we are able to estimate a theoretic lower bound for the weekly number of H1N1pdm infections. Specifically, we multiply the weekly ILI incidence to the number of laboratory confirmed cases divided by the number of tested specimens. Tested specimens have been sampled between the ILI cases identified by physicians participating to the national surveillance system.

As for the weekly ILI incidence (analyzed in the main text), this different dataset is characterized by two distinct exponential growth phases (especially appreciable in the

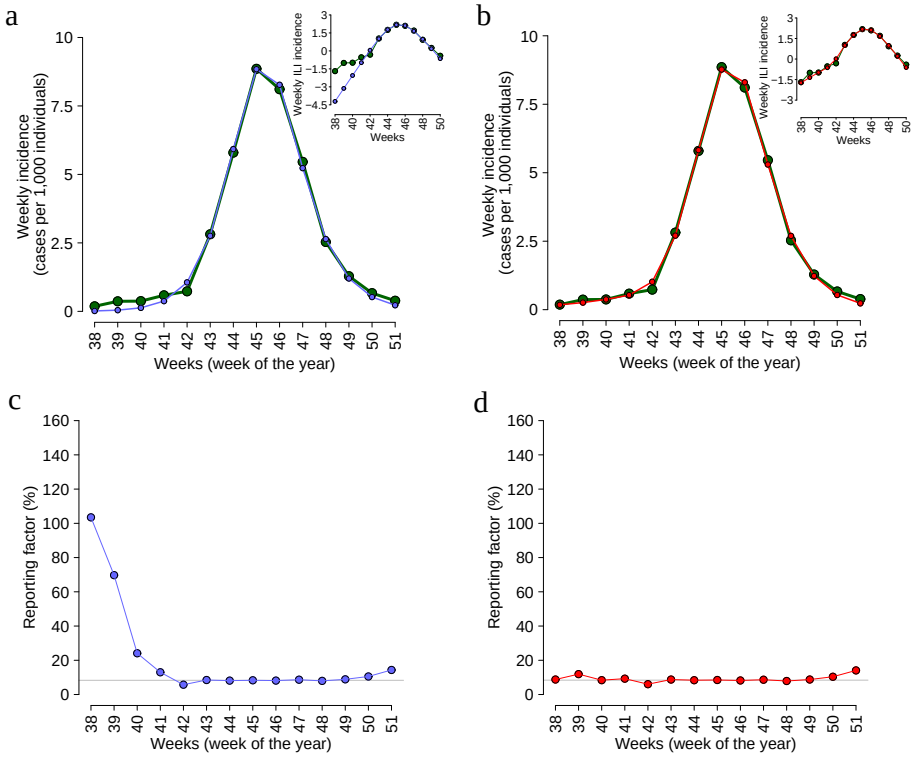

Figure 8.8: **a** Weekly incidence as obtained by combining epidemiological and virological surveillance data for the 2009 pandemic in Italy (green) and weekly incidence simulated by a "simple" SIR model with a constant reporting factor (blue). Sub–panel shows the same curves in a logarithmic scale. Parameter values used in the simulation are set as follows: the generation time $1/\gamma$ is assumed 2.5 days (in agreement with [63, 165]); $S(0) = 0.9$ (according to [134]); $I(0) = 0.000025$, $\beta = 0.62$, fitted. **b** Weekly incidence computed as in **a** (green) and simulated by the model accounting for behavioral changes (with a constant reporting factor, red). Sub–panel shows the same curves in a logarithmic scale. Parameter values used in the simulation are set as follows: $1/\gamma = 2.5$ days; $S(0) = 0.9$; $x(0) = 10^{-8}$, assumed; $M(0) = 10.17$, $I(0) = 0.00054$, $q = 0.815$, $m = 0.104$, $\rho = 70$, $\theta = 0.0046$, $\beta = 0.62$, fitted. **c** Weekly reporting factor estimates that enable the "simple" SIR model (parameters as in **a**) to exactly fit the influenza incidence (as computed in **a**). The horizontal gray line represents the average reporting factor as computed over the weeks 42–51. **d** As in **c** but for the model accounting for behavioral changes.

log scale, see Fig. 8.8a). By fitting a simple SIR model and the proposed model to such data, we obtain substantially the same results discussed in the main text: the SIR model is unable to account for the initial phases of the epidemic, while the model including behavioral changes performs much better (see Fig. 8.8a, b).

We found that a simple SIR model with a time dependent reporting factor is able to capture the initial phase of pandemic only by considering extremely large values of the reporting factor (even above 100%, see Fig. 8.8c). Since this new dataset can be interpreted as a theoretic lower bound for the number of H1N1pdm infections, reporting factor values above 100% in principle cannot be observable. On the contrary, the model considering behavioral changes does not require such large values for the reporting factor (see Fig. 8.8d). In conclusion, this analysis suggests that a variable reporting factor does not seem to be able to explain alone the observed pattern.

8.3 Appendix C

8.3.1 Properties and more details

The biomathematical properties listed in section 3 may be demonstrated as follows:
Property A Let us define, to simplify the notation, the parameter:

$$\Psi = kh\left(I_e\right)\left(1-h\left(I_e\right)\right). \tag{8.8}$$

Linearizing at E_e yields the following characteristic polynomial with positive coefficients:

$$\lambda^3 + \left(\Psi+\mu+\beta I_e\right)\lambda^2 + \left(\left(\mu+\beta I_e\right)\Psi + (\mu+\nu)\beta I_e\right)\lambda + \beta I_e\left(\mu+\nu+\mu h'\left(I_e\right)\right)\Psi, \tag{8.9}$$

for which the Routh-Hurwitz condition yields this inequality in the variable Ψ:

$$RH(\Psi) = \left(\mu+\beta I_e\right)\Psi^2 + \left(\left(\mu+\beta I_e\right)^2 - \beta I_e \mu h'\left(I_e\right) +\right)\Psi + \left(\mu+\beta I_e\right)\beta I_e(\mu+\nu) > 0. \tag{8.10}$$

Since the coefficients of power 0 and 2 of eq. (8.10) are positive, and taking also into account the sign of the coefficient of power 1, it is easy to show that if (6.12) holds then E_{beh} is LAS.
Property B If (6.13) holds then there are two positive values $0 < k_1 < k_2$ such that if $k < k_1$ or $k > k_2$ then E_{beh} is LAS; moreover, if $k_1 < k < k_2$ then E_{beh} is unstable and k_1 and k_2 are Hopf points. After some algebra it is easy to verify that at the Hopf points there are Hopf bifurcations since the nonzero speed condition $Re\left((d\lambda/dk)|_{\lambda=\pm i\omega_{Hopf}}\right) \neq 0$ is fulfilled.
Property C As regards the Yabucovitch oscillations, note that: *i)* the bounded set

$$A = \{(S,I,p) \in R_+ | 0 \leq S+I \leq 1-h(0), h(0) \leq p \leq 1\}$$

is positively invariant and attractive; *ii)* E_{beh} is unstable, and E_{dfe}, which is in the boundary of A, has as the stable manifold the line $(w,0,1)$ $w \in [0,1]$ to which E_{beh} does not

belong, excluding heterocline orbits. Thus we may apply the Yabucovitch theorem.
Property D Since asymptotically $p(t) \geq h(0)$, it follows that for large times:

$$S' \leq \mu \left(1 - h(0) - S\right),$$

i.e. asymptotically $S(t) \leq (1 - h(0))$. This in turn implies:

$$I' \leq \beta I \left(1 - h(0) - R_0^{-1}\right) = \beta \left(p_c - h(0)\right) I.$$

Thus, if $h(0) > p_c$ then $I(t) \to 0$ implying $p(t) \to h(0)$ and $S(t) \to 1 - h(0)$, i.e. E_{dfe} is GAS.
Let us now discuss the case of an exponentially fading memory in the perceived risk of vaccination with linear $h(I) = \vartheta I$. The Routh-Hurwitz stability condition reads:

$$G(\Psi, b) = c_2(b)\Psi^2 + c_1(b)\Psi + c_0(b) > 0 \tag{8.11}$$

where Ψ is as in eq. (8.8), and the coefficients are third order polynomials in the delay parameter b. Thus, for each b there are at most two bifurcation values for k, whereas for each k there may be at most three bifurcation values for b.

Bibliography

[1] F. R. Adler and J. M. Losada. *Adaptive Dynamics of Infectious Diseases: In Pursuit of Virulence Management*. Cambridge University Press, 2002.

[2] A. Ahituv, V. J. Hotz, and T. Philipson. The Responsiveness of the Demand for Condoms to the Local Prevalence of AIDS. *J Hum Resour*, 31(4):869–897, 1996.

[3] M. Ajelli, M. Iannelli, P. Manfredi, and M. L. Ciofi degli Atti. Basic mathematical models for the temporal dynamics of HAV in medium-endemicity Italian areas. *Vaccine*, 26(13):1697–1707, 2008.

[4] M. Ajelli, S. Merler, A. Pugliese, and C. Rizzo. Model predictions and evaluation of possible control strategies for the 2009 A/H1N1v influenza pandemic in Italy. *Epidemiol Infect*, Published Online by Cambridge University Press 14 June 2010, 2010.

[5] R. M. Anderson and R. M. May. *Infectious diseases of humans: dynamics and control*. Oxford, UK: Oxford University Press, 1991.

[6] R. M. Anderson and R. M. May. *Infectious diseases of humans: dynamics and control*. Oxford, UK: Oxford University Pres, 1992.

[7] V. Andreasen, J. Lin, and S. Levin. The dynamics of cocirculating influenza strains conferring partial cross-immunity. *J Math Biol*, 35(7):825–842, 1997.

[8] D. A. Asch, J. Baron, J. C. Hershey, H. Kunreuther, J. Meszaros, I. Ritov, and M. Spranca. Omission bias and pertussis vaccination. *Medical Decision Making*, 14(2):118–23, 1994.

[9] F. Bagnoli, P. Liò, and L. Sguanci. Risk perception in epidemic modeling. *Phys Rev E*, 76(6):061904–061911, 2007.

[10] M. Baguelin, A. J. V. Hoek, M. Jit, S. Flasche, P. J. White, and W. J. Edmunds. Vaccination against pandemic influenza A/H1N1v in England: A real-time economic evaluation. *Vaccine*, 28(12):2370–2384, 2010.

[11] D. Balcan, V. Colizza, B. Gonçalves, H. Hu, J. J. Ramasco, and A. Vespignani. Multiscale mobility networks and the spatial spreading of infectious diseases. *Proc Natl Acad Sci USA*, 106(51):21484–21489, 2009.

[12] D. Balcan, H. Hu, B. Goncalves, P. Bajardi, C. Poletto, J. J. Ramasco, D. Paolotti, N. Perra, M. Tizzoni, W. V. Broeck, V. Colizza, and A. Vespignani. Seasonal transmission potential and activity peaks of the new influenza A (H 1 N 1): a Monte Carlo likelihood analysis based on human mobility. *BMC Med*, 7(1):45, 2009.

[13] S. Barrett. Global disease eradication. *Journal of European Economic Association*, 1(2,3):591–600, 2003.

[14] S. Basu, G. B. Chapman, and A. P. Galvani. Integrating epidemiology, psychology, and economics to achieve HPV vaccination targets. *Proc Natl Acad Sci USA*, 105:19018–19023, 2008.

[15] C. T. Bauch. Imitation dynamics predict vaccinating behaviour. *Proc R Soc B*, 27:1669–1675, 2005.

[16] C. T. Bauch and D. J. D. Earn. Vaccination and the theory of games. *Proc Natl Acad Sci USA*, 101:13391–13394, 2004.

[17] C. T. Bauch, A. P. Galvani, and D. J. D. Earn. Group interest versus self-interest in smallpox vaccination policy. *Proc Natl Acad Sci USA*, 100(18):10564–10567, 2003.

[18] H. Bedford and M. Lansley. More vaccines for children? Parents' views. *MVaccine*, 25:7818–7823, 2007.

[19] S. Bonhoeffer and M. A. Nowak. Mutation and the evolution of virulence. *Proc R Soc B*, 258:133–140, 1994.

[20] M. Boni, J. Gog, V. Andreasen, and F. Christiansen. Influenza drift and epidemic size: the race between generating and escaping immunity. *Theor Popul Biol*, 65:179–191, 2004.

[21] M. C. J. Bootsma and N. M. Ferguson. The effect of public health measures on the 1918 influenza pandemic in US cities. *Proc Natl Acad Sci USA*, 104(18):7588–7593, 2007.

[22] R. Breban, R.and Vardavas and S. Blower. Mean-field analysis of an inductive reasoning game: Application to influenza vaccination. *Phys Rev E*, 76(3):031127, 2007.

[23] D. L. Brito, E. Sheshinski, and M. D. Intriligator. Externalities and compulsory vaccinations. *Journal of Public Economics*, 45:69–90, 1991.

[24] G. L. Campbell and J. M. Hughes. Plague in India: A New Warning from an Old Nemesis. *Ann Intern Med*, 122(2):151–153, 1995.

[25] V. Capasso and G. Serio. A generalization of the Kermack-McKendrick deterministic epidemic model. *Mathematical Biosciences*, 42(1-2):43–61, 1978.

[26] C. Castillo-Chavez, H. Hethcote, V. Andreasen, S. A. Levin, and W. M. Liu. Epidemiological models with age structure, proportionate mixing, and cross-immunity. *J Math Biol*, 89(27):233–258, 1989.

[27] S. Cauchemez, C. Ferguson, N. M.and Wachtel, A. Tegnell, G. Saour, B. Duncan, and A. Nicoll. Closure of schools during an infuenza pandemic. *Lancet*, 9:473–481, 2009.

[28] S. Cauchemez, A. Valleron, P. Boelle, A. Flahault, and N. M. Ferguson. Estimating the impact of school closure on influenza transmission from Sentinel data. *Nature*, 452:750 – 754, 2007.

[29] F. H. Chen. A Susceptible-infected Epidemic Model with Voluntary Vaccinations . *J Math Biol*, 53(2):253–272, 2006.

[30] R. T. Chen and W. A. Orenstein. Epidemiologic Methods in Immunization Programs. *Epidemiologic Reviews*, 18(2):99–117, 1996.

[31] G. Chowell, C. E. Ammon, N. W. Hengartner, and J. M Hyman. Estimation of the reproductive number of the spanish flu epidemic in geneva, switzerland. *Vaccine*, 24:p6747–6750, 2006.

[32] G. Chowell, C. E. Ammon, N. W. Hengartner, and J. M. Hyman. Transmission dynamics of the great influenza pandemic of 1918 in geneva, switzerland: Assessing the effects of hypothetical interventions. *J Theor Biol*, 241:193–204, 2006.

[33] M. L. Ciofi degli Atti, S. Merler, C. Rizzo, M. Ajelli, M. Massari, P. Manfredi, C. Furlanello, G. Scalia Tomba, and M. Iannelli. Mitigation measures for pandemic influenza in Italy: an individual based model considering different scenarios. *PLoS ONE*, 3(3):e1790, 2008.

[34] C.T. Codeço, P.M. Luz, F. Coelho, A.P. Galvani, and C. Struchiner. Vaccinating in disease-free regions: a vaccine model with application to yellow fever. *J R Soc Interface*, 4(17):1742–5689, 2007.

[35] S. Cohuet, A. Bukasa, R Heathcock, J. White, K. Brown, M. Ramsay, and G. Fraser. A measles outbreak in the Irish traveller ethnic group after attending a funeral in England, March–June 2007. *Epidemiol and Infect*, 12:1–7, 2009.

[36] M. G. Cojocaru, C. T. Bauch, and M. D. Johnston. Dynamics of vaccination strategies via projected dynamical systems. *Bulletin of Mathematical Biology*, 69:1453–1476, 2007.

[37] V. Colizza, A. Barrat, M. Barthélemy, A.-J. Valleron, and A. Vespignani. Modeling the worldwide spread of pandemic influenza: baseline case and containment interventions. *PLoS Med*, 4(1):e13, 2007.

[38] V. Colizza, A. Barrat, M. Barthélemy, and A. Vespignani. The role of the airline transportation network in the prediction and predictability of global epidemics. *Proc Natl Acad Sci USA*, 103(7):2015–2020, 2006.

[39] B.J. Cowling, DM Ng, DK Ip, Q. Liao, WW Lam, J.T. Wu, JT Lau, S.M. Griffiths, and R. Fielding. Community Psychological and Behavioral Responses through the First Wave of the 2009 Influenza A (H1N1) Pandemic in Hong Kong. *J Infect Dis*, 202(6):867–876, 2010.

[40] A. W. Crosby. *America's forgotten pandemic: the influenza of 1918*. Cambridge, UK: Cambridge University Press, 1990.

[41] V. J. Davey, R. J. Glass, H. J. Min, W. E. Beyeler, and L. M. Glass. Effective, robust design of community mitigation for pandemic influenza: a systematic examination of proposed US guidance. *PLoS ONE*, 3(7):e2606, 2008.

[42] S. Del Valle, H. Hethcote, J. M. Hyman, and C. Castillo-Chavez. Effects of behavioral changes in a smallpox attack model. *Math Biosci*, 195(2):228–251, 2005.

[43] Istituto Superiore di Sanità. Surveillance of adverse events, 1999.

[44] O. Diekmann, J. A. P Heesterbeek, and J. A. J. Metz. On the definition and the computation of the basic reproduction ratio R0 in models for infectious diseases in heterogeneous populations. *J Math Biol*, 28(4):365–382, 1990.

[45] A. d'Onofrio and P. Manfredi. Information-related changes in contact patterns may trigger oscillations in the endemic prevalence of infectious diseases. *J Theor Biol*, 256(3):473–478, 2008.

[46] A. d'Onofrio and P. Manfredi. Vaccine demand driven by vaccine side effects: dynamic implications for SIR diseases. *J Theor Biol*, 264:237–252, 2010.

[47] A. d'Onofrio, P. Manfredi, and E. Salinelli. Bifurcation threshold in an SIR model with information dependent vaccination. *Mathematical Modelling of Natural Phenomena*, 2:323–38, 2007.

[48] A. d'Onofrio, P. Manfredi, and E. Salinelli. Vaccinating behaviour, information, and the dynamics of SIR vaccine preventable diseases. *Theor Popul Biol*, 71(3):301–317, 2007.

[49] A. d'Onofrio, P. Manfredi, and E. Salinelli. Fatal SIR diseases and rational exemption to vaccination. *Mathematical Medicine and Biology*, 25(4):337–357, 2008.

[50] K. T. D. Eames. Networks of influence and infection: parental choices and childhood disease. *J R Soc Interface*, 6(38):811–814, 2009.

[51] D. Edwards, J. C. Man, P. Brand, J. P. Katsra, K. Sommerer, H. A. Stone, E. Nardell, and G. Scheuch. Inhaling to mitigate exhaled bioaerosols. *Proc Natl Acad Sci USA*, 101(50):17383–17388, 2004.

[52] J. M. Epstein. Modelling to contain pandemics. *Nature*, 460(7256):687, 2009.

[53] J. M. Epstein, J. Parker, D. Cummings, and R. A. Hammond. Coupled contagion dynamics of fear and disease: mathematical and computational explorations. *PLoS One*, 3(12):e3955, 2008.

[54] European Commission. Organisation of school time in Europe, Primary and general secondary education, 2009/10 school year, 2009.

[55] D. Farchy. A common good: whither the global eradication of the measles virus. *Working Paper World Bank*, 2006.

[56] N. Ferguson. Capturing human behaviour. *Nature*, 446(7137):733, 2007.

[57] N. M. Ferguson, D. A. Cummings, S. Cauchemez, C. Fraser, S. Riley, A. Meeyai, S. Iamsirithaworn, and D. S. Burke. Strategies for containing an emerging influenza pandemic in Southeast Asia. *Nature*, 437(7056):209–214, 2005.

[58] N. M. Ferguson, D. A. Cummings, C. Fraser, J. C. Cajka, and P. C. Cooley. Strategies for mitigating an influenza pandemic. *Nature*, 442(7101):448–452, 2006.

[59] N. M. Ferguson, D. A. Cummings, C. Fraser, J. C. Cajka, P. C. Cooley, and D. S. Burke. Strategies for mitigating an influenza pandemic. *Nature*, 442:448–452, 2006.

[60] A. Ferro, S. Cinquetti, T. Menegon, G. Napoletano, L. Bertoncello, and M. Valsecchi. Overcoming mandatory vaccination policy: first steps. *Annali di Igiene*, 20:3–8, 2008.

[61] P. E. M. Fine and J. A. Clarkson. Individual versus public priorities in the determination of optimal vaccination policies. *Am J Epidemiol*, 124:1012–1020, 1986.

[62] Center for Disease Control. Vaccine safety, 1999.

[63] C. Fraser, C. A. Donnelly, S. Cauchemez, W. P. Hanage, M. D. Van Kerkhove, T. D. Hollingsworth, J. Griffin, R. F. Baggaley, H. E. Jenkins, E. J. Lyons, T. Jombart, W. R. Hinsley, N. C. Grassly, F. Balloux, A. C. Ghani, N. M. Ferguson, A. Rambaut, O. G. Pybus, H. Lopez-Gatell, C. M. Alpuche-Aranda, I. Bojorquez Chapela, E. Palacios Zavala, D. M. Espejo Guevara, F. Checchi, E. Garcia, S. Hugonnet, C. Roth, and The WHO Rapid Pandemic Assessment Collaboration. Pandemic Potential of a Strain of Influenza A (H1N1) : Early Findings. *Science*, 324(5934):1557–1561, 2009.

[64] V. Friederichs, J. C. Cameron, and Robertson C. Impact of adverse publicity on MMR vaccine uptake: a population based analysis of vaccine uptake records for one million children, born 1987–2004. *Arch. Diseases Childood*, 91(6):465–468, 2006.

[65] K. Frost, E. Frank, and E. Maibach. Relative risk in the news media: a quantification of misrepresentation. *American Journal of Public Health*, 87(5):842–845, 1997.

[66] S. Funk, E. Gilad, and V. A. A. Jansen. Endemic disease, awareness, and local behavioural response. *J Theor Biol*, 264(2):501–509, 2010.

[67] S. Funk, E. Gilad, C. Watkins, and V. A. A. Jansen. The spread of awareness and its impact on epidemic outbreaks. *Proc Natl Acad Sci USA*, 106(16):6872–6877, 2009.

[68] S. Funk, M. Salathé, and V. A. A. Jansen. Modelling the influence of human behaviour on the spread of infectious diseases: a review. *J R Soc Interface*, 7(50):1247–1256, 2010.

[69] A. P. Galvani, T. C. Reluga, and G. B. Chapman. Long-standing influenza vaccination policy is in accord with individual self-interest but not with the utilitarian optimum. *Proc Natl Acad Sci USA*, 104(13):5692–5697, 2007.

[70] E. J. Gangarosa, A. M. Galazka, C. R. Wolfe, R. E. Phillips, L. M. Gangarosa, Miller E., and R. T. Chen. Impact of anti-vaccine movements on pertussis control: the untold story. *Lancet*, 351:356–61, 1998.

[71] G. P. Garnett and R. M. Anderson. Sexually transmitted diseases and sexual behavior: insights from mathematical models. *J Infect Dis*, 174:150–161, 1996.

[72] P.Y. Geoffard and T. Philipson. Disease eradication: private versus public vaccination. *Am Econ Rev*, 87:222–230, 1997.

[73] T. C. Germann, K. Kadau, I. M. J. Longini, and C. A. Macken. Mitigation strategies for pandemic influenza in the United States. *Proc Natl Acad Sci USA*, 103(15):5935–5940, 2006.

[74] A. C. Ghani, M. Baguelin, J. Griffin, S. Flasche, A. J. Van Hoek, S. Cauchemez, C. Donnelly, C. Robertson, M White, J Truscott, C Fraser, T Garske, P White, S Leach, I Hall, H Jenkins, N Ferguson, and B Cooper. The early transmission dynamics of H1N1pdm influenza in the United Kingdom. *PLoS Curr Influenza*, 2:RRN1130, 2009.

[75] M. Z. Gojovic, B. Sander, D. Fisman, M. D. Krahn, and C. T. Bauch. Modelling mitigation strategies for pandemic (H1N1) 2009. *Can Med Assoc J*, 181(10):673–680, 2009.

[76] M. C. González, C. A. Hidalgo, and A. L. Barabási. Understanding individual human mobility patterns. *Nature*, 453(7196):779–782, 2008.

[77] T. Gross, C. J. D. D'Lima, and B. Blasius. Epidemic Dynamics on an Adaptive Network. *Phys Rev Lett*, 96(20):208701, 2006.

[78] M. E. Halloran, N. M. Ferguson, S. Eubank, I. M. Longini Jr, D. A. T. Cummings, B. Lewis, S. Xu, C. Fraser, A. Vullikanti, T. C. Germann, D. Wagener, R. Beckman, K. Kadau, C. Barrett, C. A. Macken, D. S. Burke, and P. Cooley. Modeling targeted layered containment of an influenza pandemic in the United States. *Proc Natl Acad Sci USA*, 105(12):4639–4645, 2008.

[79] B. Hanratty, O Holt, E. Duffell, W. Patterson, J. M. Ramsay, M. White, and P. Jin, L.and Litton. UK measles outbreak in non-immune anthroposophic communities: the implications for the elimination of measles from Europe. *Epidemiol Infect*, 125:377–383, 2000.

[80] R. J. Hatchett, C. E. Mecher, and M. Lipsitch. Public health interventions and epidemic intensity during the 1918 influenza pandemic. *Proc Natl Acad Sci USA*, 104(18):7582–7587, 2007.

[81] J. Hofbauer and K. Sigmund. *Evolutionary Games and Population Dynamics*. Cambridge University Press, 1998.

[82] S. Holly, H. Anita, M.L. Mary-Louise, W. Kirsten, L. Chris, V. Debbie, and M. I. C. Raina. Why do I need it? I am not at risk! Public perceptions towards the pandemic (H1N1) 2009 vaccine. *BMC Infect Dis*, 10:1471–2334, 2010.

[83] F. Hoppensteadt. Singular Perturbations on the Infinite Interval. *Transactions of the American Mathematical Society*, 123:521–535, 1966.

[84] L. Hufnagel, D. Brockmann, and T. Geisel. Forecast and control of epidemics in a globalized world. *Proc Natl Acad Sci USA*, 101(42):15124–15129, 2004.

[85] Istituto Superiore di Sanitá. FluNews Aggiornamento epidemiologico settimanale numero 14, 25-31 January 2010., 2010. (In Italian).

[86] Istituto Superiore di Sanitá. FluNews Aggiornamento epidemiologico settimanale numero 22, 22-28 March 2010., 2010. (In Italian).

[87] Istituto Superiore di Sanitá. Stagione influenzale 2009/2010: Sorveglianza epidemiologica, 2010. (Available in Italian at `http://www.iss.it/iflu/risu/cont.php?id=141&lang=1&tipo=5`).

[88] Italian Ministry of Health. Sorveglianza virologica dell'influenza, 2010. (Available in Italian at `http://www.nuovainfluenza.salute.gov.it/nuovainfluenza/andamentoEpidemiaNuovaInfluenza.jsp?id=1223`).

[89] V. A. A. Jansen, N. Stollenwerk, H. J. Jensen, M. E. Ramsay, W. J. Edmunds, and C. J. Rhodes. Measles Outbreaks in a Population with Declining Vaccine Uptake. *Science*, 301(5634):804, 2003.

[90] J. H. Jones and M. Salathé. Early assessment of anxiety and behavioral response to novel swine-origin influenza A (H1N1). *PloS One*, 4:e8032, 2009.

[91] R.E. Kasperson, O. Renn, P. Slovic, H.S. Brown, J. Emel, R. Goble, J.X. Kasperson, and S. Ratick. The social amplification of risk: A conceptual framework. *Risk analysis*, 8(2):177–187, 1988.

[92] M. J. Keeling, M. E. J. Woolhouse, R. M. May, G. Davies, and B. T. Grenfell. Modelling vaccination strategies against foot-and-mouth disease. *Nature*, 421(6919):136–142, 2002.

[93] I. Z. Kiss, J. Cassell, M. Recker, and P. L. Simon. The impact of information transmission on epidemic outbreaks. *Math Biosci*, 225(1):1–10, 2010.

[94] La Repubblica (National newspaper). Caso sospetto di influenza A la scuola chiude per 2 giorni (September 29, 2009), 2009. (In Italian, article available at `http://ricerca.repubblica.it/repubblica/archivio/repubblica/2009/09/29/caso-sospetto-di-influenza-la-scuola-chiude.html`).

[95] La Repubblica (National newspaper). Davanti a scuola sorpresa e paura ma c'é pure chi brinda alla vacanza (October 9, 2009), 2009. (In Italian, article available at `http://ricerca.repubblica.it/repubblica/archivio/repubblica/2009/10/09/davanti-scuola-sorpresa-paura-ma-pure.html`).

[96] La Repubblica (National newspaper). Influenza: un caso di virus A scuola chiusa, riapre oggi, 2009. (In Italian, article available at `http://ricerca.repubblica.it/repubblica/archivio/repubblica/2009/10/06/influenza-un-caso-di-virus-scuola-chiusa.html`).

[97] La Repubblica (National newspaper). Virus A, chiusa scuola a Pomigliano (October 4, 2009), 2009. (In Italian, article available at `http://ricerca.repubblica.it/repubblica/archivio/repubblica/2009/10/04/virus-chiusa-scuola-pomigliano.html`).

[98] JT Lau, H. Tsui, M. Lau, and X. Yang. SARS transmission, risk factors, and prevention in Hong Kong. *Emerg Infect Dis*, 10(4):587–92, 2004.

[99] B. Y. Lee, S. T. Brown, G. Korch, P. C. Cooley, R. K. Zimmerman, W. D. Wheaton, S. M. Zimmer, J. J. Grefenstette, R. R. Bailey, T. M. Assi, and Burke D. S. A computer simulation of vaccine prioritization, allocation, and rationing during the 2009 H1N1 influenza pandemic. *Vaccine*, 28(31):4875–4879, 2010.

[100] W. Liu, H. W. Hethcote, and S. A. Levin. Dynamical behavior of epidemiological models with nonlinear incidence rates . *J Math Biol*, 25(4):359–380, 1987.

[101] W. Liu, S. A. Levin, and Y. Iwasa. Influence of nonlinear incidence rates upon the behavior of SIRS epidemiological models. *J Math Biol*, 23(2):187–204, 1986.

[102] J. O. Lloyd-Smith, S. J. Schreiber, P. E. Koop, and W. M. Getz. Superspreading and the effect of individual variation on disease emergence. *Nature*, 438:355–359, 2005.

[103] I. M. J. Longini, M. E. Halloran, A. Nizam, and Y. Yang. Containing Pandemic Influenza with Antiviral Agents. *Am J Epidemiol*, 159(7):623–633, 2004.

[104] I. M. J. Longini, A. Nizam, S. Xu, K. Ungchusak, W. Hanshaoworakul, D. A. Cummings, and M. E. Halloran. Containing pandemic influenza at the source. *Science*, 309(5737):1083–1087, 2005.

[105] Jr I. M. Longini, J. S. Koopman, M. Haber, and G. A. Cotsonis. Statistical inference for infectious diseases: risk-specific household and community transmission parameters. *Am J Epidemiol*, 128(4):845–859, 1988.

[106] E. T. Luman, Fiore A. E., Strine T. W., and L. E. Barker. Impact of thimerosal-related changes in hepatitis B vaccine, birth-dose recommendations. *J. American Medical Association*, 291:2351–2358, 2004.

[107] A. Maayan-Metzger, P. Kedem-Friedrich, and J. Kuint. To vaccinate or not to vaccinate: that is the question: why are some mothers opposed to giving their infants hepatitis B vaccine? *Vaccine*, 23:1941–1948, 2004.

[108] P. Manfredi, A. D'Onofrio, P. della Posta, and E. Salinelli. Rational exemption to vaccination: from dynamics to behaviour. *Epidemics Conference, Asilomar (CA)*, December 2009.

[109] P. Manfredi, P. D. Posta, A. d'Onofrio, E. Salinelli, F. Centrone, C. Meo, and P. Poletti. Optimal vaccination choice, vaccination games, and rational exemption: An appraisal. *Vaccine*, 28(1):98–109, 2009.

[110] A. Mas Colell and M. D. Whinston. *Microeconomic theory*. Oxford, UK: Oxford University Press, 1995.

[111] R.M. May and M.A. Nowak. Coinfection and the evolution of parasite virulence. *Proceedings: Biological Sciences*, 261(1361):209–215, 1995.

[112] S. Merler and M. Ajelli. The role of population heterogeneity and human mobility in the spread of pandemic influenza. *Proc R Soc B*, 277(1681):557–565, 2010.

[113] S. Merler, M. Ajelli, and C. Rizzo. Age-prioritized use of antivirals during an influenza pandemic. *BMC Infect Dis*, 9:117, 2009.

[114] S. Merler, P. Poletti, M. Ajelli, B. Caprile, and P. Manfredi. Coinfection can trigger multiple pandemic waves. *J Theor Biol*, 254(2):499–507, 2008.

[115] C. E. Mills, J. M. Robins, and M. Lipsitch. Transmissibility of 1918 pandemic influenza. *Nature*, 432:904–906, 2004.

[116] V. Molina and Y. Shoenfeld. Infection, vaccines and other environmental triggers of autoimmunity. *Autoimmunity*, 38:235–245, 2005.

[117] I. A. Moneim. The effect of using different types of periodic contact rate on the behaviour of infectious diseases: A simulation study. *Computers in Biology and Medicine*, 37, 2007.

[118] C. V. Munayco, J. Gomez, V. A. Laguna-Torres, J. Arrasco, TJ Kochel, V. Fiestas, J. Garcia, J. Perez, I. Torres, F. Condori, H. Nishiura, and G. Chowell. Epidemiological and transmissibility analysis of influenza a (h1n1) v in a southern hemisphere setting: Peru. *Eurosurveill*, 14:pii: 19299, 2009.

[119] K. M. Neuzil, C. Hohlbein, and Y. Zhu. Illness among schoolchildren during influenza season: effect on school absenteeism, parental absenteeism from work, and secondary illness in families. *Arch Pediatr Adolesc Med*, 156(10):986–991, 2002.

[120] A. Nicoll, D. Elliman, and E. Ross. MMR vaccination and autism 1998. *Br med J*, 316:715–716, 1998.

[121] H. Nishiura. Time variations in the transmissibility of pandemic influenza in Prussia, Germany, from 1918-19. *Theoretical Biology and Medical Modelling*, 4:20, 2007.

[122] M. A. Nowak and K. Sigmund. Evolutionary Dynamics of Biological Games. *Science*, 303:793–799, 2004.

[123] R.E. O'Malley Jr. *Singular perturbation methods for ordinary differential equations.* Springer-Verlag, 1991.

[124] A. Perisic and C. T. Bauch. Social contact networks and disease eradicability under voluntary vaccination. *PLoS Comp Biol*, 5(2):e1000280, 2009.

[125] T. Philipwon. Private Vaccination and Public Health: An Empirical Examination for U.S. Measles. *J Hum Resour*, 31(3):611–630, 1996.

[126] S. Plotkin. Lessons learned concerning vaccine safety. *Vaccine*, 20(Suppl. 1):S16–S19, 2002.

[127] P. Poletti, B. Caprile, M. Ajelli, A. Pugliese, and S. Merler. Spontaneous behavioural changes in response to epidemics. *J Theor Biol*, 260(1):31–40, 2009.

[128] A. M. Presanis, D. De Angelis, The New York City Swine Flu Investigation Team, A. Hagy, C. Reed, S. Riley, B. S. Cooper, L. Finelli, P. Biedrzycki, and M. Lipsitch. The Severity of Pandemic H1N1 Influenza in the United States, from April to July 2009: A Bayesian Analysis. *PLoS Med*, 6(12):e1000207, 2009.

[129] T. C. Reluga. An SIS epidemiology game with two subpopulations. *Journal of Biological Dynamics*, 200:1–19, 2008.

[130] T. C. Reluga. Game theory of social distancing in response to an epidemic. *PLoS Comp Biol*, 6(5):e1000793, 2010.

[131] T. C. Reluga, C. T. Bauch, and A. P. Galvani. Evolving public perceptions and stability in vaccine uptake. *Mathematical Biosciences*, 204(2):185–198, 2006.

[132] S. Riley, C. Fraser, C. A. Donnelly, A. C. Ghani, L. J. Abu-Raddad, A. J. Hedley, G. M. Leung, L. Ho, T. Lam, T. Q. Thach, K. Chau, P. Chan, S. Lo, T. Leung, P. Tsang, W. Ho, K. Lee, E. M. C. Lau, N. M. Ferguson, and R. M. Anderson. Transmission Dynamics of the Etiological Agent of SARS in Hong Kong: Impact of Public Health Interventions. *Science*, 300(5627):1961 – 1966, 2003.

[133] S. Risau-Gusman and D. H. Zanette. Contact switching as a control strategy for epidemic outbreaks. *arXiv[q-bio.PE]:0806.1872*, 2008.

[134] C. Rizzo, M. C. Rota, A. Bella, V. Alfonsi, S. Declich, M. G. Caporali, A. Ranghiasci, G. Lapini, S. Piccirella, S. Salmaso, and E Montomoli. Cross-reactive antibody responses to the 2009 A/H1N1v influenza virus in the Italian population in the prepandemic period. *Vaccine*, 28(10):3558–3562, 2010.

[135] R. J. Roberts, Q. D. Sandifer, Evans M. R., Nolan-Farrell M. Z., and Davis P. M. Reasons for non-uptake of measles, mumps and rubella catch up immunisation in a measles epidemic and side effects of the vaccine. *British Medical Journal*, 310:1629–1639, 1995.

[136] G. J. Rubin, R. Amlot, L. Page, and S. Wessely. Public perceptions, anxiety, and behaviour change in relation to the swine flu outbreak: cross sectional telephone survey. *Br Med J*, 339:b2651, 2009.

[137] M. Z. Sadique, W. J. Edmunds, R. D. Smith, W. J. Meerding, O. de Zwart, J. Brug, and P. Beutels. Precautionary behavior in response to perceived threat of pandemic influenza. *Emerg Infect Dis*, 13(9):1307–1313, 2007.

[138] M. Salathé and S. Bonhoeffer. The effect of opinion clustering on disease outbreaks. *J R Soc Interface*, 5(29):1505–1508, 2008.

[139] D. A. Salmon, S. P. Teret, C. R. MacIntyre, D. Salisbury, M. A. Burgess, and N. A. Halsey. Compulsory vaccination and conscientious or philosophical exemptions: past, present and future. *Lancet*, 367:436–442, 2006.

[140] A. Schotter. *Microeconomics: a modern approach*. New York, Harper Collins College Publishers, 1994.

[141] L. B. Shaw and I. B. Schwartz. Fluctuating epidemics on adaptive networks. *Phys Rev E*, 77:066101, 2008.

[142] A. Smith, J. Yarwood, and D. M. Salisbury. Tracking mothers' attitudes to MMR immunisation 1996–2006. *Vaccine*, 25:33996–4002, 2007.

[143] J. Solomon and C. J. L.. Murray. The epidemiological transition revisited: new compositional models for causes of death by age and sex. *Pop Dev Rev*, 28:205–228, 2006.

[144] G. K. SteelFisher, R. J. Blendon, M. M. Bekheit, and K. Lubell. The Public's Response to the 2009 H1N1 Influenza Pandemic. *N Engl J Med*, 365:e65, 2010.

[145] J. P. Stiglitz. *Economics of the Public Sector*. New York, W.W. Norton & Company, 2000.

[146] K Stratton, A. Gable, P. Shtty, and M. McCormick. *Immunization safety review: measles-mumps-rubella vaccine and autism*. Washington DC: The National Academies Press, 2004.

[147] M. M. Tanaka, J. Kumm, and M. W. Feldman. Coevolution of pathogens and cultural practices: a new look at behavioral heterogeneity in epidemics. *Theor Popul Biol*, 62(2):111–119, 2002.

[148] A. Tikhonov. Systems of differential equations containing a small parameter multiplying the derivative. *Matematicheskii Sbornik (N.S.)*, 73(31):576–585, 1952.

[149] A. Traulsen, C. Hauert, H. De Silva, M. A. Nowak, and K. Sigmund. Exploration dynamics in evolutionary games. *Proc Natl Acad Sci USA*, 106(3):709–712, 2009.

[150] R. Vardavas, R. Breban, and S. Blower. Can influenza epidemics be prevented by voluntary vaccination? *PLoS Comp Biol*, 3(5):e85, 2007.

[151] C. Viboud, O. N. Bjornstad, D. L. Smith, L. Simonsen, M. A. Miller, and B. T. Grenfell. Synchrony, waves, and spatial hierarchies in the spread of influenza. *Science*, 312(5772):447–451, 2006.

[152] S. D. Von Allmen, R. H. Lopez-Correa, J. P. Woodall, D. M. Morens, J. Chiriboga, and A. Casta-Velez. Epidemic dengue fever in Puerto Rico, 1977: a cost analysis. *Am J Trop Med Hyg*, 28(6):1040–1044, 1979.

[153] J. Von Neuman and O. Morgenstern. *Theory of games and economic behavior*. NJ: Princeton, 1947.

[154] J. von Neumann and O. Morgenstern. *The Theory of Games and Economic Behavior*. Princeton University Press, 1947.

[155] E. Vynnycky, N. J. Gay, and F. T. Cutts. The predicted impact of private sector MMR vaccination on the burden of Congenital Rubella Syndrome. *Vaccine*, 21:2708–2719, 2003.

[156] J. Wallinga, W. J. Edmunds, and M. Kretzschmar. Perspective: human contact patterns and the spread of airborne infectious diseases. *Trends Microbiol*, 7(9):372–377, 1999.

[157] J. Wallinga and P. Teunis. Different epidemic curves for severe acute respiratory syndrome reveal similar impacts of control measures. *Am J Epidemiol*, 160(6):509, 2004.

[158] J. W. Weibull. *Evolutionary game theory*. The MIT press, 1997.

[159] W.H.O. Guidelines for managers of immunization programmes on reporting and investigating adverse events following immunization (WPRO/EPI/99.01.), 1999.

[160] W.H.O. Immunization safety, 1999.

[161] World Health Organization. Mitigating the impact of the new influenza A(H1N1): options for public health measures. (Available at urlhttp://www.wpro.who.int/NR/rdonlyres/9274FF90-8862-41F6-B858-D672E46C1C78/0/options_ph.pdf). (Accessed May 18, 2010).

[162] World Health Organization. Situation updates - Pandemic (H1N1) 2009. Influenza-like illness in the United States and Mexico. 2009. (Available at `http://www.who.int/csr/don/2009_04_24/en/index.html`), 2009. (Accessed May 18, 2010).

[163] J. A. Wright and C. Polack. Understanding variation in measles—mumps–rubella immunization coverage: a population-based study. *European J. Public Health*, 16(2):137–142, 2005.

[164] J. T. Wu, S. Riley, C. Fraser, and G. M. Leung. Reducing the impact of the next influenza pandemic using household-based public health interventions. *PLoS Med*, 3(9):e361, 2006.

[165] Y. Yang, J. D. Sugimoto, M. E. Halloran, N. E. Basta, D. L. Chao, L. Matrajt, G. Potter, E. Kenah, and I. M. Longini Jr. The transmissibility and control of pandemic influenza A (H1N1) virus. *Science*, 326(5953):729–733, 2009.

[166] M.E. Young, G.R. Norman, and K.R. Humphreys. Medicine in the popular press: the influence of the media on perceptions of disease. *PLoS One*, 3(10):e3552, 2008.

[167] D. H. Zanette and S. Risau-Gusman. A generalization of the Kermack-McKendrick deterministic epidemic model. *Journal of Biological Physics*, 34(1-2):135–148, 2008.